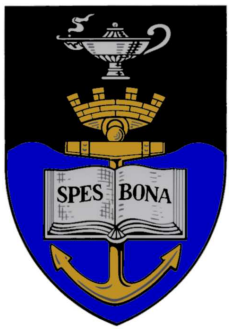

Modelling Seasonality in South African Agricultural Futures

Richard Kirk

Submitted to the Department of Mathematics
in partial fulfilment of the requirements for the degree of

Master of Science in Financial Mathematics
at the
UNIVERSITY OF CAPE TOWN

December 5, 2007

Supervisor: Dr. D. Wilcox

Abstract

This study investigates the seasonality in agricultural commodity futures prices. Futures prices are modelled using the model developed by Sørensen (2002). The model defines the commodity spot price as the sum of a non-stationary state variable, a stationary state variable and a deterministic seasonal component. Standard no-arbitrage arguments are applied in order to derive futures and option prices. Model parameters are estimated using Kalman filter methodology and maximum likelihood estimation. Model parameters are estimated for white maize, yellow maize and wheat futures traded on the South African Futures Exchange (SAFEX). Furthermore, this research considers other models for commodity derivatives as well as pricing futures contracts in the presence of price limits.

Keywords: Commodity futures, options, seasonality, Kalman filter, SAFEX, price limits.

Plagiarism Declaration

1. This dissertation is my own work. It has not been submitted before for any degree or examination to any other University.

2. I have not allowed, and will not allow, anyone to copy my work with the intention of passing it off as his or her own work.

3. Each significant contribution to, and quotation in, this dissertation from the work of other people has been cited and referenced.

_____

Signature

_____

Date

Acknowledgements

Firstly, I would like to thank my supervisor, Dr Dr Diane Wilcox, for her guidance and advice throughout. Secondly, I would like to thank Dr Jaco Maritz for his assistance in selecting a topic as well as being a source of constant guidance. Finally, I'd like to thank Gus Louw of Cadiz for helping me understand the intricacies of the South African Agricultural Futures Market.

Contents

List of Figures

List of Tables

Chapter 1

Introduction

The market for trading commodity based financial instruments has grown rapidly in recent years. Commodity futures and option contracts are traded extensively as a form of hedging, speculation and diversification. The futures exchanges upon which the instruments are traded have become well regarded and investors have become more confident in trading commodity derivatives. This is a result of a greater understanding by market participants of the dynamics of commodities and commodity based contracts as well as a significant development in the modelling and pricing of these instruments.

The first major development by Black (1975) assumed commodity prices followed a 'random walk' described by geometric Brownian motion. This model followed the ground-breaking Black-Scholes option pricing formula. The major shortfall of this model is that commodity prices are assumed to increase at a constant rate, independently of previous price movements, and the variance in future spot prices is assumed to increase in proportion to time.

Laughton and Jacoby (1993, 1995) showed that commodity prices exhibit mean-reversion. In an equilibrium setting, one would expect high commodity prices to correspond to an increase in the supply of the commodity, as producers enter the market, and hence a fall in price of the specific commodity. Conversely, if commodity prices fall, one would expect higher cost producers to exit the market, which would lead to lower commodity prices as the supply of the commodity is reduced. This dynamic has lead to the development of pricing models which incorporate mean-reverting stochastic factors.

This study investigates the dynamics of futures prices using a model proposed by Sørensen (2002). The Sørensen model defines the (log-) commodity spot price as the sum of a non-stationary state variable, a stationary state

variable as well as a deterministic seasonal component. The non-stationary state variable represents the long-term equilibrium level of the commodity spot price and is modelled as the logarithm of a geometric diffusion process. The stationary state variable, representing short-term deviations in the price of the commodity from its equilibrium level, is modelled as an Ornstein-Uhlenbeck process reverting to 0. Lastly, a seasonal component is included to capture the consistent seasonal fluctuations in commodity prices caused by the specific harvesting periods of commodities. A deterministic parameterised linear combination of trigonometric functions, with seasonal frequencies, denotes the seasonal component of the model.

Commodity prices display a consistent seasonal pattern year-on-year. Prices are generally highest prior to harvesting periods and lowest after harvesting periods. This pattern is a direct consequence of the forces of supply and demand. Before the harvest supply is at its lowest and hence prices are high. After the harvest prices fall as a result of the increase in supply.

The state variables and the seasonal component of commodity spot prices cannot be inferred directly from spot prices as such assets are not traded on exchanges and hence spot price data is unavailable. Futures prices are thus used in order to deduce information about the state variables and the seasonality of commodity prices. At any point in time, various futures contracts are available for different expiry months. Intuitively, the equilibrium level is determined using prices of all available futures contracts, the short-term deviation determined by comparing futures prices for short-dated and long-dated contracts, and lastly the seasonality determined by comparing prices of contracts for different expiry months.

A key tool needed in order to estimate the parameters of the model is the state space formulation. Once the model is presented in the state space form, Kalman filtering techniques may be used to estimate the model parameters. The model parameters are estimated by means of maximum likelihood estimation of the error decomposition of the log-likelihood function. The Matlab function 'fmincon' is used as the numerical optimisation tool to find the maximum likelihood estimates.

The properties of three agricultural commodities, namely white maize, yellow maize and wheat, are investigated throughout this thesis. Time series data for the futures prices of these commodities is obtained from the South African Futures Exchange (SAFEX).

The structure of this study is as follows: Chapter 3 explores the advance in the models used to value and price commodity contingent claims. Chapter 2 discusses the South African agricultural market as well as the Agricultural Products Division of the SAFEX, the exchange on which agricultural commodities futures are traded. Chapter 4 presents the dynamics and properties of the Sørensen model and derives closed form solutions for the price of futures and option contracts. Chapter 5 establishes the procedure for estimating the model parameters by means of state space formulation and Kalman filtering. Chapter 6 presents an initial investigation of the properties of price of white maize, yellow maize and wheat futures contracts. Chapter 7 explores the estimated seasonal parameters of the model for each commodity. The resulting seasonal components together with their implied influence on futures prices is analysed. Similarly, chapter 8 explores the non-seasonal parameter estimates and discusses their meaning. Chapter 9 considers pricing futures contracts in the presence of price limits. Finally chapter 10 concludes.

Chapter 2

The South African Agricultural Market and the SAFEX Agricultural Products Division

This chapter serves as a brief introduction to the South African agricultural market with specific focus on the commodities that are investigated throughout this research project.

The Agricultural Products Division (APD) is also discussed as this is the exchange on which the instruments analysed in this study are traded.

2.1 South African Agricultural Market

2.1.1 Brief Background

The South African agricultural economy can be regarded as a dual economy. On the one hand there is a significant commercial sector and on the other a subsistence-oriented sector.

Primary agriculture in South Africa contributes significantly towards the economy. It accounts for approximately 2.6% of gross domestic product (GDP) and provides almost 9% of formal employment in South Africa. On average, agricultural exports account for 8% of South African exports.

Under normal circumstances, South Africa is self-sufficient and a net exporter of agricultural products. The greatest concern to the agricultural industry is rainfall. Rainfall is distributed unevenly across the country and

Crop	Area Planted 2005/06 Ha	Seventh Estimate 2005/06 Tons	Area Planted 2004/05 Ha	Final Crop 2004/05 Tons	Change (Tons) 04/05 to 05/06 % Change
White Maize	985 000	3 635 300	1 700 000	6 540 700	-44.4
Yellow Maize	567 200	2 355 050	1 110 000	4 909 300	-52.0
Total Maize	1 552 200	5 990 350	2 810 000	11 450 000	-47.7

Table 2.1: Area planted and sixth production estimates of white and yellow maize for 2005/06. Area planted and final crop values for the 2004/05 season are included. Percentage change reflects the estimated change in total tons produced from 2004/05 to 2005/06.

rainfall is highly variable between seasons. This implies that the agricultural industry itself is very susceptible to changes in weather patterns.

The business of agriculture is termed agribusiness. There are approximately 1000 primary agricultural co-operatives and agribusinesses throughout the country as well as 15 central co-operatives.

The agricultural sector was deregulated in 1994. In 1996, legislation abolished the control boards for each sector of agriculture.

2.1.2 White Maize, Yellow Maize and Wheat

Throughout this study, white maize, yellow maize and wheat derivatives are investigated. It is not only important to understand the dynamics of the derivative instruments themselves, but also the underlying assets. Hence, this section aims at providing a greater understanding of white maize, yellow maize and wheat crops.

Maize (white and yellow) followed by wheat, accounts for the largest area of farmland planted in South Africa. Maize is a summer crop and its season begins on 1 May and ends on 30 April. Wheat is a winter crop and its season runs from 1 October to 30 September.

Note, all tables presented in this section display data for commercial agriculture only. Total area planted and forecasts for the crop sizes are released by the Crop Estimates Committee (CEC). All values presented here are in accordance with the CEC's report of the meeting on the 22 August 2006.

Table 3.1 displays the values for the total area planted and final crop estimates of maize for both the 2004/05 and 2005/06 season. The total area that South African commercial maize producers have planted for maize dur-

Crop	Area Planted 2006/07 Ha	Area Planted 2005/06 Ha	Final Crop 2005/06 Tons	Area Planted 2004/05 Ha	Final Crop 2004/05 Tons	Change (Tons) 04/05 to 05/06 % Change
Wheat	792 300	805 000	1 905 000	830 000	1 680 000	13.4

Table 2.2: Area planted and final crop values of wheat for 2005/06 and 2004/05. Area planted for the 2006/07 season is included. Percentage change reflects the change in total tons produced from 2004/05 to 2005/06.

ing the 2005/06 season is 1.552 million ha. The total maize crop forecast for the 2005/06 season is 5.990 million tons, which is 47.7% lower than the 2004/05 season. The considerable reduction in maize production is due to a marked reduction in the area planted, coupled with a delayed start to the 2005/06 season across many parts of the country.

White maize plantings for 2005/06 are down from 1.7 million ha to 985 000 ha, while yellow maize planting are down from 1.11 million ha to 567 200 ha. The ratio of white maize to yellow maize plantings is 63:37 versus the previous seasons 60:40.

Table 3.2 presents the total area planted and final crop values of wheat for the 2004/05 and 2005/06 seasons. As wheat is a winter crop values for the 2006/07 area planted are available.

The total size of the area planted for wheat decreased from 830 000 ha in 2004/05 to 805 000 ha in 2005/06. Despite this, total crop output increased 13.4% from 1.68 million tons to 1.905 million tons. The total area planted for the 2006/07 is down 1.6% from the 2005/06 season to 792 300 ha.

Table 3.3 displays the area planted and final crop productions for white maize, yellow maize and wheat by each province in the 2005/06 season. The majority of South Africa's maize is produced in the Free State, Mpumalanga and North West provinces. Wheat is mainly produced in the Western Cape, Free State and Northern Cape provinces. It is interesting to note that the Northern Cape accounted for 6.02% of the area planted for wheat in 2005/06 but accounted for 16.06% of the total crop produced.

Finally table 3.4 displays the gross incomes attributable to the major field crops for the periods April 2004 to March 2005 and the period April 2005 to March 2006. In 2005/06 maize (R7.5 million) generated the greatest income, followed by sugar cane (R3.1 million) and wheat (R1.9 million). Maize and

Province	Area Planted 2005/06 ha			Seventh Estimate / Final Crop 2005/06 Tons		
	White Maize	Yellow Maize	Wheat	White Maize	Yellow Maize	Wheat
Western Cape	0	2 700	302 000	0	27 000	645 000
Northern Cape	12 000	25 000	48 500	126 000	275 000	306 000
Free State	345 000	190 000	380 000	1 311 000	684 000	580 000
Eastern Cape	3 000	10 000	4 000	16 200	56 000	14 500
KwaZulu Natal	32 000	27 000	9 000	172 800	140 400	41 500
Mpumalanga	156 000	180 000	18 000	702 000	783 000	92 000
Limpopo	12 000	5 500	11 000	40 800	15 400	50 000
Gauteng	45 000	20 000	2 500	202 500	80 000	14 000
North West	380 000	107 000	30 000	1 064 000	294 250	162 000
Total	985 000	567 200	805 000	3 635 300	2 355 050	1 905 000

Table 2.3: Area planted and final crop values for white maize, yellow maize and wheat for 2005/06 attributable to each province.

Crops	April '05 to March '06 R million	April '04 to March '05 R million	Change %
Maize	7 482	7 879	-5.0
Wheat	1 940	1 814	6.9
Sugar Cane	3 134	2 460	27.4
Sunflower seed	1 022	1 142	-10.5
Tobacco	204	351	-41.9
All field crops	15 563	16 375	-5.0

Table 2.4: Gross income generated for the major field crops for the period April '05 to March '06 and April 2004 to March 2005 together with the year-on-year percentage change.

wheat accounted for 48% and 12.5% of total field crop income for the period April 2005 to March 2006 respectively.

2.2 SAFEX Agricultural Products

The South African Futures Exchange (SAFEX) Agricultural Markets Division (AMD) was opened in January 1995. It was established as a separate division to the already existing Financial Derivatives Market. The deregulation of the South African market in 1994 made the establishment of an exchange trading grains futures viable.

The AMD began trading white and yellow maize futures in May 1996. In 1997 the exchange introduced a wheat futures contract. Options on all grains traded were introduced in 1998. Today white maize, yellow maize, wheat, soybean and sunflower futures and option contracts are traded on the exchange.

In July 2001 the JSE bought out SAFEX and the Agricultural Derivatives Division was renamed to SAFEX Agricultural Derivatives. The SAFEX branding was retained as the SAFEX name had built up considerable value as a proficient exchange. SAFEX Agricultural Derivatives Division was subsequently renamed the SAFEX Agricultural Products Division (APD).

2.2.1 Futures

Recall, a Futures contract is defined as an obligation to purchase or sell an asset at an agreed-upon price on a specified future date. The long position is held by the trader who commits to purchase. The short position is held by the trader who commits to sell. Futures differ from forward contracts in their standardisation, exchange trading, margin requirements and daily settling (marking to market).

The Safex defines two different types of expiry months for futures contracts, namely hedging months and constanct delivery months. Hedging month futures contracts generally become available for trade one year before their expiration, however they may be introduced earlier should there be a demand for it. Constant delivery months on the other hand become available 20 business days prior to expiry.

The contract specifications of futures contracts traded on the APD are set by the JSE Securities Exchange. An abridged version of the Agricultural Products Division Contract Specifications is presented:

1. **Commodities**
    - White Maize
    - Yellow Maize
    - Wheat
    - Sunflower Seeds
    - Soybean
2. **Contract Unit**
    - White Maize: 100 metric tons
    - Yellow Maize 100 metric tons
    - Wheat: 50 metric tons
    - Sunflower: 50 metric tons
    - Soybean: 25 metric tons
3. **Expiry Months**
    - Hedging months: March, May, July, September and December
    - Constant delivery months: January, February, April, June, August, October and November
    - Hedging months futures contracts are available at all times. Constant delivery month futures become available 20 business days prior to the constant delivery month.
    - The same contract specifications applying to hedging months apply to constant delivery.
    - Note: Only hedging months futures are considered in this study.
4. **Trading Days**
    - All business days are considered trading days for agricultural products, except days deemed by the JSE as non trading days for the market as a whole.
    - The last trading day for a specific contract is defined as the seventh business day preceding the last business day of the expiry month.

- Note: For all modelling purposes the last trading day is regarded as the expiry date.

5. **Margins**
   - Initial margin payable in terms of the contract is determined from time to time by the JSE
   - Initial margin is held until all delivery obligations are met.
   - Variation margin may be required if deemed necessary by the JSE to preserve the security of the contract.

2.2.2 Options

Recall, an option contract gives the purchaser the right to buy or sell the underlying asset at a predetermined time in the future for a predetermined price. A call option is the right to buy the underlying and put option is the right to sell the underlying. The purchaser of an option is said to hold a long position and the seller of an option holds a short position.

Option contracts for agricultural commodities are also traded on the APD. Again, the contract specifications are set by the JSE:

1. **Commodities**
   - White Maize
   - Yellow Maize
   - Wheat
   - Soybean
   - Sunflower Seeds
2. **Underlying Instrument**
   - The underlying instrument is a futures contract on the particular commodity.
3. **Option Type**
   - Options are American in style.
4. **Contract Size**
   - White Maize: 100 metric tons

- Yellow Maize 100 metric tons
- Wheat: 50 metric tons
- Sunflower: 50 metric tons
- Soybean: 25 metric tons

5. **Contract Months**
   - Only options on hedging months are available, i.e.. March, May, July, September and December.
6. **Strike Price**
   - Option strike prices are available in intervals of R20.00 per ton.
7. **Expiry**
   - Close of trade occurs on the fifth last trading day of the month prior to the expiry month of the underlying futures contract.
8. **Exercise**
   - The holder of a long position may exercise at any time prior to and including the expiry date.
9. **Mark-to-Market**
   - The mark-to-market price of the option is calculated from volatility quotes for at-the-money options using the Black options pricing formula.

Chapter 3

Existing Models for Commodity Derivatives

This chapter examines four models for pricing commodity contracts. The models are presented in the chronological order in which they were published. The order thus represents the development of the methods used for pricing commodity derivatives.

The first model examined is the model presented by Black (1975). This model represents the first significant attempt at modelling the specific dynamics of commodities. Black's model is the most widely used model for pricing commodity derivatives.

One particular feature of commodities that differentiates them from other asset classes is the presence of a convenience yield for each particular commodity. The convenience yield of a commodity can be defined as the net "dividend" yield accruing to the holder of the physical commodity. The second model explored is one developed by Gibson & Schwartz (1990) which includes a stochastic convenience yield.

The next model considered is the short-term/long-term model proposed by Schwartz & Smith (2000). This model defines the spot price as the sum of two stochastic factors, one representing the the long-term equilibrium level and the other the short-term deviations in the long-term level.

Finally, a model proposed by Korn (2005) is examined. Korn's model is an extension of the Gibson-Schwartz model where both the stochastic factors are mean-reverting.

3.1 Black's Model

3.1.1 Introduction

Black & Scholes (1973) produced the first pricing formula for stock options that did not depend on arbitrary parameters. Black (1975) extends the methodology used in the Black-Scholes formula to develop a means to value commodity futures, forwards and options.

Black (1975) identifies three fundamental differences between commodities and stocks. Firstly, commodities tend to exhibit a seasonal pattern. The spot price of commodities tends to be high just before a harvest and low just after a harvest. Secondly, commodities do not pay dividends in the same manner that stocks do. However, the convenience yield can be considered as a dividend payable to the holder of the commodity. Finally, commodities need to be stored, and thus a storage cost is associated with commodities.

Commodity markets themselves are very different from stock markets. Trades on commodity exchanges are dominated by futures and, to a lesser extent, options. Trades on stock markets however are dominated the purchasing and selling of stocks at spot prices.

As a result, Black (1975) developed pricing formulae specifically for commodity forward and option contracts in terms of the futures price and other non-arbitrary variables.

3.1.2 Properties of commodity contracts

Three types of commodity contracts need to be defined, namely forward contracts, futures contracts and option contracts.

A forward contract is a contract to buy or sell the underlying asset at a prespecified date in the future for a prespecified price. The prespecified date and price at which the contract is struck are known as the exercise price and expiry date respectively.

A futures contract is similar to a forward contract expect that a futures contract is settled every day and rewritten at the new futures price. A futures contract is like a series of forward contracts. Each day, the previous day's contract is settled, and the current day's contract is written with a contract price equal to the futures price with the same expiry time as the

futures contract.

An option contract gives the holder the right to buy or sell the underlying asset at a prespecified date in the future for a prespecified price. A call option gives the holder the right to purchase the underlying, and a put option gives the holder the right to sell the underlying. The purchaser of the option is said to hold a long position and the seller of the option holds a short position.

Define:

$$\begin{aligned}
t &= \text{observation time,}\\
t_0 &= \text{time of contract initiation,}\\
T &= \text{expiry time,}\\
P_t = P(t) &= \text{spot price of the commodity at time } t,\\
F = F_t(T) = F(t,T) &= \text{futures price at time } t \text{ for expiry at } T,\\
X &= \text{exercise price of forward contract,}\\
K &= \text{exercise price of option contract,}\\
u_t(F) = u(t,F,X,T) &= \text{value of futures contract,}\\
v_t(F) = v(t,F,X,T) &= \text{value of forward contract,}\\
T_1 &= \text{expiry time of option contract,}\\
T_2 &= \text{expiry time of underlying asset,}\\
C_{\mathrm{E},t} = C_{\mathrm{E}}(t,F,K,T_1,T_2) &= \text{value of a European call option,}\\
P_{\mathrm{E},t} = P_{\mathrm{E}}(t,F,K,T_1,T_2) &= \text{value of a European put option.}
\end{aligned}$$

The futures price is defined as the price at which a forward contract has an initial value of 0. Therefore

$$v(t_0,F,X,T) = 0, \tag{3.1}$$

and

$$X = F_t(T). \tag{3.2}$$

At expiry the value of a forward is equal to the futures price minus the price at which the contract is struck:

$$v(T,F,X,T) = F - X. \tag{3.3}$$

The value of a futures contract is reset to 0 every day. Gains and losses are settled at the end of every day. Therefore

$$u_t(F) = 0. \tag{3.4}$$

Equation 3.4 is only valid at the beginning and end of each trading day once the contract has been rewritten. During the course of a trading day the value of a futures contract does not necessarily equal to 0.

An option contract gives the holder the right, not the obligation, to exercise at expiry. For this reason the payoff at expiry for a call option is different to the payoff of a long forward. The payoff of a call option at expiry is:

$$\begin{aligned} C_{\mathrm{E},t}(F, K, T_1, T_2) &= F - K \qquad \text{if } F \geq K \\ &= 0 \qquad \text{if } F < K. \end{aligned} \tag{3.5}$$

The payoff of a put option is:

$$\begin{aligned} P_{\mathrm{E},t}(F, K, T_1, T_2) &= K - F \qquad \text{if } F < K \\ &= 0 \qquad \text{if } F \geq K. \end{aligned} \tag{3.6}$$

3.1.3 Model Assumptions

Black's model makes the following assumptions:

- Markets are efficient.
- There are no taxes or transaction costs.
- The capital asset pricing model (CAPM) holds at each instant of time and all parameters are constant though time.
- There are no dividends or distributions over the period of the contract.
- There are no price limits set by the futures exchange.
- Options can only be exercised at maturity, ie. European type.
- It is possible to borrow and lend at a constant risk-free interest rate.
- Trading in the underlying instrument is continuous.
- The change in the futures price over any time period is log-normally distributed with a known variance, σ^2.

3.1.4 The Behaviour of the Futures Price

The total return to an investor over the duration of a futures contract is a function of the futures price over the same period. Since the net investment of a futures contract is only the initial margin posted, it is inaccurate to refer to the percentage return. Rather the expected return must be defined in nominal terms.

The usual CAPM formula is:

$$\mathrm{E}(R_i) - R_f = \beta_i[\mathrm{E}(R_m) - R_f], \tag{3.7}$$

where

$$\begin{aligned} R_i &= \text{return on asset } i, \\ R_f &= \text{risk-free rate}, \\ R_m &= \text{return on the market portfolio}, \\ \beta_i &= \text{measure of systematic risk of asset } i \\ &= \frac{\mathrm{Cov}(R_i, R_m)}{\mathrm{Var}(R_m)}. \end{aligned}$$

The market portfolio referred to above is purely theoretical. It is assumed to include all corporate securities, personal assets and assets held by non-corporate businesses. Commodity contracts however are not included in the market portfolio. For every commodity contract there is both a long position and a short position. Thus when summing all commodity contracts together, they net to 0.

Equation 3.7 can be rearranged in terms of an assets starting and ending price. Let P_{i0} denote the starting price of asset i and P_{i1} the ending price.

$$\mathrm{E}[\frac{(P_{i1} - P_{i0})}{P_{i0}}] - R_f = \frac{\mathrm{Cov}[(P_{i1} - P_{i0})/P_{i0}, R_m]}{\mathrm{Var}(R_m)}[\mathrm{E}(R_m) - R_f]. \tag{3.8}$$

Multiplying through by P_{i0}:

$$\mathrm{E}[(P_{i1} - P_{i0})] - R_f P_{i0} = \frac{\mathrm{Cov}[(P_{i1} - P_{i0}), R_m]}{\mathrm{Var}(R_m)}[\mathrm{E}(R_m) - R_f]. \tag{3.9}$$

Now, since the value a futures contract is equal to 0 at initiation, P_{i0} is set to 0. At the end of the period, before the contract is reset, the value of the futures contract is equal to the change in the futures price over the period.

Thus P_{i1} is equal to ΔP.

Now, equation 3.9 can be written as:

$$\begin{aligned} \mathrm{E}[\Delta P] &= \frac{\mathrm{Cov}[(\Delta P), R_m]}{\mathrm{Var}(R_m)}[\mathrm{E}(R_m) - R_f] \\ &= \beta^*[\mathrm{E}(R_m) - R_f]. \end{aligned} \tag{3.10}$$

Where β^* can be regarded as the 'nominal beta' of the futures price.

Equation 3.10 implies that the expected change in the futures price is a function of β^* and the expected market premium, $\mathrm{E}(R_m) - R_f$.

If $\beta^* = 0$, the expected change in the futures price will equal 0. β^* will equal 0 if $\mathrm{Cov}[(\Delta P), R_m]$ equals 0. Recall, commodity contracts can be regarded as bets on the movement of the underlying asset. Commodity contracts are not included in the market portfolio, thus it is reasonable to assume that changes in commodity futures prices are not associated with movements in the market portfolio. $\mathrm{Cov}[(\Delta P), R_m]$ will not exactly equal 0, but it may be approximately equal to 0. Therefore:

$$\mathrm{E}[\Delta P] \approx 0, \qquad \text{when} \qquad \mathrm{Cov}[(\Delta P), R_m] \approx 0. \tag{3.11}$$

3.1.5 Pricing Forwards and Options

Option Contracts

The derivation of the price of commodity options follows the same methodology used in the derivation stock options by Black & Scholes (1973).

Consider a call option. The first step requires the construction of a portfolio constituting a long position in a call option and a short position in $\frac{\partial}{\partial F}C_{\mathrm{E},t}(F)$ futures contracts, with the same dates of expiry. This portfolio is considered riskless, as a movement in the price of the underlying futures contract results in movements in the two positions which are equal in size but opposite in direction.

The change in value of the portfolio over any arbitrary short time interval Δt is:

$$\Delta C_{\mathrm{E}} - C_{\mathrm{E}}^{1}\Delta F, \tag{3.12}$$

where

$$C_{\mathrm{E}}^{1}(F) = C_{\mathrm{E}}^{1} \;=\; \frac{\partial}{\partial F}C_{\mathrm{E}}(F). \tag{3.13}$$

Let r denote the continuously compounded risk free rate. Since the portfolio is riskless the change in the value of the portfolio over the interval Δt should be proportional to the risk free rate r. The size of the equity position of the portfolio is simply the value of the position in the option contract, as the value of a futures contract is always 0.

Thus, the change in the portfolio value over the interval Δt is equal to $C_{\mathrm{E}} r \Delta t$. i.e.

$$\Delta C_{\mathrm{E}} - C_{\mathrm{E}}^{1}\Delta F = C_{\mathrm{E}} r \Delta t. \tag{3.14}$$

ΔC_{E} can now be expanded:

$$\begin{aligned} \Delta C_{\mathrm{E}} &= C_{\mathrm{E}}(F + \Delta F, t + \Delta t) \\ &= \vdots \\ &= C_{\mathrm{E}}^{1}\Delta x + \frac{1}{2}C_{\mathrm{E}}^{11}\sigma^2 F^2 \Delta t + C_{\mathrm{E}}^{2}\Delta t, \end{aligned} \tag{3.15}$$

where

$$C_{\mathrm{E}}^{11} \;=\; \frac{\partial^2}{\partial F \partial t}C_E(t, F), \tag{3.16}$$

$$C_{\mathrm{E}}^{2} \;=\; \frac{\partial^2}{\partial t^2}C_E(t, F). \tag{3.17}$$

$$\tag{3.18}$$

Substituting 3.14 into 3.15:

$$C_{\mathrm{E}}^{1}\Delta F + \frac{1}{2}C_{\mathrm{E}}^{11}\sigma^2 F^2 \Delta t + C_{\mathrm{E}}^{2}\Delta t - C_{\mathrm{E}}^{1}\Delta F = C_{\mathrm{E}} r \Delta t. \tag{3.19}$$

Simplifying and dividing through by Δt results in the following differential equation:

$$C_{\mathrm{E}}^{2} = rC_{\mathrm{E}} - \frac{1}{2}\sigma^2 F^2 C_{\mathrm{E}}^{11}. \tag{3.20}$$

The boundary condition for this equation is:

$$\begin{aligned} C_{\mathrm{E}}(F, T_1) &= F - K \qquad \text{if } F \geq K \\ &= 0 \qquad \text{if } F < K. \end{aligned} \tag{3.21}$$

Solving equations 3.20 and 3.21, the following formula for the value of a call option is obtained:

$$C_{\mathrm{E},t}(F, K, T_1, T_2) = e^{-r(T_1 - t)}[FN(d_1) - KN(d_2)], \tag{3.22}$$

where

$$d_1 = \frac{\ln\frac{F}{K} + \frac{\sigma^2}{2}(T_1 - t)}{\sigma\sqrt{T_1 - t}}, \tag{3.23}$$

$$d_2 = \frac{\ln\frac{F}{K} - \frac{\sigma^2}{2}(T_1 - t)}{\sigma\sqrt{T_1 - t}}, \tag{3.24}$$

$$\begin{aligned} F &= F_t(T_2), \\ N(x) &= \text{standard normal cumulative distribution} \\ &= \frac{1}{\sqrt{2\pi}} \int_{-\infty}^{x} e^{-\frac{t^2}{2}} dt. \end{aligned}$$

The value of a put option can be derived using the same methodology just with different boundary conditions:

$$P_{\mathrm{E},t}(F, K, T_1, T_2) = e^{-r(T_1 - t)}[KN(-d_2) - FN(-d_1)]. \tag{3.25}$$

Equations 3.22 and 3.25 represent the values of European type options. These options may only be exercised at expiry. The value of American type options, those that may be exercised at any point in time prior to and including expiry, are much more difficult to calculate. Black (1975) does not consider American options but merely states that their value depends on, among other things, the spot price and futures price at various transaction dates prior to expiry.

Forward Contracts

The derivation of the value of a forward contract follows the same methodology used in the derivation of option values.

The differential equation that needs to be satisfied is essentially the same, replacing $C_{\mathrm{E},t}(F)$ with $v_t(F)$. The differential equation becomes:

$$v^2 = rv - \frac{1}{2}\sigma^2 x^2 v^{11}. \tag{3.26}$$

The boundary conditions are:

$$\begin{aligned} v_T(F) &= F - X, \\ v_{t_0}(F) &= 0. \end{aligned} \tag{3.27}$$

Solving equations 3.26 and 3.27 results in the expression for the value of a forward contract at any time $t_0 \leq t \leq T$:

$$v_t(F, X, T) = (F - X)e^{-r(T-t)}. \tag{3.28}$$

3.1.6 Model Limitations

The assumption that investors can borrow and lend at a constant risk-free rate of interest, R_f, is unrealistic. Firstly, interest rates can fluctuate fairly regularly especially when central banks alter lending rates as part of their monetary policy. Secondly, investors generally borrow at a higher rate than at which they lend.

The volatility of the underlying, σ^2, is assumed to be constant and known throughout the term of the contract. In reality, the actual volatility of the futures contract over the term of the option is unknown and cannot be observed at the outset of the contract. Investors can consider either historical volatility or implied volatility. Historical volatility is a measure of the variance of the price of futures in the past. Choosing the period to measure volatility and whether or not past variance is a good measure of future variance are issues that need to be considered. Implied volatility on the other hand is volatility measure assuming the market price is equal to the theoretical price.

Historical distributions of futures prices often depart significantly from a lognormal distribution. Historical prices/returns often show fatter tails which imply that dramatic moves occur with greater frequency.

3.2 The Gibson-Schwartz Model

3.2.1 Introduction

According to Brennan (1986) and Fama and French (1987, 1988), the convenience yield of a commodity is a key determinant of the relationship between

future prices and spot prices.

Gibson & Schwartz (1990) extend this notion by including a stochastic convenience in a two-factor contingent claims pricing model. The Gibson-Schwartz model was first applied to the case of oil futures but can be extended to all commodities that exhibit a convenience yield.

At the time of publishing, the Gibson-Schwartz model had no closed form solutions for the values of futures and option contracts. It was not until Jamshidian & Fein (1990) and Bjerksund (1991) found the solution to the partial differential equation that futures and option contracts need to satisfy, that a closed form solution could be obtained. Schwartz (1997) presents the model with closed form solutions for the values of futures and option contracts.

3.2.2 Model Assumptions

- The risk-free rate of interest rate is deterministic.
- The instantaneous convience yield and the market price of convience yield are known and constant throughout term of the contract.

3.2.3 The Pricing Model

The dynamics of the Gibson-Schwartz model are defined as follows:

$$\frac{dP_t}{P_t} = (\mu - \delta)dt + \sigma_1 dW_{1t}, \tag{3.29}$$

$$d\delta = \kappa(\alpha - \delta)dt + \sigma_2 dW_{2t}, \tag{3.30}$$

where

$$\begin{aligned}
P = P_t &= \text{commodity spot price at time } t,\\
\delta &= \text{instantaneous convenience yield},\\
\kappa &= \text{mean-reversion coefficient},\\
\mu, \alpha &= \text{drift parameters},\\
\sigma_1, \sigma_2 &= \text{volatility parameters},\\
dW_{1t}, dW_{2t} &= \text{correlated increments of standard Brownian motion},\\
dW_{1t}dW_{2t} &= \rho dt,\\
\rho &= \text{correlation between 2 Brownian processes.}
\end{aligned}$$

By letting $p_t = \ln P_t$ and applying Ito's Lemma, the instantaneous change in p_t can be written as:

$$dp_t = (\mu - \delta - \frac{1}{2}\sigma_1^2)dt + \sigma_1 dW_{1t}. \tag{3.31}$$

In order to derive pricing formulae for contingent claims, the 'risk-neutral' environment must be considered. The dynamics of the model under the risk-neutral measure Q can be expressed as:

$$\begin{aligned} dP_t &= P_t(r-\delta)dt + \sigma_1 P_t dW_{1t}^Q, && (3.32)\\ d\delta &= [\kappa(\alpha-\delta) - \lambda]dt + \sigma_2 dW_{2t}^Q, && (3.33)\\ dW_{1t}^Q dW_{2t}^Q &= \rho dt. && (3.34) \end{aligned}$$

where λ denotes the market price per unit of convenience yield risk. dW_{1t}^Q and dW_{2t}^Q are increments of a standard Brownian motion process under the risk-neutral measure Q.

Let $F_t(P, \delta, T)$ denote the price of a futures contract at time t for expiry at time T.

By assuming the standard perfect market assumptions, it can be shown that the futures price must satisfy the following partial differential equation (PDE):

$$\frac{1}{2}F_{PP}P^2\sigma_1^2 + \frac{1}{2}F_{\delta\delta}\sigma_2^2 + F_{P\delta}P\rho\sigma_1\sigma_2 + F_P P(r-\delta) + F_\delta(\kappa(\alpha-\delta) - \lambda) - F_\tau = 0, \tag{3.35}$$

subject to the boundary condition:

$$F_t(P, \delta, t) = P_t. \tag{3.36}$$

The solution to 3.35 and 3.36, as shown by Jamshidian & Fein (1990) and Bjerksund (1991), is:

$$F_t(P, \delta, T) = S_t \exp[-\delta\frac{(1 - e^{-\kappa(T-t)})}{\kappa} + A(T-t)]. \tag{3.37}$$

Expressed as a log:

$$\ln F(P, \delta, t, T) = \ln P - \delta\frac{(1 - e^{-\kappa(T-t)})}{\kappa} + A(T-t), \tag{3.38}$$

where

$$\begin{aligned} A(T-t) &= (r-\hat{\alpha}+\frac{1}{2}\frac{\sigma_2^2}{\kappa^2}-\frac{\sigma_1\sigma_2\rho}{\kappa})(T-t)+\frac{1}{4}\sigma_2^2\frac{(1-e^{-2\kappa(T-t)})}{\kappa^3} \\ &\quad +(\hat{\alpha}\kappa+\sigma_1\sigma_2\rho-\frac{\sigma_2^2}{\kappa})\frac{(1-e^{-\kappa*(T-t)})}{\kappa^2}, \qquad (3.39) \\ \hat{\alpha} &= \alpha-\frac{\lambda}{\kappa}. \end{aligned}$$

Similarly, the prices of European call and put options, with strike price K and underlying asset F, can be obtained, subject to the following boundary conditions:

$$C_{\mathrm{E},T}(F,\delta,T)=\max[0,F-K], \qquad (3.40)$$

$$P_{\mathrm{E},T}(F,\delta,T)=\max[0,K-F], \qquad (3.41)$$

where $C_{\mathrm{E},T}(F,\delta,T)$ and $P_{\mathrm{E},T}(F,\delta,T)$ denote the values of call and put options at expiry respectively.

3.2.4 Model Limitations

The assumption of a constant interest rates is unrealistic. For longer time horizons the uncertainty about future interest rates becomes more significant. Non-stochastic interest rates also imply that futures and forward prices are always equal.

Black's model contained only one parameter that is not directly observable in the market, namely volatility σ^2. The addition of numerous non-observable parameters in the Gibson-Schwarz model namely, the instantaneous convenience yield δ, the mean-reversion coefficient κ, the drift parameters μ, α, the volatility parameters σ_1, σ_2, and the correlation ρ greatly increase the complexity of the model. All these paramaters need to be estimated using historical data. Fitting the model to past data and using maximum likelihood estimation is required to generate estimates for these parameters.

The addition of complexity has a number of drawbacks. Firstly a large sample of data is required to produce accurate and meaningful estimates. These estimates will be based on past data and one needs to assess whether

or not these estimates are likely to persist in the future. Another consideration is the choice of the sample period used to produce the estimates. Finally, greater computing power is required to produce estimates for large sample sizes especially when running similations, such as Monte Carlo simulations, to measure the reliability of these estimates. However the issue of computing power is becoming less of an issue as computers have become more powerful and more freely available.

The above comments on model complexity due to the increased number of parameters apply to next two model discussed as well.

3.3 The Short-Term/Long-Term Model

3.3.1 Model Dynamics

The short-term/long-term model was proposed by Schwartz & Smith (2000). It is a simple two-factor model that allows for mean-reversion in short-term prices and uncertainty in the long-term equilibrium level to which the prices revert.

The intuition behind this model is that long-dated futures contracts provide information about the equilibrium level, and differences between the prices of long- and short-dated contracts provide information about short-term movements in prices.

The model is defined as follows:

Assume the logarithm of the spot price can be decomposed as the sum of two stochastic factors:

$$p_t = \ln(P_t) = x_t + z_t, \tag{3.42}$$

where

$$\begin{aligned} P_t &= \text{commodity spot price at time } t, \\ x_t &= \text{equilibrium price level}, \\ z_t &= \text{short-term deviation in prices.} \end{aligned}$$

x_t and z_t are known as the state variables of the model. They are stochastic factors and have the following dynamics:

$$dx_t = \mu_x dt + \sigma_x dW_{1t}, \tag{3.43}$$
$$dz_t = -\kappa z_t dt + \sigma_z dW_{2t}, \tag{3.44}$$

where

dW_{1t}, dW_{2t} = correlated increments of a standard Brownian motion,
$dW_{1t}dW_{2t}$ = $\rho_{xz}dt$,
κ = mean-reversion coefficient,
σ_x, σ_z = volatility coefficients,
μ_x = equilibrium drift rate.

3.3.2 Model Assumptions

- The equilibrium level process, x_t, follows a geometric Brownian motion with drift μ_x.
- The short-term deviation, z_t, follows an Ornstein-Uhlenbeck process that reverts to 0.
- The mean-reversion coefficient, κ, the volatility coefficients σ_x, σ_z, and the drift rate, μ_x, are constant throughout the term of the contract.

3.3.3 Pricing Futures and Options

The dynamics of x_t and z_t under the risk neutral measure Q become:

$$dx_t = (\mu_x - \lambda_x)dt + \sigma_x dW_{1t}^Q, \tag{3.45}$$
$$dz_t = (-\kappa z_t - \lambda_z)dt + \sigma_z dW_{2t}^Q, \tag{3.46}$$

where λ_x and λ_z denote the market price of risk for the state variables x_t and z_t respectively. dW_{1t}^Q and dW_{2t}^Q are the usual increments of a standard Brownian motion process under the risk-neutral measure Q, and $dW_{1t}^Q dW_{2t}^Q = \rho_{xz}dt$.

Before proceeding, values of $\mathrm{E}^*[p_t]$ and $\mathrm{Var}^*[p_t]$ must to be obtained. $\mathrm{E}^*[p_t]$ and $\mathrm{Var}^*[p_t]$ denote the expected value and variance of p_t under the risk-neutral measure respectively. These values will be used in the derivation of the futures and option prices.

x_t and z_t are jointly normally distributed with mean and variance:

$$\mathrm{E}^* \begin{bmatrix} x_t \\ z_t \end{bmatrix} = \begin{bmatrix} x_0 + (\mu - \lambda_x)t \\ e^{-\kappa t} z_0 - \frac{(1-e^{-\kappa t})}{\kappa}\lambda_z \end{bmatrix}, \tag{3.47}$$

$$\mathrm{Cov}^* \begin{bmatrix} x_t \\ z_t \end{bmatrix} = \begin{bmatrix} \sigma_x^2 t & (\frac{1-e^{-\kappa t}}{\kappa})\rho_{xz}\sigma_x\sigma_z \\ (\frac{1-e^{-\kappa t}}{\kappa})\rho_{xz}\sigma_x\sigma_z & \frac{(1-e^{-2\kappa t})}{2\kappa}\sigma_z^2 2\kappa \end{bmatrix}. \tag{3.48}$$

Since $\ln(P_t) = x_t + z_t$ is a linear function of normally distributed variables, $\ln(P_t)$ is itself normally distributed with mean and variance:

$$\mathrm{E}^*[p_t] = x_0 + e^{-\kappa t} z_0 + (\mu - \lambda_x)t - \frac{(1 - e^{-\kappa t})}{\kappa}\lambda_z, \tag{3.49}$$

$$\mathrm{Var}^*[p_t] = \sigma_x^2 t + \frac{(1 - e^{-2\kappa t})}{2\kappa}\sigma_z^2 + 2(\frac{1 - e^{-\kappa t}}{\kappa})\rho_{xz}\sigma_x\sigma_z. \tag{3.50}$$

Futures Contracts

The value of expressing the model dynamics under a risk-neutral framework is that the value of any contingent claim can be determined as the expected future claim. Thus the futures price of a commodity is equal to the expected future spot price of the commodity under the risk-neutral measure.

Let $F_t(T)$ denote the price of a futures contract at time t expiring at time T.

$$\begin{aligned} \ln[F_t(T)] &= \ln[\mathrm{E}^*(P_T)|\mathcal{F}_t] \\ &= \mathrm{E}^*[\ln(P_T)|\mathcal{F}_t] + \frac{1}{2}\mathrm{Var}^*[\ln(P_T)|\mathcal{F}_t] \\ &= x_t + e^{-\kappa(T-t)} z_t + A(T-t), \end{aligned} \tag{3.51}$$

where

$$\begin{aligned} A(T-t) &= (\mu - \lambda_x)(T-t) - \frac{(1 - e^{-\kappa(T-t)})}{\kappa}\lambda_z \\ &\quad + \frac{1}{2}[\sigma_x^2(T-t) + \frac{(1 - e^{-2\kappa(T-t)})}{2\kappa}\sigma_z^2 \\ &\quad + 2(\frac{1 - e^{-\kappa(T-t)}}{\kappa})\rho_{xz}\sigma_x\sigma_z]. \end{aligned} \tag{3.52}$$

Option Contracts

Again, the risk-neutral approach is used to derive pricing formula for the value of option contracts. The value of an option is derived by discounting the expected payoff under the risk-neutral measure at the risk free rate. In this case, option contracts refers to European type options where the underlying asset is a futures contract.

The mean and variance of $\ln^*[F_t(T)]$ is needed. Recall, equation 3.51 is a linear function of the state variables x_t and z_t, which have been shown to be jointly normally distributed. Hence, $\ln^*[F_t(T)]$ is also normally distributed with mean and variance:

$$\begin{aligned} \mathrm{E}^*[\ln[F_t(T)]] &= \mathrm{E}^*[x_t] + e^{-\kappa(T-t)}\mathrm{E}^*[z_t] + A(T-t) \\ &= x_0 + (\mu - \lambda_x)t + e^{-\kappa(T-t)}z_0 + A(T-t), \end{aligned} \tag{3.53}$$

$$\begin{aligned} \mathrm{Var}^*[\ln[F_t(T)]] &= \mathrm{Var}^*[x_t] + e^{-2\kappa(T-t)}\mathrm{Var}^*[z_t] \\ &\quad + 2e^{-2\kappa(T-t)}\mathrm{Cov}^*[x_t, z_t] \\ &= \sigma_x^2 t + e^{-2\kappa(T-t)}\frac{(1-e^{-2\kappa t})}{2\kappa}\sigma_z^2 \\ &\quad + 2(\frac{1-e^{-\kappa t}}{\kappa})\rho_{xz}\sigma_x\sigma_z. \end{aligned} \tag{3.54}$$

A closed form expression for the value of a European option can now be calculated.

Let $C_{E,t}(T_1, T_2) = C_{E,t}(F, T_1, T_2, K..)$ denote the value of a European call option on a future at time t. The option expires at time T_1 and the underlying futures contract expires at time T_2. The strike price of the option is K. Likewise, let $P_{E,t}(T_1, T_2)$ denote the value of a European put option.

$$\begin{aligned} C_{\mathrm{E},t} &= e^{-r(T_1-t)}\mathrm{E}^*[\max[F_t(T_2) - K, 0]] \\ &= e^{-r(T_1-t)}[F_t(T_2)N(d_1) - KN(d_2)], \end{aligned} \tag{3.55}$$

$$\begin{aligned} P_{\mathrm{E},t} &= e^{-r(T_1-t)}\mathrm{E}^*[\max[K - F_t(T_2), 0]] \\ &= e^{-r(T_1 t)}[KN(-d_2) - F_t(T_2)N(-d_1)], \end{aligned} \tag{3.56}$$

where

$$d_1 = \frac{\ln(F_t(T_2)/K)}{\sqrt{\text{Var}^*[\ln(F_t(T_2)]}} + \frac{1}{2}\sqrt{\text{Var}^*[\ln(F_t(T_2))]}, \tag{3.57}$$

$$d_2 = \frac{\ln(F_t(T_2)/K)}{\sqrt{\text{Var}^*[\ln(F_t(T_2))]}} - \frac{1}{2}\sqrt{\text{Var}^*[\ln(F_t(T_2))]}. \tag{3.58}$$

3.3.4 Model Limitations

The long-term equilibrium level is non-stationary. For certain instruments and for longer time horizons a stationary process for the equilibrium process would be more accurate.

There are many coefficients that are assumed constant where a stochastic nature would be more accurate. However the value of the increase in accuracy may not justify the addition of complexity.

3.4 Korn's Model

Korn (2005) extends the short-term long-term model by Schwartz & Smith (2000) by allowing for two mean-reverting stochastic factors. The implication of this model is that both the spot and futures price can be stationary. Korn (2005) shows that this model works just as well for short-term contracts but leads to an improvement in valuing longer-term contracts.

3.4.1 Model Dynamics

The spot price, P_t, is defined as follows:

$$\ln P_t = p_t = \frac{\kappa}{\kappa - \gamma} x_t + z_t - \frac{\gamma\theta}{\kappa - \gamma}, \tag{3.59}$$

where

$$\begin{aligned} x_t &= \text{long-term price level,} \\ z_t &= \text{short-term deviations from long-term level,} \\ dx_t &= \gamma(\theta - x_t)dt + \sigma_x dW_{1t}, \qquad (3.60) \\ dz_t &= -\kappa z_t dt + \sigma_z dW_{2t}. \qquad (3.61) \end{aligned}$$

The parameters γ and κ represent mean-reversion coefficients of the state variables x_t and z_t respectively. σ_x and σ_z are volatility parameters and

$dW_{1t}dW_{2t} = \rho_{xz}dt$. Finally θ denotes the stationary mean of x_t.

The Korn model represents a reduced form affine two-factor model where both stochastic factors are mean-reverting.

3.4.2 Pricing Futures

The standard methodology for deriving prices of contingent claims is followed. The dynamics of the state variables need to be expressed under a risk-neutral measure. This involves the introduction of two new parameters, namely the market of risk for x_t, λ_x, and the market price of risk for z_t, λ_z.

The risk-neutral dynamics become:

$$dx_t = -\gamma(x_t - \theta + \frac{\lambda_x}{\gamma})dt + \sigma_x dW_{1t}^Q, \tag{3.62}$$

$$dz_t = -\kappa(z_t + \frac{\lambda_z}{\kappa})dt + \sigma_z dW_{2t}^Q. \tag{3.63}$$

Now, the futures price, F, equals the expected future spot price under risk-neutral measure. As usual, let $F_t(T)$ denote the futures price at time t for expiry at time T.

$$F_t(T) = exp[\frac{\kappa}{\kappa - \gamma}e^{-\gamma(T-t)}x_t + e^{-\kappa T}z_t + A(T-t)], \tag{3.64}$$

where

$$\begin{aligned} A(T-t) = & \frac{\kappa}{\kappa - \lambda}[(1 - e^{-\gamma(T-t)})(\theta - \frac{\lambda_x}{\gamma})] - \frac{\gamma\theta}{\kappa - \gamma} - (1 - e^{-\kappa(T-t)})\frac{\lambda_z}{\kappa} \\ & + \frac{\kappa^2}{(\kappa - \gamma)^2}(1 - e^{-2\gamma(T-t)})\frac{\sigma_x^2}{4\gamma} + (1 - e^{-2\kappa(T-t)})\frac{\sigma_z^2}{4\kappa} \\ & + \frac{\kappa}{\kappa - \gamma}(1 - e^{-(\kappa+\gamma)(T-t)})\frac{\rho_{xz}\sigma_x\sigma_z}{\kappa + \gamma}. \end{aligned} \tag{3.65}$$

3.4.3 Model Limitations

Korn's model is shown to produce better results for longer-term contracts. However, most traded futures and options contracts are short-dated. Hence it can be argued that the added complexity is not justified.

Chapter 4

The Sørensen Model

This chapter presents the specifications of the Sørensen model. The dynamics of the model are discussed and the resulting properties are investigated. Finally, prices for commodity futures and options on commodity futures are derived.

The Sørensen model is the basis for all empirical tests conducted throughout this study. The properties of white maize, yellow maize and wheat futures are investigated assuming the futures prices are determined by the Sørensen model.

4.1 Model Dynamics

Let P_t be the commodity spot price at time t. The (natural) logarithm of P_t, $p_t = \ln P_t$, is modelled and is decomposed into three parts:

$$p_t = s(t) + x_t + z_t, \tag{4.1}$$

where

$$s(t) = \sum_{k=1}^{K} (\gamma_k \cos(2\pi kt) + \gamma_k^* \sin(2\pi kt)). \tag{4.2}$$

x_t and z_t have dynamics:

$$dx_t = (\mu - \frac{1}{2}\sigma^2)dt + \sigma dW_{1t}, \tag{4.3}$$

$$dz_t = -\kappa z_t dt + \nu dW_{2t}. \tag{4.4}$$

dW_{1t} dW_{2t} are correlated increments of standard Brownian motion processes with constant correlation coefficient , i.e $\rho = dW_{1t}dW_{2t}$ .The filtration generated by the two-dimensional Brownian process is assumed to describe all

the available information in the economy.

$s(t)$ denotes the seasonal component of the model. K represents the number of term in the summation. t is measured in years. Hence the first term repeats itself yearly, the second term repeats itself twice per annum and so on. γ_k and γ_k^* are constant parameters, hence $s(t)$ is deterministic. By varying the parameters K, γ_k and γ_k^*, the seasonal component $s(t)$ can take any form. $s(t)$ is the Fourier series suggested by Hannan, Turrel and Tuckwell (1970).

x_t follows a non-stationary Wiener process. μ and σ are constant drift parameters. x_t reflects the equilibrium level of the commodity prices. Changes in x_t represent permanent prices changes caused by permanent changes in demand and/or supply.

z_t follows an Ornstein-Uhlenbeck process with constant parameters κ and ν. κ is regarded to as the mean-reversion coefficient. κ determines the rate at which the process reverts to 0. z_t reflects short-term deviations from the equilibrium level x_t. Changes in z_t represent temporary changes in prices caused by unexpected 'shocks' to demand and/or supply. An example might be unusual weather that affects crop levels.

x_t and z_t are referred to as the state variables of the model. They are unobservable but, as will be shown, can be estimated from the futures prices. Intuitively, movements in prices for long-maturity contracts provide information about the equilibrium price level. According to Schwartz and Smith (2000) the difference between prices for long- and short- maturity contracts provides information about short-term variations in prices.

The joint distribution of the state variables x_t and z_t is stated in appendix A. The distribution of the state variables can be used to forecast future spot prices.

Given x_0 and z_0, $(x_t, z_t)'$ is jointly normally distributed with mean vector and covariance matrix:

$$\mathrm{E}\begin{bmatrix} x_t \\ z_t \end{bmatrix} = \begin{bmatrix} x_0 + t(\mu - \frac{1}{2}\sigma^2) \\ e^{-\kappa t} z_0 \end{bmatrix}, \tag{4.5}$$

$$\mathrm{Cov}\begin{bmatrix} x_t \\ z_t \end{bmatrix} = \begin{bmatrix} \sigma^2 t & (\frac{1-e^{-\kappa t}}{\kappa})\rho\sigma\nu \\ (\frac{1-e^{-\kappa t}}{\kappa})\rho\sigma\nu & (\frac{1-e^{-2\kappa t}}{2\kappa})\nu^2 \end{bmatrix}. \tag{4.6}$$

Since p_t is a linear function of the state variables x_t and z_t, p_t is itself normally distributed with mean and variance:

$$\mathrm{E}[p_t] = x_0 + t(\mu - \frac{1}{2}\sigma^2) + e^{-\kappa t}z_0 + s(t), \tag{4.7}$$

$$\mathrm{Var}[p_t] = \sigma^2 t + (\frac{1 - e^{-2\kappa t}}{2\kappa})\nu^2 + 2(\frac{1 - e^{-\kappa t}}{\kappa})\rho\sigma\nu. \tag{4.8}$$

This is a key result. Given the dynamics of the state variable in equation 4.3 and 4.4, as well as the initial values x_0 and z_0, the distribution of the log of spot price can been derived.

Equation 4.7 shows that the expectation of p_t is a function of the initial state variables x_0 and z_0, the mean reversion coefficient κ, drift coefficient μ, standard deviation σ, as well as time t. The term $(\mu - \frac{1}{2}\sigma^2)$ can be regarded as the expected growth rate of the (ln-) spot price p_t. The term $e^{-\kappa t}$ approaches 0 as t gets larger and can be thought of as the effect of the short term deviation at time 0 on the expected price at time t. The further the forecast, the less the significance of the initial deviation z_0.

Since $p_t = \ln P_t$ is normally distributed, the spot price P_t is log normally distributed. The expectation of P_t is given by:

$$\mathrm{E}[P_t] = e^{\mu t} exp\{x_0 + s(t) + e^{-\kappa t}z_0 + \frac{1}{2}[(\frac{1 - e^{-2\kappa t}}{2\kappa})\nu^2 + 2(\frac{1 - e^{-\kappa t}}{\kappa})\rho\sigma\nu]\}. \tag{4.9}$$

From the expectation it can be seen that the spot price is expected to grow at rate μ. This gives insight as into the choice of the drift term $(\mu - \frac{1}{2}\sigma^2)$ in the dynamics of x_t.

Equations 4.7 and 4.9 give expectations of p_t and P_t conditional on information at time 0 respectively. i.e. $\mathrm{E}[p_t|\mathcal{F}_0]$ and $\mathrm{E}[P_t|\mathcal{F}_0]$, where $\mathcal{F}_0$ is the filtration at time 0.

These expectations can be extended to $\mathrm{E}[p_t|\mathcal{F}_s]$ and $\mathrm{E}[P_t|\mathcal{F}_s]$, where $t > s$ and $\mathcal{F}_s$ is the filtration at time s. $\mathcal{F}_s = \sigma(\mathcal{F}_u : 0 \leq u \leq s)$ is the usual sigma algebra which denotes all available information at time s. $\mathrm{E}[p_t|\mathcal{F}_s]$ is the expected value of p_t given all information up to and including time s, i.e.. assuming all parameters including x_s and z_s are known at time s

The forecast of the (ln-) spot price p_t at time s, as well as the variance of the forecast, is given by $\mathrm{E}[p_t|\mathcal{F}_s]$ and $\mathrm{Var}[p_t|\mathcal{F}_s]$:

$$\mathrm{E}[p_t|\mathcal{F}_s] = x_s + (t-s)(\mu - \frac{1}{2}\sigma^2) + e^{-\kappa(t-s)}z_s + s(t), \tag{4.10}$$

$$\mathrm{Var}[p_t|\mathcal{F}_s] = \sigma^2(t-s) + (\frac{1-e^{-2\kappa(t-s)}}{2\kappa})\nu^2 + 2(\frac{1-e^{-\kappa(t-s)}}{\kappa})\rho\sigma\nu. \tag{4.11}$$

Likewise, the expectation of the spot price P_t given information up to and including time s is:

$$\begin{aligned}\mathrm{E}[P_t|\mathcal{F}_s] &= e^{\mu(t-s)}exp\{x_s + s(t) + e^{-\kappa(t-s)}z_s + \\ &\quad \frac{1}{2}[(\frac{1-e^{-2\kappa(t-s)}}{2\kappa})\nu^2 + 2(\frac{1-e^{-\kappa(t-s)}}{\kappa})\rho\sigma\nu]\}. \end{aligned}\tag{4.12}$$

When comparing equations 4.7 and 4.9 to equations 4.10 and 4.12 it can be seen that the drift and mean reversion terms are the same. The difference in the equations is caused by the different forecast periods and the different starting values of the state variables. Forecasting from time 0 to t implies a forecast period of $t-0=t$ with initial state variables x_0 and z_0. Forecasting from time s to t has a forecast period of $t-s$ and starting state variables x_s and z_s. Intuitively, one would expect the variance of the forecast to reduce with a reduced forecast period. This is confirmed by comparing equation 4.8 to 4.11.

Equations 4.10, 4.11 and 4.12 can be updated further if it assumed that the parameters μ, σ, κ, ρ, ν are not constant over time.

4.2 Risk-Neutral Processes and Valuation

4.2.1 Risk-Neutral Dynamics

In order to value futures contracts using risk-neutral valuation, one needs to develop a 'risk-neutral' version of the model. The state variable dynamics become:

$$dx_t = (\mu - \lambda_x - \frac{1}{2}\sigma^2)dt + \sigma dW_{1t}^Q, \tag{4.13}$$

$$dz_t = -(\lambda_z + kz_t)dt + \nu dW_{2t}^Q. \tag{4.14}$$

W_{1t}^Q and W_{2t}^Q are Wiener processes under the risk-neutral measure Q. Once again, the correlation between the 2 processes is constant, i.e.. $dW_{1t}^Q dW_{2t}^Q =$

ρdt.

Two new parameters have been introduced in the dynamics above, namely λ_x and λ_z. They represent constant market prices of risk associated with x_t and z_t respectively. In essence they reduce the drift of x_t and z_t. The drift of x_t under the risk-neutral measure Q is now $\mu - \lambda_x - \frac{1}{2}\sigma^2$ as apposed to its real world drift of $\mu - \frac{1}{2}\sigma^2$. z_t now follows an Ornstein-Uhlenbeck process that reverts to $-\lambda_z/\kappa$ instead of 0.

Under these new dynamics, the distributions of p_t and P_t can be derived. The full derivation is presented in appendix A.

$p_t|\mathcal{F}_s$ follows a normal distribution with mean and variance:

$$\mathrm{E}^*[p_t|\mathcal{F}_s] = x_s + (t-s)(\mu - \frac{1}{2}\sigma^2 - \lambda_x) + e^{-\kappa(t-s)}z_s - (e^{-\kappa s} - e^{-\kappa t}) + s(t), \quad (4.15)$$

$$\mathrm{Var}^*[p_t|\mathcal{F}_s] = \mathrm{Var}[p_t|\mathcal{F}_s]. \quad (4.16)$$

Comparing equation 4.15 to its real world counterpart, equation 4.7, it can be seen that the expected (ln-) spot price has been decreased by the term $(e^{-\kappa s} - e^{-\kappa t})$ and its drift has been reduced by the term λ_x. The variance however remains unchanged.

Again, the spot price $P_t|\mathcal{F}_s$ follows a log-normal distribution with mean $\mathrm{E}^*[P_t|\mathcal{F}_s]$ and variance $\mathrm{Var}^*[P_t|\mathcal{F}_s]$. For the purpose of pricing futures and option contracts, only the expectation is required.

$$\begin{aligned}\mathrm{E}^*[P_t|\mathcal{F}_s] &= e^{(\mu-\lambda_x)(t-s)} exp\{x_s + s(t) + e^{-\kappa(t-s)}z_s - (e^{-\kappa s} - e^{-\kappa t}) \\ &\quad + \frac{1}{2}[(\frac{1 - e^{-2\kappa(t-s)}}{2\kappa})\nu^2 + 2(\frac{1 - e^{-\kappa(t-s)}}{\kappa})\rho\sigma\nu]\}. \quad (4.17)\end{aligned}$$

Comparing equations 4.17 and 4.9 it can be seen that the expected spot price under the risk neutral measure has a drift of $\mu - \lambda_x$ instead of μ, and its expectation has been reduced multiplicatively by the term $exp[-(1 - e^{-\kappa t})]$.

4.2.2 Valuing Futures Contracts

The price of a futures contract can now be derived. According to Cox *et al.* (1981) the price of a futures contract is equal to the expected future spot

price.

Assume the futures contract expires at time T. Let $F_t(T)$ denote the futures price at time t, expiring at time T. The price of a futures contract under the Sørensen model is:

$$\begin{aligned} F_t(T) &= \mathrm{E}[P_T|\mathcal{F}_t] \\ &= \mathrm{E}[exp(s(T)+x_T+z_T)] \\ &= exp[s(T)+A(T-t)+x_t+z_te^{-\kappa(T-t)}], \end{aligned} \tag{4.18}$$

where

$$\begin{aligned} A(T-t) &= (\mu-\lambda_x)(T-t)-\frac{\lambda_z-\rho\sigma\nu}{\kappa}(1-e^{-\kappa(T-t)}) \\ &\quad +\frac{\nu^2}{4\kappa}(1-e^{-2\kappa(T-t)}). \end{aligned} \tag{4.19}$$

The derivation of the above formula is presented in appendix A.

This is a closed form solution for the price of any futures contract, with the dynamics described above, at any time t for expiry at time T. An important feature of this result is that $\ln F_t(T)$ is an affine function of the state variables x_t and z_t:

$$\begin{aligned} f_t(T) &= \ln F_t(T) \\ &= s(T)+A(T-t)+x_t+z_te^{-\kappa(T-t)}. \end{aligned} \tag{4.20}$$

Since we know the distribution of the state variables x_t and z_t, the distribution of $f_t(T)$ can be derived. In appendix A, $f_t(T)$ is shown to be normally distributed with mean and variance:

$$\begin{aligned} \mathrm{E}^*[f_t(T)|\mathcal{F}_0] &= s(T)+A(T-t)+x_0+t(\mu-\frac{1}{2}\sigma^2-\lambda_x)+e^{-\kappa T}z_0 \\ &\quad +[e^{-\kappa T}-e^{-\kappa(T-t)}]\frac{\lambda_z}{\kappa}, \end{aligned} \tag{4.21}$$

$$\mathrm{Var}^*[f_t(T)|\mathcal{F}_0]=\sigma^2t+\frac{e^{-2\kappa T}}{2\kappa}\nu^2(e^{2\kappa t}-1)+\frac{2e^{-\kappa T}}{\kappa}\rho\sigma\nu(e^{-\kappa t}-1). \tag{4.22}$$

Equation 4.21 gives a forecast of the price of a futures contract at time t for expiry at time T, forecast from time 0. Equation 4.22 gives the variance of this forecast.

Equations 4.21 and 4.22 can be extended to allow for evaluation at any time s where $0 \leq s \leq t$:

$$\begin{aligned} \mathrm{E}^*[f_t(T)|\mathcal{F}_s] &= s(T) + A(T-t) + x_s + (t-s)(\mu - \frac{1}{2}\sigma^2 - \lambda_x) + e^{-\kappa(T-s)}z_s \\ &\quad + [e^{-\kappa(T-s)} - e^{-\kappa(T-t)}]\frac{\lambda_z}{\kappa}, \end{aligned} \tag{4.23}$$

$$\mathrm{Var}^*[f_t(T)|\mathcal{F}_s] = \sigma^2(t-s) + \frac{e^{-2\kappa T}}{2\kappa}\nu^2(e^{2\kappa t} - e^{2\kappa s}) + \frac{2e^{-\kappa T}}{\kappa}\rho\sigma\nu(e^{\kappa t} - e^{\kappa s}). \tag{4.24}$$

Equations 4.21 and 4.23 indicate that the term $(\mu - \frac{1}{2}\sigma^2 - \lambda_x)$ can be regarded as the long term expected appreciation of the (ln-) futures price. This term is not affected by the actual expiry of the futures contract T, only its time until observation $t - s$.

Letting $s = t$:

$$\begin{aligned} \mathrm{E}^*[f_t(T)|\mathcal{F}_t] &= s(T) + A(T-t) + x_t + (t-t)(\mu - \frac{1}{2}\sigma^2 - \lambda_x) + e^{-\kappa(T-t)}z_t \\ &\quad + [e^{-\kappa(T-t)} - e^{-\kappa(T-t)}]\frac{\lambda_z}{\kappa} \\ &= s(T) + A(T-t) + x_t + e^{-\kappa(T-t)}z_t \\ &= f_t(T), \end{aligned}$$

$$\begin{aligned} \mathrm{Var}^*[f_t(T)|\mathcal{F}_t] &= \sigma^2(t-t) + \frac{e^{-2\kappa T}}{2\kappa}\nu^2(e^{2\kappa t} - e^{2\kappa t}) + \frac{2e^{-\kappa T}}{\kappa}\rho\sigma\nu(e^{\kappa t} - e^{\kappa t}) \\ &= 0. \end{aligned}$$

This makes intuitive sense, as the futures price $f_t(T)$ is equal to the expected future spot price. Also, given information available at time t the expected (ln-) futures price is simply equal to the (ln-) future price according to equation 4.20.

4.2.3 Valuing Option Contracts

This section derives values for options where the underlying asset is a futures contract. Both European and American option values are determined.

When valuing options on futures it is important to distinguish between the expiry time of the option and the expiry time of the underlying future. Let T_1 denote the expiry time of the option and T_2 denote the expiry time of the underlying future. Clearly, T_1 must be less than, or equal to, T_2.

Let t denote the valuation date throughout. The derivations of all the formulae below are presented in appendix A.

Standard Black

The Standard Black differential equation produces prices for European style options. European options may only be exercised on expiry. Standard Black formulae are used internationally.

The traditional option pricing formulae are modified slightly in order to incorporate the Sørensen model for pricing futures contracts.

Let $C_{\mathrm{E},t}$ and $P_{\mathrm{E},t}$ denote the value of a European call and a European put at valuation date t respectively.

$$C_{\mathrm{E},t} = e^{-r(T_1-t)}[F_t(T_2)N(d_1) - KN(d_2)], \tag{4.25}$$

$$P_{\mathrm{E},t} = e^{-r(T_1-t)}[KN(-d_2) - F_t(T_2)N(-d_1)], \tag{4.26}$$

where

$$d_1 = \frac{\ln(F_t(T_2)/K) + \sigma_\phi^2(t,T_1,T_2)/2}{\sigma_\phi(t,T_1,T_2)}, \tag{4.27}$$

$$d_2 = \frac{\ln(F_t(T_2)/K) - \sigma_\phi^2(t,T_1,T_2)/2}{\sigma_\phi(t,T_1,T_2)}, \tag{4.28}$$

$$\begin{aligned} t &= \text{valuation date,} \\ T_1 &= \text{option expiry date,} \\ T_2 &= \text{underlying futures expiry date,} \\ r &= \text{risk free rate,} \\ K &= \text{option strike price,} \\ N(x) &= \text{standard normal cumulative distribution} \end{aligned}$$

$$
\begin{aligned}
&= \frac{1}{\sqrt{2\pi}} \int_{-\infty}^{x} e^{-\frac{t^2}{2}} dt, \\
F_t(T_2) &= \text{futures price at } t \text{ for expiry at } T_2, \\
\sigma_\phi^2(t, T_1, T_2) &= \text{variance of } f_{t_1}(T_2) \text{ conditioned at time } t.
\end{aligned}
$$

$F_t(T_2)$ is the price of a futures contract at t for expiry at T_2, defined by equation 4.18.

$$F_t(T_2) = exp[s(T_2) + A(T_2 - t) + x_t + z_t e^{-\kappa(T_2 - t)}], \tag{4.29}$$

where

$$A(T_2 - t) = \alpha(T_2 - t) - \frac{\lambda_z - \rho\sigma\nu}{\kappa}(1 - e^{-\kappa(T_2 - t)}) + \frac{\nu^2}{4\kappa}(1 - e^{-2\kappa(T_2 - t)}).$$

ϕ is defined as the distribution of $\ln F_{T_1}(T_2)$, i.e. $\phi \equiv f_{T_1}(T_2)$. At valuation date t, ϕ is normally distributed with mean $\mu_\phi(t, T_1, T_2)$ and variance $\sigma_\phi^2(t, T_1, T_2)$:

$$
\begin{aligned}
\mu_\phi(t, T_1, T_2) &= \mathrm{E}[f_{T_1}(T_2)|\mathcal{F}_t] \\
&= s(T_2) + A(T_2 - T_1) + x_t + (T_1 - t)(\mu - \frac{1}{2}\sigma^2 - \lambda_x) \\
&\quad + e^{-\kappa(T_2 - t)} z_t + [e^{-\kappa(T_2 - t)} - e^{-\kappa(T_2 - T_1)}]\frac{\lambda_z}{\kappa},
\end{aligned} \tag{4.30}
$$

$$
\begin{aligned}
\sigma_\phi^2(t, T_1, T_2) &= \mathrm{Var}[f_{T_1}(T_2)|\mathcal{F}_t] \\
&= \sigma^2(T_1 - t) + \frac{e^{-2\kappa T_2}}{2\kappa}\nu^2(e^{2\kappa T_1} - e^{2\kappa t}) \\
&= + \frac{2e^{-\kappa T_2}}{\kappa}\rho\sigma\nu(e^{\kappa T_1} - e^{\kappa t}).
\end{aligned} \tag{4.31}
$$

SAFEX Black

The SAFEX Black differential equation produces prices for American style options. These formula are used for options on futures that are traded on the SAFEX. American options differ from European options in that they may be exercised at any time prior to and including the expiry date.

Let $C_{\mathrm{A},t}$ and $P_{\mathrm{A},t}$ denote the value of an American call and put option at valuation date t respectively.

$$C_{\mathrm{A},t} = [F_t(T_2)N(d_1) - KN(d_2)], \tag{4.32}$$

$$P_{\mathrm{A},t} = [KN(-d_2) - F_t(T_2)N(-d_1)], \tag{4.33}$$

where

$$d_1 = \frac{\ln(F_t(T_2)/X) + \sigma_\phi^2(t, T_1, T_2)/2}{\sigma_\phi(t, T_1, T_2)},$$
$$d_2 = \frac{\ln(F_t(T_2)/X) - \sigma_\phi^2(t, T_1, T_2)/2}{\sigma_\phi(t, T_1, T_2)}.$$

All terms in these formulae are identical to those used in the Standard Black model.

The only difference between the SAFEX Black prices and the Standard Black prices is the discount factor $e^{-r(T_1-t)}$.

Chapter 5

Procedure for Estimating Model Parameters

The state variables x_t and z_t are not directly observable. However, they can be estimated from the futures prices. The way in which the state variables are estimated is via the Kalman filter.

In brief, the procedure for estimating the model parameters is as follows. Initially the model parameters are assumed (initial estimates). A Kalman filter procedure is then run. The Kalman filter is a recursive procedure that produces updated estimates of the state variables x_t and z_t, at each observation time t, based on observations up to and including time t. Once the Kalman filter has been run for the whole sample of observations, the log-likelihood function can be calculated. The parameters are then varied and the Kalman filter rerun to produce another value for the log-likelihood. The parameters that maximise the log-likelihood are chosen as the model parameters.

The structure of this chapter is as follows: Section 5.1 discusses the Kalman filter in greater detail as well as the state space form required to run a Kalman filter. Section 5.2 looks at the state space specification of the Sørensen model. Finally section 5.3 discusses the form of the log-likelihood function.

5.1 The State Space Form and the Kalman Filter

The Kalman filter is a recursive procedure for computing estimates of unobservable state variables based on observations that depend on these state

variables.

In order for a Kalman filter to be applied to a time series model, the model needs to be arranged into the state space form.

An extensive account of the Kalman Filter procedure is provided by Harvey (1989). The notation throughout this text is consistent with the notation used by Harvey (1989).

5.1.1 The State Space Form

The state space form consists of two equations, namely the measurement equation and the transition equation. The measurement equation describes the relationship between the observable variables, in this case the futures prices, and the unobservable state variables. The transition equation describes the evolution of the state variables.

The general (reduced) form of the measurement and transition equations is presented.

The measurement equation is defined as:

$$\mathbf{y}_n = \mathbf{Z}_n\alpha_n + \mathbf{d}_n + \varepsilon_n, \qquad n = 1, \ldots, N, \tag{5.1}$$

where $\mathbf{y}_n$ is a $N \times 1$ vector containing the observable variables at time n. α_n is a $m \times 1$ state vector containing the state variables. $\mathbf{Z}_n$ is a $N \times m$ matrix, $\mathbf{d}_n$ is a $N \times 1$ vector and ε_n is a $N \times 1$ vector of serially uncorrelated disturbances, such that:

$$\mathrm{E}(\varepsilon_n) = 0 \quad \text{and} \quad \mathrm{Var}(\varepsilon_n) = \mathbf{H}_n. \tag{5.2}$$

The transition equation takes the following form:

$$\alpha_n = \mathbf{T}_n\alpha_{n-1} + \mathbf{c}_n + \eta_n, \qquad n = 1, \ldots, T. \tag{5.3}$$

Again α_n is the state vector, $\mathbf{T}_n$ is a $m \times m$ matrix, $\mathbf{c}_n$ a $m \times 1$ vector and η_n a $m \times 1$ vector of errors, such that:

$$\mathrm{E}(\eta_n) = 0 \quad \text{and} \quad \mathrm{Var}(\eta_n) = \mathbf{Q}_n. \tag{5.4}$$

Two assumptions are required before the Kalman filter can be applied:

1. A prior distribution for the state variables α_0 needs to be specified. It is assumed that α_0 is multivariate normal with $\mathrm{E}(\alpha_0) = \mathbf{a}_0$ and $\mathrm{Var}(\alpha_0) = \mathbf{P}_0$.

2. The error terms ε_n and η_n are assumed to be uncorrelated with each other over all time periods and uncorrelated with the initial the state vector α_0, i.e.:

$$\begin{aligned} \mathrm{E}(\varepsilon_i \eta'_j) &= 0 \qquad \forall i, j = 1, \ldots, N, & (5.5)\\ \mathrm{E}(\varepsilon_i \alpha'_0) &= 0 \qquad i = 1, \ldots, N, & (5.6)\\ \mathrm{E}(\eta_i \alpha'_0) &= 0 \qquad i = 1, \ldots, N. & (5.7) \end{aligned}$$

5.1.2 The Kalman Filter

Once in the state space form the Kalman filter can be applied to a time series model. An extremely valuable result of the Kalman filter is that, under certain assumptions, the likelihood function can be calculated. These assumptions are that the initial state vector α_0, as well as the disturbances ε_n and η_n are normally distributed. The assumption of the distribution of α_0 is stated in section 5.1.1. The distribution of the error terms is defined in section 5.2.

The general form of the Kalman filter procedure follows.

Let $\mathbf{a}_{n-1}$ denote the optimal estimator of α_{n-1} based on observations up to and including time $n-1$. Let $\mathbf{P_{n-1}}$ denote the $m \times m$ covariance of the estimation error:

$$\mathbf{P_{n-1}} = \mathrm{E}[(\alpha_{n-1} - \mathbf{a}_{n-1})(\alpha_{n-1} - \mathbf{a}_{n-1})']. \tag{5.8}$$

Given $\mathbf{a}_{n-1}$ and $\mathbf{P_{n-1}}$, the optimal estimator of α_n and $\mathbf{P}_n$ is given by:

$$\begin{aligned} \mathbf{a}_{n|n-1} &= \mathbf{T}_n \alpha_{n-1} + \mathbf{c}_n \qquad n = 1, \ldots, N, & (5.9)\\ \mathbf{P}_{n|n-1} &= \mathbf{T}_n \mathbf{P}_{n-1} \mathbf{T}'_n + \mathbf{Q}_n \qquad n = 1, \ldots, N. & (5.10) \end{aligned}$$

Equation 5.9 follows from equation 5.3. Equation 5.9 and 5.10 are called the prediction equations.

When the observation $\mathbf{y}_n$ becomes available $\mathbf{a}_{n|n-1}$ and $\mathbf{P}_{n|n-1}$ can be updated:

$$\begin{aligned} \mathbf{a}_n &= \mathbf{a}_{n|n-1} + \mathbf{P}_{n|n-1} \mathbf{Z}'_n \mathbf{F}_n^{-1} (\mathbf{y}_n - \mathbf{Z}_n \mathbf{a}_{n|n-1} - \mathbf{d}_n), & (5.11)\\ \mathbf{P}_n &= \mathbf{P}_{n|n-1} - \mathbf{P}_{n|n-1} \mathbf{Z}'_n \mathbf{F}_n^{-1} \mathbf{Z}_n \mathbf{P}_{n|n-1}, & (5.12) \end{aligned}$$

where

$$\mathbf{F}_n = \mathbf{Z}_n \mathbf{P}_{n|n-1} \mathbf{Z}_n' + \mathbf{H}_n. \tag{5.13}$$

Equations 5.9 to 5.13 make up the Kalman filter.

The starting values for the Kalman filter procedure are $\mathbf{a}_0$ and $\mathbf{P}_0$. Once these have been specified the Kalman filter yields the optimal estimator of the state vector as each new observation becomes available.

5.2 The State Space Form of the Sørensen Model

In this section the Sørensen model is arranged into the state space form discussed in 5.1.1. The first step is to recognise that the Kalman filter works in discrete time steps. Hence the Sørensen model needs to be presented in discrete form.

Let $\Delta = t_n - t_{n-1}$ be the distance between any two observation points, $t_n, n = 1, \ldots, N$. It is assumed that all observations times are equidistant.

The measurement equation is derived from 4.20 which defines the relationship between the (ln-) futures price and the state variables. The measurement equation needs to be an affine function of the state variables, thus the (natural) logarithm of the futures price, $f_{t_n}(T) = \ln F_{t_n}(T)$, is modelled.

The measurement equation thus has the following form:

$$\mathbf{y}_n = \mathbf{Z}_n \alpha_n + \mathbf{d}_n + \varepsilon_n, \qquad n = 1, \ldots, N, \tag{5.14}$$

where

$$\mathbf{y}_n = \begin{pmatrix} f_{t_n}(T_t^1) \\ \vdots \\ f_t(T_t^n) \end{pmatrix}, \tag{5.15}$$

$$\mathbf{Z}_t = \begin{pmatrix} 1 & e^{-\kappa(T_n^1 - t_n)} \\ \vdots & \vdots \\ 1 & e^{-\kappa(T_{t_n}^{M_n} - t)} \end{pmatrix}, \tag{5.16}$$

$$\alpha_n = \begin{pmatrix} x_n \\ z_n \end{pmatrix}, \tag{5.17}$$

$$\mathbf{d}_n = \begin{pmatrix} s(T_n^1) + A(T_n^1 - t_n) \\ \vdots \\ s(T_n^{M_n}) + A(T_n^{M_n} - t_n) \end{pmatrix}. \tag{5.18}$$

ε_n, $n = 1, \ldots, N$ is a $M_n \times 1$ vector of errors that are independently normally distributed:

$$\mathrm{E}(\varepsilon_n) = 0, \qquad \mathrm{Var}(\varepsilon_n) = \mathbf{H}_n = \sigma_\varepsilon^2 I_{M_n}. \tag{5.19}$$

ε_n allows for noise in the sampling of the data. The form of H_n is chosen so that only one parameter, σ_ε, needs to be estimated.

The number of futures contracts available at each time point varies. M_n denotes the number of futures contracts available at time n. T_n^1 and $T_n^{M_n}$ thus denote the expiry time of the closest and furthest to maturity contracts available at time n respectively. This model thus allows the dimensionality of the model to change at each observation time n, depending on the number of futures contracts available at that time M_n.

The transition equation follows from equations 4.3 and 4.4. This equation describes the stochastic evolution of the unobservable state vector:

$$\alpha_n = \mathbf{T}_n \alpha_{n-1} + \mathbf{c}_n + \eta_n, \qquad n = 1, \ldots, N,$$

where

$$\alpha_n = \begin{pmatrix} x_n \\ z_n \end{pmatrix}, \tag{5.20}$$

$$\mathbf{T}_n = \begin{pmatrix} 1 & 0 \\ 0 & e^{-\kappa\Delta} \end{pmatrix}, \tag{5.21}$$

$$\mathbf{c}_n = \begin{pmatrix} \mu - \frac{1}{2}\sigma^2 \\ 0 \end{pmatrix}. \tag{5.22}$$

η_n, $n = 1, \ldots, N$ is a 2×1 vector of errors that are independently normally distributed:

$$\mathrm{E}(\eta_n) = 0, \tag{5.23}$$

$$\mathrm{Var}(\eta_n) = \begin{pmatrix} \sigma^2\Delta & \frac{\rho\sigma\nu}{\kappa}(1 - e^{-\kappa\Delta}) \\ \frac{\rho\sigma\nu}{\kappa}(1 - e^{-\kappa\Delta}) & \frac{\nu^2}{2\kappa}(1 - e^{-2\kappa\Delta}) \end{pmatrix}. \tag{5.24}$$

5.3 The Log Likelihood Function

As previously mentioned, it is assumed that the disturbances, as well as the initial state vector are normally distributed. Thus it is possible to calculate

the likelihood function.

The (ln-) likelihood function is defined as:

$$\ln L = -\frac{1}{2}\sum_{n=1}^{N} \ln |\mathbf{F}_n| - \frac{1}{2}\sum_{n=1}^{N} \mathbf{v}_n' \mathbf{F}_n^{-1} \mathbf{v}_n - \sum_{t=n}^{N} \frac{M_n}{2} \ln 2\pi, \tag{5.25}$$

where

$$\mathbf{v}_n = \mathbf{y}_n - \tilde{\mathbf{y}}_{n|n-1}. \tag{5.26}$$

$\tilde{\mathbf{y}}_{n|n-1}$ is the conditional expectation of $\mathbf{y}_n$ given information up to and including time $n-1$:

$$\tilde{\mathbf{y}}_{n|n-1} \quad = \quad \mathrm{E}(\mathbf{y}_n|\mathcal{F}_{n-1}) \quad = \quad \mathbf{Z}_n \mathbf{a}_{n|n-1} + \mathbf{d}_n, \tag{5.27}$$

where $\mathcal{F}_n$ has its usual meaning as the filtration at time n.

$\mathbf{F}_n$ is the conditional covariance matrix introduced in equation 5.13.

$\mathbf{a}_{n|n-1}$ and $\mathbf{F}_n$ are calculated for each time period via the Kalman filter procedure. M_n, the number of traded futures contracts available at time n, and N, the total number of observation times are known at each time point n. Thus all the variables required to calculated $\ln L$ are available.

5.25 is often referred to as the error decomposition form of the likelihood. This is because $\mathbf{v}_n$ can be regarded as the vector of prediction errors.

Now that the likelihood function can be calculated explicitly, there exists a platform from which to estimate the model parameters. Let Ψ denote the vector of model parameters. There are 9 parameters plus the seasonal parameters. Ψ has the general form:

$$\Psi = \begin{pmatrix} \mu \\ \kappa \\ \sigma \\ \nu \\ \rho \\ \alpha \\ \lambda_z \\ x_1 \\ \sigma_\varepsilon \\ \mathcal{S} \end{pmatrix}, \tag{5.28}$$

where $\mathcal{S}$ denotes the seasonal component of the model. The number of parameters in $\mathcal{S}$ depends on the choice of K:

$$\mathcal{S} = \begin{pmatrix} \gamma_1 \\ \gamma_1^* \\ \vdots \\ \gamma_K \\ \gamma_K^* \end{pmatrix}. \tag{5.29}$$

Thus, if $K = 1$ then there are 2 parameters in $\mathcal{S}$ and a total of 11 in parameters to be estimated in Ψ.

For ease Ψ can be presented as:

$$\Psi = \begin{pmatrix} \mathcal{N} \\ \mathcal{S} \end{pmatrix}, \tag{5.30}$$

where N denotes the set of non-seasonal parameters,

$$\mathcal{N} = \begin{pmatrix} \mu \\ \kappa \\ \sigma \\ \nu \\ \rho \\ \alpha \\ \lambda_z \\ x_1 \\ \sigma_\varepsilon \end{pmatrix}. \tag{5.31}$$

It should be noted that x_1, the initial value of the equilibrium level, is treated as an extra parameter to be estimated. On the other hand, the other state variable z_1 is assumed to be distributed according to its steady state distribution.

Chapter 6

The Data

Three different agricultural commodities are examined throughout this study, namely white maize, yellow maize and wheat. For each commodity the parameters of the Sørensen model are estimated for varying samples.

The full dataset for white and yellow maize consists of weekly closing prices for futures contracts for the period 08 Jan 1997 to 31 May 2006. The dataset for wheat consists of weekly closing prices for the period 07 Jan 1998 to 31 May 2006. Weekly closing prices refer to the closing prices on Wednesdays (or Tuesdays if Wednesdays are unavailable). According to Sørensen (2002) weekly sampling is chosen in order to reduce problems associated with micro-structural issues such as price limits imposed by exchanges. At each observation time t, there are a number of futures contracts available with different times to maturity. The number of contracts available varies over time and across commodities.

In this study the sample is reduced to include only closest and furthest to maturity contracts at each observation time. This eases that calculation of the likelihood function, as $M_n = 2$ for all discrete observation time points n, but still manages to capture the short- and long-term dynamics of the futures market.

According to Schwartz and Smith (2000), an observed vector with varying times to maturity results in little uncertainty about the state-variables. The number of futures contracts required to achieve this can be as few as two.

Including closest and furthest to maturity contracts as apposed to any other two observations makes intuitive sense. The intuition behind this is that movements in long-maturity futures prices provide information about

the equilibrium level x_t, and the differences between long- and short-dated futures prices provide information about short-term variations in prices z_t. Thus it makes sense to include these two contracts.

For each commodity various subsamples are modelled and their respective parameters estimated. The subsamples are chosen based on a plot of the futures closing prices for the full sample period. Subsamples are modelled in order to test the consistency of certain parameters as well as to identify changes in the underlying dynamics of the commodity futures market over certain periods.

The Sørensen model requires the time to maturity, $\tau = T - t$, as an input of the model. The terms of the futures contracts traded on the SAFEX state that the last trading day of a futures contract is the seventh business day preceding the last business day of the delivery month. Although delivery can take place any time up to an including the last business day of the month, the convention, for modelling purposes, is that the last trading day is regarded as the expiry date.

6.1 Preliminary Data Analysis

This sections investigates the basic features of the data under consideration. Time series plots for each commodity are investigated. Summary statistics for the prices of futures contracts for different close-out months are also presented. The aim is to get a basic idea of the features of the futures prices before presenting the empirical results.

For each commodity a time series plot presented. The time series plots 6.1, 6.2 and 6.3 display the closing (ln-) futures prices for both nearest and farthest to maturity contracts. The plots indicate that the closest and furthest to maturity closing prices move closely together. The strength of this relationship is measured by the correlation coefficient. Correlation is a bivariate measure of the strength and direction of the relationship between two variables, measuring between -1 and +1 where -1 indicates a perfectly negative correlation, 0 no correlation, and +1 perfect correlation. The correlation coefficients for all three plots are close to 0.96. This means there is an extremely strong positive relationship between front month and back month futures prices and the degree to which the prices vary together is 96%.

The plots seem to display a seasonal pattern. Recall, $f_t(T)$ $(= \ln F_t(T))$ is

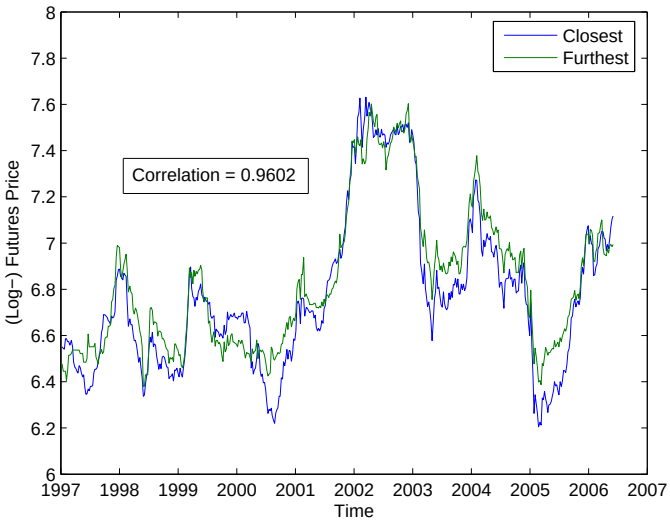

Figure 6.1: Plot of weekly closing futures prices for nearest- and farthest- to maturity white maize contracts. Sample period: 08 Jan 1997 to 31 May 2006.

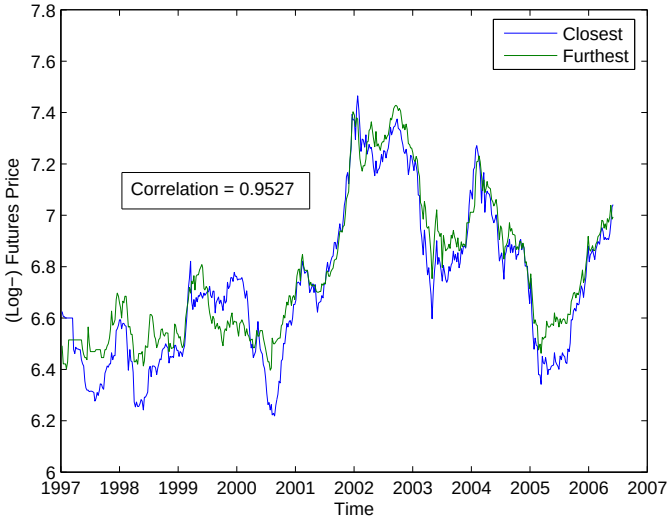

Figure 6.2: Plot of weekly closing futures prices for nearest- and farthest- to maturity yellow maize contracts. Sample period: 08 Jan 1997 to 31 May 2006.

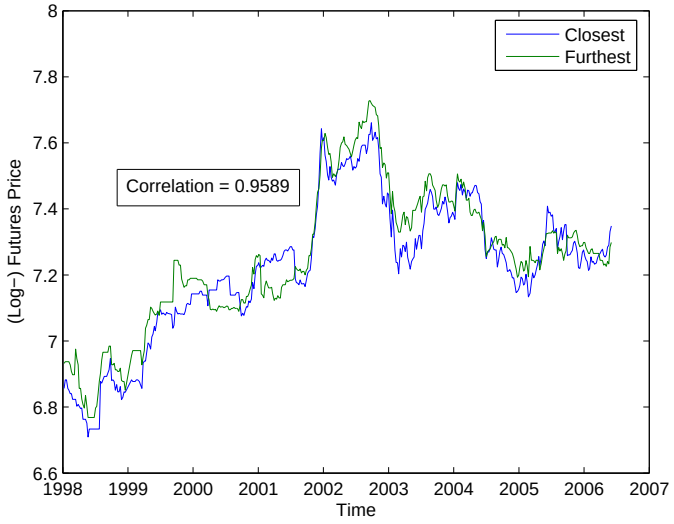

Figure 6.3: Plot of weekly closing futures prices for nearest- and farthest- to maturity wheat contracts. Sample period: 07 Jan 1998 to 31 May 2006.

an affine function of the seasonal component $s(T)$ and the state variables x_t and z_t. The plots suggest that the inclusion of a seasonal component in the futures prices of white maize, yellow maize and wheat is appropriate.

It is important to note that there are five possible expiry months for each futures contract, namely March, May, July, September and December. At each observation time t there are a number of futures contracts available with different expiry months. Only futures prices for nearest to maturity contracts are presented in the summary statistics. The main features of the futures prices are captured sufficiently by the closest to maturity contracts as they are the most liquid and thus accurately reflect the dynamics of the futures prices.

Tables 6.1, 6.2 and 6.3 present the summary statistics for white maize, yellow maize and wheat contracts respectively. The tables portray the number of observations, the average closing prices as well as the standard deviations of the prices of closest-to-maturity futures contracts for each expiry month.

The summary statistics highlight the effect of seasonality on the price of futures contracts. Table 6.1 shows that prices of March-expiry white maize futures are on average the highest and prices of July-expiry contracts seem on

Expiry Month	No. obs	Average Price	Std Dev
Mar	130	1000.5	373.5
May	89	918.8	384.3
Jul	80	852.7	341.6
Sep	76	879.6	348.1
Dec	116	960.5	346.3

Table 6.1: Number of observations, average price and standard deviation for nearest to maturity weekly closing prices of white maize futures for different close-out months. Sample period: 08 Jan 1997 to 31 May 2006.

Expiry Month	No. obs	Average Price	Std Dev
Mar	130	951.0	295.1
May	89	847.6	261.7
Jul	80	805.1	249.1
Sep	76	829.4	296.0
Dec	116	898.5	262.8

Table 6.2: Number of observations, average price and standard deviation for nearest to maturity weekly closing prices of yellow maize futures for different close-out months. Sample period: 08 Jan 1997 to 31 May 2006.

Expiry Month	No. obs	Average Price	Std Dev
Mar	117	1384.6	284.4
May	78	1395.2	298.4
Jul	73	1395.1	291.3
Sep	59	1457.9	308.4
Dec	112	1385.9	281.4

Table 6.3: Number of observations, average price and standard deviation for nearest to maturity weekly closing prices of wheat futures for different close-out months. Sample period: 07 Jan 1998 to 31 May 2006.

average to be the lowest. The same seasonal pattern appears to be affecting yellow maize futures prices, as is evident by considering table 6.2.

The seasonal component of wheat futures prices, indicated by table 6.3 seems to be a lot different to that of maize futures. September close-out futures contracts are on average the highest with March and December prices appearing to be the lowest.

The final column in table 6.1, 6.2 and 6.3 shows the standard deviation of prices for each particular expiry month. White maize futures prices are the most volatile, followed by yellow maize and wheat futures. The standard deviations seem to indicate that prices for expiry months that are generally more 'expensive' have greater volatility and expiry months that are generally 'cheaper' are less volatile.

6.2 Influence of Rand/Dollar Exchange Rate

The level of the ZAR/USD exchange rate has a significant affect on the spot price, P_t, of agricultural commodities and hence on the futures prices $F_t(T)$.

Figures 6.4, 6.5 and 6.6 plot the time series of the (ln-) futures price and the exchange rate on the same set of axes. It is evident that there is a significant positive correlation between all three commodities and the ZAR/USD exchange rate.

The plots suggest that the steep rise in commodity prices in March 2001 and the steep fall in February 2003 was caused by the decline in value of the rand and its subsequent recovery.

The correlation coeffients of the commodity prices and the ZAR/USD exchange rate range between 0.7 to 0.75. In this case there is a causality relationship between the ZAR/USD exchange rate and the commodity prices. The most liquid exchange for these commodities is the Chicago Board of Trade (CBOT) which trades in dollars. The dollar price of these commodities thus has a major influence on the rand price of the these commodities. A correlation coeffient of 0.7 implies that fluctuations in the ZAR/USD rates cause 70% of the fluctuations in the ZAR denominated commodities price. The strong correlation between commodity prices (in rands) and the ZAR/USD exchange rate suggests that modelling the dollar price of commodity futures may be appropriate.

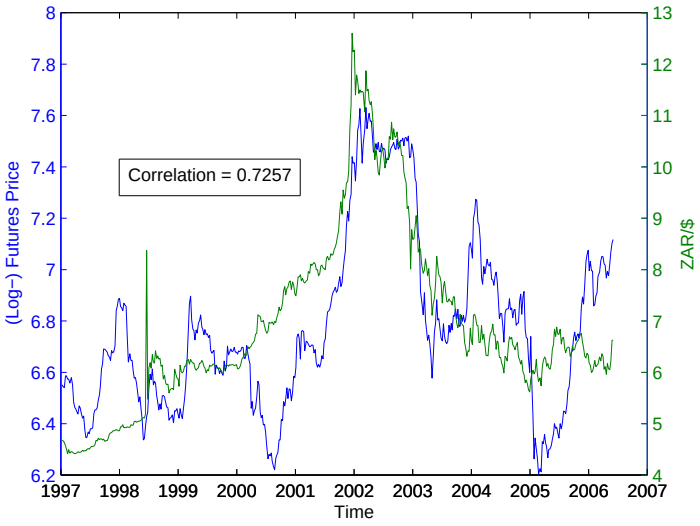

Figure 6.4: Plot of weekly closing nearest-to-maturity white maize futures prices versus the ZAR/USD exchange rate. Sample period: 08 Jan 1997 to 31 May 2006.

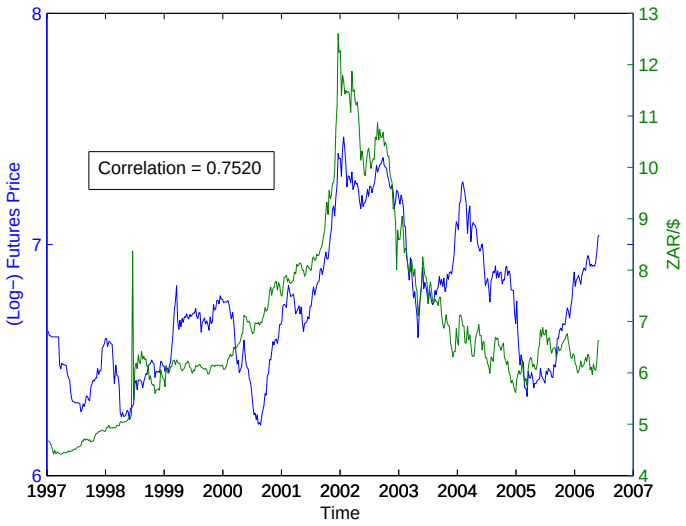

Figure 6.5: Plot of weekly closing nearest-to-maturity yellow maize futures prices versus the ZAR/USD exchange rate. Sample period: 08 Jan 1997 to 31 May 2006.

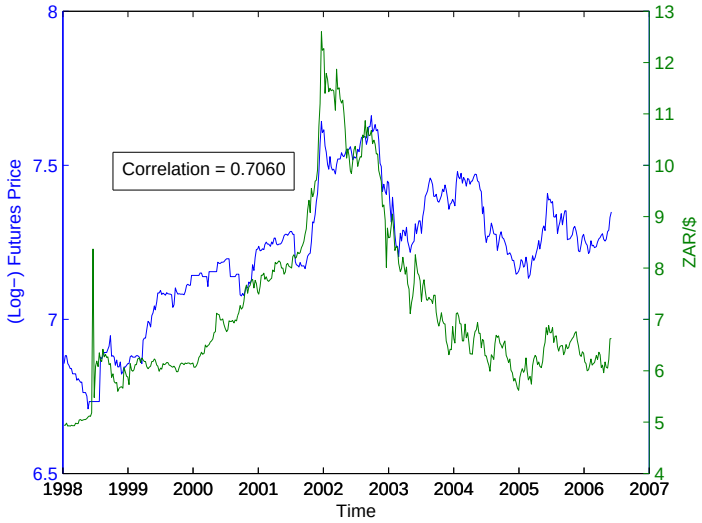

Figure 6.6: Plot of weekly closing nearest-to-maturity wheat futures prices versus the ZAR/USD exchange rate. Sample period: 07 Jan 1998 to 31 May 2006.

Chapter 7

Seasonal Model Parameters

7.1 Introduction and Methodology

In this chapter the seasonal parameter estimates are presented and discussed for white maize, yellow maize and wheat futures. Recall, Ψ denotes the vector of model parameters. The optimal value for Ψ is derived via the methodology described in chapter 5. Ψ is the complete vector of model parameters:

$$\Psi = \begin{pmatrix} \mathcal{N} \\ \mathcal{S} \end{pmatrix}.$$

In this chapter however only the seasonal parameters $\mathcal{S}$ are considered. The size of the vector $\mathcal{S}$ is determined by the number of Fourier coefficients, K, included in $S(T)$. Recall,

$$\mathcal{S} = \begin{pmatrix} \gamma_1 \\ \gamma_1^* \\ \vdots \\ \gamma_K \\ \gamma_K^* \end{pmatrix}.$$

An important feature of this section is the determination of the optimal choice of K. For each commodity different choices of K will be compared. The choice of K will ultimately be decided upon using certain information criteria.

Once the seasonal parameters $\mathcal{S}$ have been estimated for varying choices of K, the seasonal component of the Sørensen model can be calculated. Recall equation 4.20:

$$f_t(T) = s(T) + A(T-t) + x_t + z_t e^{-\kappa(T-t)},$$

where

$$s(T) = \sum_{k=1}^{K} (\gamma_k \cos(2\pi kT) + \gamma_k^* \sin(2\pi kT)).$$

$s(T)$ denotes the seasonal component of the futures price $F_t(T)$. Although the (ln-) futures price $f_t(T)$ is clearly a function of both t and T it is important to note that $s(T)$ is a function of T only.

$s(T)$ is a Fourier series, which by nature of its construction, repeats itself (at least) once every period. Formally:

$$s(T) = s(T+i), \qquad \forall i \in \mathcal{I}. \tag{7.1}$$

Therefore $s(T)$ need only be evaluated for values of T between 0 and 1. T can then be interpreted as the expiry date of a futures contract relative to its time within the calendar year. Thus $T = 0$ denotes 1 January and $T = 1$ denotes 31 December. The critical feature is that the year in which a futures contract expires is not a factor, it is only the expiry date within the year that important important.

Commodity futures traded on the SAFEX have five possible expiry dates, namely March, May, July, September and December. Therefore one should only really be concerned with these five values of T and their associated values of $s(T)$.

The first step in calculating these five values of $s(T)$ is to determine the values of T. Recall that the expiry date, for modelling purposes, is the seventh business day preceding the final business day in the close-out month, i.e. the final trading day. For each year however the exact date of the final trading day of a particular close-out month is slightly different depending on the number of weekend days and public holidays between the final trading day of the month and the last day of the month. Thus, for each year the values of T are slightly different.

The degree to which the values of the expiry times, T, change year on year is however minimal. Hence, taking an average for each value of T over all

Expiry Month	Average Expiry Date	T
March	19.4 March	0.213
May	21.1 May	0.385
July	20.9 July	0.552
September	18.9 September	0.717
December	19.1 December	0.967

Table 7.1: Average time of expiry for the five possible close-out dates. The expiry date is equal to the last day to trade (LDT) which is the seventh business day prior to the last business day of the month. The LDT changes every year, thus an average is taken over the sample period. T denotes the expiry date on a scale of 0 to 1.

years in the sample leads to a single set of T's that are both accurate and consistent. Table 7.1 shows the average values for T for each of the expiry months. These average expiry times are used for the analysis of all three commodities throughout. For the results that follow these five expiry times will be highlighted.

The rest of this chapter has the following structure: Seasonal parameters are estimated for white maize, yellow maize and wheat futures. For each commodity the choice of K is determined. Plots of the seasonal component, $s(T)$, are presented for each value of K. Once a suitable choice for K has been established the specific values and implications of $s(T)$ are examined.

This chapter considers only the full sample period for each commodity. A full account of all parameter estimates for all different samples is presented in appendix C.

7.2 White Maize Futures

The sample under consideration consists of weekly closing prices for the period 08 January 1997 to 31 May 2006.

The initial step is to find a suitable choice for K. Table 7.2 presents the seasonal parameter estimates for varying values of K. For $K = 1$ there are 2 parameters in $\mathcal{S}$, for $K = 2$ there are 4, and for $K = 3$ there are 6.

Table 7.3 presents the values of $s(T)$ for each of the five expiry months together with each choice of K. These values represent the actual seasonal component factored into the futures price.

$\mathcal{S}$	$K=1$	$K=2$	$K=3$
γ_1	0.0177	0.0198	-0.0109
γ_1^*	0.0160	0.0144	0.0065
γ_2		-0.0048	-0.0310
γ_2^*		0.0040	-0.0176
γ_3			0.0449
γ_3^*			-0.0448

Table 7.2: Seasonal parameter estimates for white maize futures for $K = 1, 2\&3$. K determines the number of Fourier coefficients included in the seasonal component $s(T)$. Sample: weekly closing nearest- and farthest- to maturity white maize futures prices. Sample period: 08 Jan 1997 to 31 May 2006. Estimates are obtained by means of maximum likelihood estimation and Kalman filtering.

		$s(T)$		
Expiry Month	T	$K=1$	$K=2$	$K=3$
March	0.213	0.0196	0.0247	0.0291
May	0.385	-0.0027	-0.0099	0.0142
July	0.558	-0.0222	-0.0245	-0.0078
September	0.717	-0.0193	-0.0122	0.0069
December	0.967	0.0140	0.0104	0.0293

Table 7.3: Seasonal component, $s(T)$, for white maize futures at the 5 expiry times, T, for $K = 1, 2\&3$. T is a measure of the relative time during a year on which the expiry date occurs. T ranges from 0 to 1. Sample: weekly closing nearest- and farthest-to maturity white maize futures prices. Sample period: 08 Jan 1997 to 31 May 2006. $s(T) = \sum_{k=1}^{K}(\gamma_k \cos(2\pi kT) + \gamma_k^* \sin(2\pi kT))$.

Figure 7.1 displays the seasonal components for different choices of K. Each figure plots $s(T)$ on the y-axis versus T on the x-axis. On each plot the five expiry dates and their associated seasonal components are highlighted.

The resulting plots of $s(T)$ for $K = 1$ and $K = 2$ are both simple and consistent with the data. Both plots depict a peak close to march and trough near July. When $K = 3$, the resulting plot of $s(T)$ suggests $s(T)$ has been over-fitted. Although the values for $s(T)$ for the five expiry months are still consistent with the data, the shape of the curve between these points does not make sense. Thus the choice of K is between $K = 1$ and $K = 2$.

The next step in deciding on a choice of K is to look at certain information

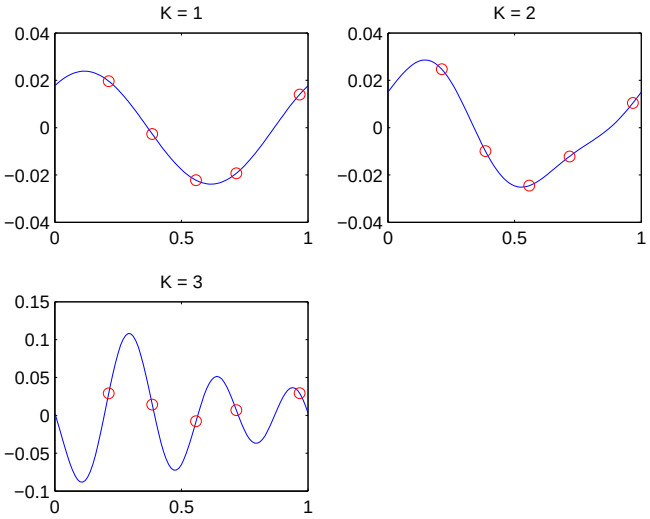

Figure 7.1: Plots of $s(T)$ vs T for white maize futures for $K = 1, 2\&3$. $s(T)$ denotes the seasonal component of a futures contract expiring at time T. Sample: Weekly closing nearest- and farthest- to maturity white maize futures prices. Sample period: 08 Jan 1997 to 31 May 2006.

criteria. Information criteria are used as a guide in model selection. Information criterion provide a measure that takes into account the goodness of fit of a model, measured by its log likelihood function, as well as the number of parameters included in the model. The notion behind an information criterion is that it is best to choose a model that fits the data well but with as few parameters as possible. Thus even though one model may accurately fit the data, it may not necessarily be the best choice if it has many parameters.

In this case the models that are being compared are the Sørensen model with $K = 1$ and the Sørensen model with $K = 2$. Two information criteria are used, namely the Akaike information criterion (AIC) and the Schwarz criterion (SC). They are defined as:

$$\begin{aligned} \text{AIC} &= -2\frac{l}{n} + 2\frac{k}{n}, \\ \text{SC} &= -2\frac{l}{n} + \frac{k}{n}\ln(n), \end{aligned}$$

where k is the number of estimated parameters, n is the number of observations, and l is the value of the log likelihood function.

	$K = 1$	$K = 2$
l	1865.1	1870.2
n	982	982
k	11	13
AIC	-3.7762	-3.7825
SC	-3.7214	-3.7178

Table 7.4: Information criteria results for white maize futures. l is the value of the (ln-) likelihood function obtained by the maximum likelihood optimisation procedure, n denotes the number of observations, and k represents the total number of parameters estimated. The Akaike information criterion (AIC) and the Schwartz criterion (SC) are presented. Sample: Weekly closing nearest- and farthest- to maturity white maize futures prices. Sample period: 08 Jan 1997 to 31 May 2006.

Table 7.4 displays the results of the information criteria for $K = 1$ and $K = 2$ for white maize futures. The log likelihood function, l, is the same function that is maximised in the parameter estimation procedure described in chapter 5. The number of parameters, k, is equal to the number of elements in Ψ. The number of observations, n, is equal to the total number of observed weekly closing prices. Since closest- and farthest-to-maturity contracts are observed, the total number of observations equals twice the number of observed time points.

Generally, the model with the lowest value for its information criterion is chosen. From table 7.2 it can seen that the model with $K = 1$ has a lower AIC value than the model with $K = 2$, but has a higher SC value. Thus, according to the AIC, $K = 1$ is a better choice, but based on the SC, $K = 2$ is better. The model with $K = 2$ is chosen in this instance because the improvement in the goodness of fit seems to justify the inclusion of two extra parameters.

7.3 Yellow Maize Futures

The analysis of the seasonal component of yellow maize futures follows the same methodology as that for white maize futures in section 7.2.

The yellow maize data under consideration consists of weekly closing prices for the period 08 January 1997 to 31 May 2006.

$\mathcal{S}$	$K=1$	$K=2$
γ_1	0.0177	0.0211
γ_1^*	0.0091	0.0097
γ_2		-0.0029
γ_2^*		0.0112

Table 7.5: Seasonal parameter estimates for yellow maize futures for $K = 1\&2$. K determines the number of Fourier coefficients included in the seasonal component $s(T)$. Sample: weekly closing nearest- and farthest- to maturity yellow maize futures prices. Sample period: 08 Jan 1997 to 31 May 2006. Estimates are obtained by means of maximum likelihood estimation and Kalman filtering.

		$s(T)$	
Expiry Month	T	$K=1$	$K=2$
March	0.213	0.0129	0.0219
May	0.385	-0.0073	-0.0209
July	0.558	-0.0198	-0.0179
September	0.717	-0.0125	-0.0067
December	0.967	0.0154	0.0115

Table 7.6: Seasonal component, $s(T)$, for yellow maize futures at the 5 possible expiry times, T, for $K = 1\&2$. T is a measure of the relative time during a year on which the expiry date occurs. T ranges from 0 to 1. Sample: weekly closing nearest- and farthest-to maturity yellow maize futures prices. Sample period: 08 Jan 1997 to 31 May 2006. $s(T) = \sum_{k=1}^{K}(\gamma_k \cos(2\pi kT) + \gamma_k^* \sin(2\pi kT))$.

Once again the initial step is to determine the most suitable value of K. The choice will be limited to $K = 1$ and $K = 2$ only. As seen in section 7.2, when $K = 3$ the estimation procedure over-fits the seasonal component $s(T)$.

The parameter estimates and the resulting seasonal components for the five expiry months for yellow maize futures are presented in table 7.5 and 7.6.

Figure 7.2 displays the plot of the seasonal component, $s(T)$, for $K = 1$ and $K = 2$. Once again the seasonal components of the five expiry months are highlighted.

Again, the plots of $s(T)$ do not give a clear indication as to which choice of K is best. The models will thus be compared using the Akaike information criterion and the Schwarz criterion. Table 7.7 indicates that $K = 1$ is a

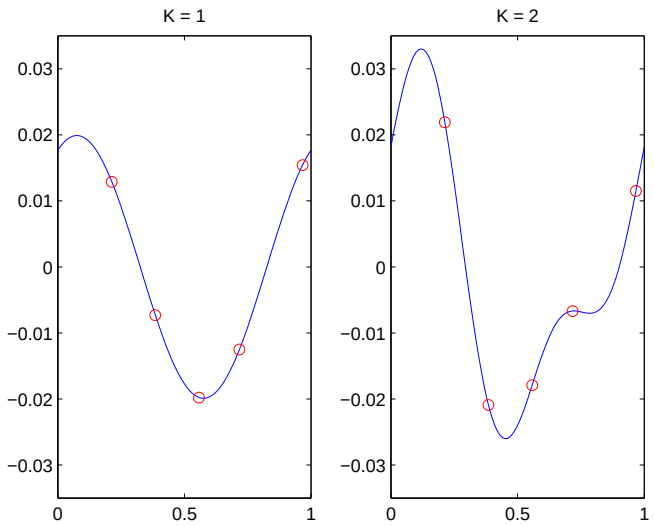

Figure 7.2: Plots of $s(T)$ vs T for yellow maize futures for $K = 1\&2$. $s(T)$ denotes the seasonal component of a futures contract expiring at time T. Sample: Weekly closing nearest- and farthest- to maturity yellow maize futures prices. Sample period: 08 Jan 1997 to 31 May 2006.

better choice under both the criteria.

7.4 Wheat Futures

Again, the same procedure is followed for the analysis of the seasonal component of wheat futures.

The wheat data consists of weekly closing prices for the period 07 January 1998 to 31 May 2006. Note, the sample is slightly smaller than that of white and yellow maize due to the fact that wheat futures began trading on the SAFEX at later stage.

Table 7.8 displays the seasonal parameter estimates for $K = 1$ and $K = 2$. The resulting values for the seasonal component, $s(T)$, are presented in table 7.9 for the possible expiry times T.

Figure 7.3 displays the plot of the seasonal component, $s(T)$, for $K = 1$ and $K = 2$. As usual $s(T)$ is highlighted for the possible expiry times.

	$K=1$	$K=2$
l	1979.4	1988.1
n	982	982
k	11	13
AIC	-4.0090	-4.0226
SC	-3.9542	-3.9579

Table 7.7: Information criteria results for yellow maize futures. l is the value of the log likelihood function obtained by the maximum likelihood optimisation procedure, n denotes the number of observations, and k represents the total number of parameters estimated. The Akaike information criterion (AIC) and the Schwartz criterion (SC) are presented. Sample: Weekly closing nearest- and farthest- to maturity yellow maize futures prices. Sample period: 08 Jan 1997 to 31 May 2006.

$\mathcal{S}$	$K=1$	$K=2$
γ_1	-0.0240	-0.0227
γ_1^*	-0.0041	-0.0110
γ_2		-0.0078
γ_2^*		-0.0041

Table 7.8: Seasonal parameter estimates for wheat futures for $K = 1\&2$. K determines the number of Fourier coefficients included in the seasonal component $s(T)$. Sample: weekly closing nearest- and farthest- to maturity wheat futures prices. Sample period: 07 Jan 1998 to 31 May 2006. Estimates are obtained by means of maximum likelihood estimation and Kalman filtering.

		$s(T)$	
Expiry Month	T	$K=1$	$K=2$
March	0.213	-0.0095	-0.0108
May	0.385	0.0153	0.0128
July	0.558	0.0239	0.0166
September	0.717	0.0090	0.0209
December	0.967	-0.0226	-0.0254

Table 7.9: Seasonal component, $s(T)$, for wheat futures at the 5 possible expiry times, T, for $K = 1\&2$. T is a measure of the relative time during a year on which an expiry date occurs. T ranges from 0 to 1. Sample: weekly closing nearest- and farthest- to maturity wheat futures prices. Sample period: 07 Jan 1998 to 31 May 2006. $s(T) = \sum_{k=1}^{K}(\gamma_k \cos(2\pi kT) + \gamma_k^* \sin(2\pi kT))$.

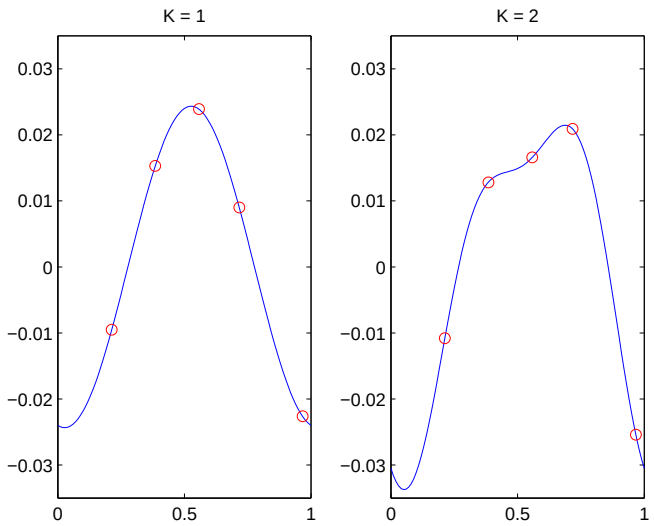

Figure 7.3: Plots of $s(T)$ vs T for wheat futures for $K = 1\&2$. $s(T)$ denotes the seasonal component of a futures contract expiring at time T. The value of $s(T)$ is highlighted for the expiry months March, May, July, September and December. Sample: Weekly closing nearest- and farthest- to maturity wheat futures prices. Sample period: 07 Jan 1998 to 31 May 2006.

Once again, the plots of $s(T)$ do not give a clear indication as to which choice of K is best. The models are thus compared using the Akaike information criterion and the Schwarz criterion. Table 7.10 presents the respective results for the information criteria.

Table 7.10 indicates that $K = 1$ is a better choice under both the Akaike information criterion and the Schwarz criterion. Thus, only the model with $K = 1$ will be considered for further investigation.

7.5 Interpreting the Seasonal Component

The outcome of sections 7.2 through 7.4 is that a seasonal component, $s(T)$, has been derived for each commodity. For white maize futures $s(T)$ is Fourier series containing coefficients of period 2, i.e. $K = 2$. For yellow maize and wheat futures K is chosen to be 1.

Table 7.11 displays the final seasonal component, $s(T)$, for each commod-

	$K = 1$	$K = 2$
l	2114.9	2125.8
n	868	868
k	11	13
AIC	-4.8477	-4.8682
SC	-4.7873	-4.7968

Table 7.10: Information criteria results for wheat futures. l is the value of the log likelihood function obtained by the maximum likelihood optimisation procedure, n denotes the number of observations, and k represents the total number of parameters estimated. The Akaike information criterion (AIC) and the Schwartz criterion (SC) are presented. Sample: Weekly closing nearest- and farthest- to maturity wheat futures prices. Sample period: 07 Jan 1998 to 31 May 2006.

	$s(T)$		
Expiry Month	White Maize	Yellow Maize	Wheat
Mar	0.0247	0.0129	-0.0095
May	-0.0099	-0.0073	0.0153
Jul	-0.0245	-0.0198	0.0239
Sep	-0.0122	-0.0125	0.0090
Dec	0.0104	0.0154	-0.0226

Table 7.11: Final seasonal component for each commodity at each possible expiry month. The seasonal component, $s(T)$, is calculated using the optimal choice of K. For white maize $K = 2$, yellow maize $K = 1$, and wheat $K = 1$.

ity at each expiry date.

The next step in the analysis of the seasonal effect on commodity futures contracts is to investigate the implication of $s(T)$ on the prices of these contracts. This section firstly examines the implied effect of $s(T)$ on the futures price $F_t(T)$ and secondly explores whether or not the effect is consistent with the data.

Recall the price of a futures contract, $F_t(T)$, observed at time t expiring at time T:

$$F_t(T) = \exp[s(T) + A(T-t) + x_t + z_t e^{-\kappa(T-t)}].$$

This can be rearranged such that:

$$F_t(T) = \exp[s(T)] exp[A(T-t) + x_t + z_t e^{-\kappa(T-t)}].$$

	$exp[s(T)]$		
Expiry Month	White Maize	Yellow Maize	Wheat
Mar	1.0250	1.0130	0.9905
May	0.9901	0.9927	1.0154
Jul	0.9758	0.9804	1.0242
Sep	0.9879	0.9876	1.0090
Dec	1.0105	1.0155	0.9777

Table 7.12: Multiplicative effect of the estimated seasonal parameters on the prices of futures contracts at different expiry months. The futures price implied by the Sørensen model is a function of the estimated parameters. The term $exp[s(T)]$ reflects the seasonal influence on the futures price.

The term $\exp[A(T-t) + x_t + z_t e^{-\kappa(T-t)}]$ can be interpreted as the futures price if there were no seasonal effect. Thus the term $\exp[s(T)]$ has a multiplicative effect on the futures price $F_t(T)$. The magnitude of the effect is equal to $\exp[s(T)]$. For instance if $s(T) = 0$, then $exp[s(T)] = 1$, and there would be no effect on the futures price. For $s(T) > 0$, the resulting futures price will be higher by the proportion $\exp[s(T)]$. Similarly if $s(T) < 0$, the resulting futures price lower by the proportion $\exp[s(T)]$.

Table 7.12displays the implied multiplicative effect on the prices of futures contracts for each of the commodities at each of the expiry dates. Estimated parameters are used to calculate the implied seasonal effect $\exp[s(T)]$.

The values presented in table 7.12 can be interpreted as follows: Consider March-expiry for white maize futures. The value of the multiplicative effect on futures prices for March expiry is estimated as 1.0250. This implies that March futures are on average 2.5% higher than they would have been had there been no seasonal effect on prices.

The accuracy of these estimates must now be examined. Tables 6.1, 6.2 and 6.3 give an initial indication as to the size and shape of the seasonal effect on future prices. The problem, however, is that these average prices are calculated by taking the average price of futures contracts for each expiry month over the entire sample period. Thus, these averages do not take into account the observation times of each futures price. The equilibrium level, x_t, and the short term deviation, z_t, at each observation time t also affect the futures price at that time. Hence, the averaged futures price for a certain expiry month will be affected by the seasonal component as well as the

Expiry Month	White Maize	Yellow Maize	Wheat
Mar	1.0294	1.0306	0.9987
May	1.0004	0.9997	1.0067
Jul	0.9774	0.9796	1.0117
Sep	0.9812	0.9798	1.0052
Dec	1.0122	1.0100	0.9836

Table 7.13: Average relative values for futures prices at different expiry months calculated from the raw data. For each observation date where futures prices are available for each expiry month, the relative value for each expiry month is calculated. The values for each month throughout the sample are then averaged. These values give an indication of the seasonal effect on futures prices.

time of the observations. For instance, if many of the March-expiry prices are observed at times when the equilibrium level, x_t, is unusually high, then the average March-expiry prices will be higher than the seasonal component itself would imply. A method of estimating the magnitude of the seasonal component for each expiry month that takes into account this problem is thus required.

A more accurate estimate of the size of the seasonal component can be achieved using the following methodology. For each observation time, t, the average of all available futures prices is calculated. The prices corresponding to each expiry month is then compared to this average. Thus at each observation date a relative value for the futures price at each expiry month can be calculated by dividing the futures price for that particular expiry month by the average price of all futures trading at that date. Then by averaging all the relative values for each expiry month, an average relative value for each expiry month can be calculated. The benefit of this methodology is that the effect of the equilibrium level, x_t, at each observation time is accounted for when relative values are calculated at each observation date t. The downside however is that short-term deviations measured by z_t will still be influencing the results.

Table 7.13 presents the results of the average relative values for each expiry month of white maize, yellow maize and wheat futures. These relative values are directly comparable to the values presented in table 7.12 as the term $\exp[s(T)]$ is also an indication of the relative magnitude of the seasonal effect.

In order to ensure that the above methodology provides accurate esti-

mations of the magnitude of the seasonal component, future prices for all possible expiry months are needed at each observation date. If prices are not available or contracts are non existent for any of the five expiry months at any observation time, then prices for that particular observation date are not considered. The dataset used in calculating the average relative prices is the same as that used for estimating the model parameters. However, daily closing prices are used as apposed to weekly closing prices in order to ensure that there is a sufficient number of observations in the sample once some of the observations have been deleted.

The sample of white and yellow maize futures is sufficiently large, once some of the observations have been deleted, to provide accurate estimations. On the other hand, the wheat futures sample is too small to provide accurate results. As a result none of the observations for wheat futures are deleted. The relative values for wheat futures thus may slightly underestimate the magnitude of the seasonal component. However these results are still useful in providing insight into the level and 'shape' of the seasonal component $s(T)$.

By comparing tables 7.12 and 7.13 one can see that the estimation of the seasonal components, $s(T)$, for each commodity is consistent with the 'crude' estimates of the seasonal effect. The results for white maize futures seem to be most accurate. This may be due to the fact that the seasonal component, $s(T)$, for white maize futures is estimated with $K = 2$. The 'crude' estimates for wheat futures seem to slightly underestimate the seasonal effects implied by the optimisation method. As mentioned, this is caused by including observation times, in the calculation of the crude estimates, where prices are not available for all possible expiry times. In general, the 'crude' estimates confirm that the estimates for $s(T)$ are in fact reasonable.

7.6 Simulated Futures

Data is simulated in order to test the accurateness of the parameter estimation methodology, in particular the seasonal parameters. Futures prices are simulated for known fixed parameters using the Sørensen model.

Simulating futures prices requires the model parameters to be set. Using the risk-neutral dynamics of the model, 4.13 and 4.14, futures prices for different observation dates and different expiry times are generated. A complete account of the procedure used to simulate the futures prices is presented in appendix **??**.

	True Parameters	Estimated Parameters
γ_1	0.01	0.0101
γ_1^*	0.02	0.0201

Table 7.14: Seasonal parameter estimates for simulated futures prices. 'True parameters' are the actual parameters used in producing the simulated dataset. 'Estimated parameters' denote the parameters derived by using Kalman filtering techniques and maximum likelihood estimation on the simulated data.

The simulated dataset consists of weekly closing prices for the period 07 January 1998 to 31 May 2006. At each observation date two futures prices are quoted, one representing the closest-to-expiry contract and the other the farthest-to-maturity contract. The simulated futures prices are also presented in appendix **??**.

The simulation is conducted using $K = 1$. Therefore the seasonal component is a function of two parameters only. The simulation could just as easily been conducted using $K = 2, 3, ...$ The parameters are estimated using the usual methodology presented in chapter 5.

The complete set of known parameters as well as the estimated parameters are presented in appendix **??**.

Table 7.14 presents the known prespecified seasonal parameters and the resulting seasonal parameter estimates. The estimated parameters are clearly very close to the actual parameters. This suggests the Kalman filtering methodology and the numerical procedure used to generate the maximum likelihood estimates is very accurate.

Chapter 8

Non-Seasonal Model Parameters

8.1 White Maize, Yellow Maize and Wheat Futures

This section discusses the estimates of the set of parameters $\mathcal{N}$, where

$$\mathcal{N} = \begin{pmatrix} \mu \\ \kappa \\ \sigma \\ \nu \\ \rho \\ \alpha \\ \lambda_z \\ x_1 \\ \sigma_\varepsilon \end{pmatrix}. \tag{8.1}$$

These parameters describe the dynamics of the state variables as well as those parameters added in the state space formulation of the Sørensen model. The estimates are presented in table 8.1 for white maize, yellow maize and wheat.

Table 8.1 presents and describes various drift measures. Table 8.2 gives estimates of these drifts for each of the commodities. The drift estimates are calculated using the relevant estimates in table 8.1.

The term μ represents the expected long term growth of the spot price P_t. This can be seen by referring to equation 4.12. The estimates for this

	White Maize	Yellow Maize	Wheat
μ	0.0815	0.1556	0.0504
κ	0.6283	0.4160	0.9144
σ	0.4986	0.5401	0.2910
ν	0.5740	0.6840	0.3783
ρ	-0.7817	-0.9030	-0.8710
λ_x	-0.0344	-0.2468	-0.0424
λ_z	-0.4580	0.2406	-0.1045
x_1	5.5449	5.9343	7.7789
σ_ε	0.0001	0.0084	0.0064

Table 8.1: Non-seasonal model parameter estimates for white maize, yellow maize and wheat futures. Parameters estimates are obtained by means of maximum likelihood estimation and Kalman filtering. For white maize $K = 2$, yellow maize $K = 1$, and wheat $K = 1$. The sample for each commodity consists of weekly closing prices for nearest- and farthest- to maturity futures contracts. White maize: 08 Jan 1997 to 31 May 2006. Yellow maize: 08 Jan 1997 to 31 May 2006. Wheat: 07 Jan 1998 to 31 May 2006.

Real World Dynamics	Description
$\mu - \frac{1}{2}\sigma^2$	Drift of x_t
	Long-term growth of p_t
μ	Long-term growth of P_t
Risk Neutral Dynamics	**Description**
$\mu - \frac{1}{2}\sigma^2 - \lambda_x$	Drift of x_t
	Long-term growth of p_t
	Long-term growth of f_t
$\mu - \lambda_x$	Long-term growth of P_t

Table 8.2: Description of various drifts. Model dynamics are introduced in the 'real world'. In order to derive the futures price F_t (and f_t), conversion to risk neutral dynamics is required.

Drift	White Maize	Yellow Maize	Wheat
μ	0.0815	0.1556	0.0504
$\mu - \frac{1}{2}\sigma^2$	-0.0428	0.0065	0.0083
$\mu - \frac{1}{2}\sigma^2 - \lambda_x$	-0.0084	0.2533	0.0507

Table 8.3: Drifts calculated from the parameter estimates in table 8.1.

	Implied Drift $(\mu - \frac{1}{2}\sigma^2 - \lambda_x)$	Actual Drift
White Maize	-0.0084	0.0448
Yellow Maize	0.2533	0.0511
Wheat	0.0507	0.0557

Table 8.4: Implied versus actual drifts for prices of white maize, yellow maize and wheat futures contracts. 'Implied drift' represents the long-term growth of futures prices predicted by the estimated model parameters. 'Actual drift' is the drift of futures prices using least squares approximation

.

term are positive for all commodities. Yellow maize (0.1556) has the greatest estimate of μ, followed by white maize (0.0815) and wheat (0.0504).

The term $\mu - \frac{1}{2}\sigma^2$ denotes the drift of the non-stationary state variable x_t as described by equation 4.3. From equation 4.10 it can be seen that this term also represents the expected long term growth of the logarithm of the spot price, p_t. Table 8.3 indicates that this drift term is negative for white maize (-0.0428). The estimates for yellow maize (0.0065) and wheat (0.0083) are positive but close to 0.

Under risk neutral dynamics, x_t has a drift of $\mu - \frac{1}{2}\sigma^2 - \lambda_x$, where λ_x denotes the risk premium associated with x_t. This term represents the expected long term growth of both p_t and the logarithm of the futures price f_t, as shown by equations 4.15 and 4.23 respectively, under the risk-neutral measure. The estimate of this term is negative and close to 0 for white maize (-0.0084). For yellow maize (0.2533) however the estimate is significantly greater than 0. The estimate for wheat is 0.0507.

Table 8.4 compares the drift of the futures price implied by the parameter estimates to the actual drift of the futures price over the same sample period. The actual drift represents the slope of a regression line using least squares approximation. The average actual drift of closest and farthest to maturity contracts is assumed to be the best estimate of the long-term growth of futures prices over the sample period.

Table 8.4 shows that the estimated drift parameters do not accurately reflect the actual drifts of the futures prices. Only estimates for wheat futures produce reasonable results. The cause of the inaccuracy for white and yel-

low maize futures is not certain, but may be caused by the high volatility of futures prices over the sample period. Another possibility may be that the size of the sample may be too small to produce accurate results. The causes of this inaccuracy are further discussed in section 8.2 when simulated futures prices and their associated parameter estimates are considered.

The parameter κ is known as the mean reversion coefficient. The estimates of κ are positive for all the commodities. This confirms that the state variable z_t is indeed stationary. Recall, z_t describes the short term deviation in p_t and has dynamics formalised by equation 4.4. The greater κ, the faster z_t is expected to revert back to its mean (0 under real world dynamics and $-\lambda_z/\kappa$ under risk-neutral dynamics). Wheat (0.9144) has the largest estimate of κ, followed by white maize (0.6283) and yellow maize (0.4160). The half-lives implied by these estimates ($-\ln(0.5)/\kappa$) are 1.1032 years, 1.6662 years and 0.7580 years respectively. Half-life estimates measure the time a deviation is expected to halve.

The volatility structure of the three commodities is depicted by the parameters σ, ν and ρ. σ represents the volatility of the non stationary state variable x_t, ν is the volatility of the stationary state variable z_t and ρ is a measure of the correlation between x_t and z_t. The estimates of σ are consistently lower than the estimates of ν. Yellow maize ($\sigma = 0.5461$, $\nu = 0.6840$) volatility estimates are the greatest implying that yellow maize futures experience the greatest volatility. White maize futures (0.4986, 0.5740) are the second most volatile and wheat futures (0.2901, 0.3783) are the least volatile.

The estimates of ρ indicate a negative correlation between x_t and z_t for each of the commodities. This implies that movements in the equilibrium level x_t are associated with movements in the opposite direction of the short term deviation z_t. The (absolute) size of ρ indicates the strength of this relationship. The estimates for yellow maize (-0.9030), wheat (-0.8710) and white maize (-0.7817) are all close to -1 and hence suggest a strong negative relationship.

λ_x and λ_z denote the risk premiums associated with x_t and z_t respectively. The estimates of λ_x are negative for all commodities. Yellow maize (-0.2468) exhibits the most significant risk premiums. The estimates of white maize (-0.0344) and wheat (-0.0424) are comparable. On the other hand, there seems to be no obvious pattern for the estimates of λ_z. White maize (-0.4580) and wheat (-0.1045) display negative risk premiums, whereas the estimate for yellow maize (0.2406) is positive. According to Sørensen (2002), the sum of

the risk premium depicts the 'instantaneous' excess return of the asset. In other words, the return over and above the risk-free rate, that an investment with its risk profile would expect to yield.

The risk premiums λ_x and λ_z also give insight into the shape of the futures curve. A futures curve is a plot of the prices of futures contracts for different maturities at a particular point in time. There are two basic shapes that futures curves can take, namely contango or normal backwardation. Contango is the case when the futures curve is rising (the prices of long dated futures are greater than short dated futures) and normal backwardation is the case of a downward sloping futures curve.

By plotting the ratio of the futures price, equation 4.18, to the expected future spot price, equation 4.12, one can get an idea of the shape of the futures curve:

$$\frac{F_t(T)}{\mathrm{E}[P_T|\mathcal{F}]} = exp[-\lambda_x(T-t) - \frac{\lambda_z}{\kappa}(1-e^{-\kappa(T-t)}] \tag{8.2}$$

Thus $F_t(T)/\mathrm{E}[P_T|\mathcal{F}]$ is a function of λ_x, λ_z, κ and the time to maturity $T-t$ only. The plot of this ratio over varying times to maturity $T-t$ gives an indication of the shape of the futures curve over the sample period. However, the plot is not a plot of the actual futures curve, it merely indicates the shape of the futures curve. For instance if the ratio $F_t(T)/\mathrm{E}[P_T|\mathcal{F}]$ is increasing with time to maturity, it implies that the futures curve itself is also increasing and hence in a state of contango. It is important to note that the parameters λ_x, λ_z, κ are assumed to be constant over the sample period. The plot can thus be considered as an indicator of the 'average' shape of the futures curve over the sample period. An actual futures curve is a plot at a specific point in time.

Figure 8.1 displays the plot of $exp[-\lambda_x(T-t)-\frac{\lambda_z}{\kappa}(1-e^{-\kappa(T-t)}]$ for varying times to maturity $T-t$. Under the sample period investigated, the furthest time to maturity is 1.42 years. As a result the ratio is plotted from $T-t=0$ to $T-t=1.5$. The ratio is 1 for all commodities at $T-t=0$ as the futures price with no time to expiry simply equals the spot price. Figure 8.1 shows that for each commodity the curve is increasing with time to maturity. The greater the time to maturity, the greater the ratio between the futures price and the expected spot price. Hence the plot implies that contango is the case for each commodity. The case for white maize futures however seems to be too extreme. Under normal circumstances, the value of $F_t(T)/\mathrm{E}[P_T|\mathcal{F}]$, for all expiry time T, should be fairly close to 1. Figure 8.1 indicates that actual

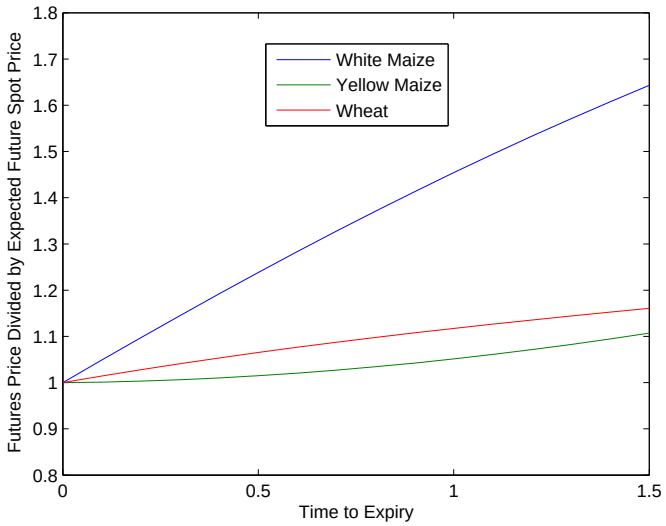

Figure 8.1: Ratio of futures price to the expected future spot price for white maize, yellow maize and wheat futures. $F_t(T)/\mathrm{E}[P_T|\mathcal{F}] = exp[-\lambda_x(T-t) - \frac{\lambda_z}{\kappa}(1-e^{-\kappa(T-t)}]$. This plot gives an indication of the 'average' shape of the futures curve over the sample period. A rising curve indicates contango and a falling curve indicates normal backwardation.

futures prices of white maize are significantly different from their associated expected spot prices. This suggests the risk premium parameters, and perhaps the mean-reversion coefficient, for white maize futures may be flawed. Again, the cause of this possible error is discussed in section 8.2.

The parameters x_1 and σ_e are included in the state space formulation. x_1 denotes the initial value of the long term equilibrium level of the (ln-) spot price p_t. More accurately $x_1 = x_{n_1}$ where n_1 signifies the time (in years) of the first observation. The estimates of x_1 for white maize (5.5449), yellow maize (5.9343) and wheat (7.7789) are all less than their associated first observed (ln-) futures prices (for both closest- and furthest-to-maturity contracts, $f_{n_1}(\tau^1)$ and $f_{n_1}(\tau^2)$). This makes intuitive sense if one recalls that the futures price is an estimate of the expected spot price at maturity. As is evident in equation 4.20, $f_t(\tau)$ is a function of $A(\tau - t)$ which itself is a function of $(\mu - \lambda_x)(\tau - t)$. $\mu - \lambda_x$ is a measure of the expected appreciation of the spot price P_t. Table 8.3 shows this term to be positive for all commodities. Thus one would generally expect the equilibrium level x_t to be lower than the futures price $f_t(\tau)$ as long as the term $(\mu - \lambda_x)(\tau - t)$ is significantly greater than 0.

	True Parameters	Estimated Parameters
μ	0.05	0.0372
κ	0.75	0.6894
σ	0.2	0.2400
ν	0.3	0.3441
ρ	-1	-1.000
λ_x	-0.05	-0.0574
λ_z	-0.1	-0.5156
x_1	5	4.9088
σ_ε	-	0.0021

Table 8.5: Non-seasonal parameter estimates for simulated futures prices. 'True parameters' are the actual parameters used in producing the simulated dataset. 'Estimated parameters' denote the parameters derived by using Kalman filtering techniques and maximum likelihood estimation on the simulated data.

σ_e is the standard deviation of the error term in the measurement equation 5.14. σ_e thus measures how well the theoretical values match the actual prices. The deviation between theoretical and observed (ln-) futures prices can be regarded as the 'noise'. According to Sørensen (2002), noise' may be caused by a number of factors. Possible sources of noise include effects of price limits, handling of bid-offer spreads, errors in the registration of data and the fact that actual settlement prices are set by administrators at SAFEX. The estimates of σ_e for all commodities are close to 0 which indicates little error in the measurement equation, and hence a good model fit. The measurement equation for white maize (0.001) exhibits the least noise, followed by wheat (0.0064) and yellow maize (0.0084).

8.2 Simulated Futures

This section presents the fixed non-seasonal parameters used to generate simulated futures prices together with the resulting estimates of these parameters using the methodology presented in chapter 5.

The complete set of fixed parameters, the resulting simulated futures prices and estimated parameters can be found in appendix **??**.

Table 8.5 presents the known inputed non-seasonal parameters and the resulting non-seasonal parameter estimates. Although not considerably ac-

curate, the estimated parameters are close enough to the true parameters to suggest the methodology and process of parameter estimation is correct.

The only parameter to show an unreasonable difference between its estimated and true value is λ_z. λ_z represents the risk premium associated with the stationary state variable z_t. One possible reason for the error in estimation is the short time period of the sample and hence the small number of observations. A small number of observation may cause the parameter estimates to not accurately reflect the true model parameters. A larger sample would thus be required in order to achieve more rigorous estimates.

Agricultural futures have only been trading since 1996. Thus it is not possible to work with a larger sample by extending the time period of the sample. The two possible means of expanding the sample are firstly by considering daily futures prices as opposed to weekly futures prices and secondly by including more futures contracts than just the closest and furthest to expiry contracts.

However, it is not clear whether or not these methods of expanding the sample size lead to significant improvements in the parameter estimates, as this study only considers weekly closing prices. Modelling daily closing prices for all available contracts would thus be the natural extension to this research.

Chapter 9

Pricing Futures Contracts in the Presence of Price Limits

This chapter considers a possible extension to the models considered throughout this study. The Sørensen model, as well as the models introduced in chapter 3, assume that there are no restrictions on the movements of prices of futures contracts. In reality however, most exchanges, including the SAFEX, set limits on the range of futures price movements for each trading day. Therefore, a model that takes into account price limits will be a better reflection of reality and thus price futures contracts more accurately. This chapter thus presents a procedure to price futures contracts whose movements are constrained by price limits.

9.1 Introduction

Trading halts serve the purpose of bringing order to markets in times of high volatility. Trading halts may take a variety of forms, the most common being a price limit. A price limit is defined as a preset level such that the price of an asset cannot deviate, either up or down, by more than the price limit during a prespecified trading session.

On a futures exchange, the price limit L is set by the exchange itself. A price limit usually applies for one trading day. At the start of a trading day, the price limit applies to the closing price on the previous trading date F^c_{t-1}. If a limit is 'hit', trading ceases until a time when a trade takes place within the price limits, or until the next trading day when the limits are reset at the closing price of the current trading day. The process of trading being halted due to a limit being 'hit' is known as a limit move.

Two hypotheses exist that substantiate the need for price limits to be imposed on exchanges, based on their causes of market volatility. These are the information and the overreaction hypotheses.

The information hypothesis assumes that prices are driven by the arrival of new information. This information is available to all traders and all traders are assumed to process the information in the same way. The true price is thus known by all traders at all times. If the true price moves outside the price limit range, trading will halt, and the the actual futures price will equal the particular limit that the true futures price breached. According to Holder *et al.* (2002), under the information hypothesis, price limits serve the purpose of delaying trade until a time when the true price falls within the allowed trading range.

The overreaction hypothesis assumes that traders do not process the information in an efficient manner and hence their estimate of the futures price is not necessarily equal to the true futures price. Most notable, traders seem to overreact to the arrival of new information causing greater volatility than that implied by the arrival of the new information. Under this hypothesis, price limits serve the purpose of halting trade until a time when the market has had time to process the information and establish a price within the allowed trading range. If the true price actually lies beyond the limit range on a particular trading day, then the limit will effectively be serving the purpose of a limit under the information hypothesis.

Holder *et al.* (2002) propose a model to price actual futures prices in the presence of price limits. A procedure is then developed to unbundle the true futures price from the actual futures price in order to compare the true prices to actual prices. By examining the true prices and actual prices around limit moves, the two hypotheses can be tested.

9.2 The Pricing Model

Holder *et al.* (2002) show that movements in futures prices, in the presence of price limits, can be replicated by a portfolio consisting of a risk-free investment together with two positions in synthetic option contracts. The value of the futures contract therefore equals the value of the portfolio.

The following assumptions are made:

1. The same futures contract is traded both in a market with price limits and in a market without price limits. The price in the market without price limits is the true price of the futures contract and is denoted F_t^*. The price in the limit market is the actual observed futures price and is denoted F_t.

2. Options are traded on futures contracts without price limits. In other words, the option prices are reflective of the true futures price of the underlying asset.

3. The actual futures contracts traded in the limit market are marked-to-market at the end of each trading day.

4. The options are marked-to-market at the true futures prices at the end of the day.

Throughout, the market for the true futures contract is known as a synthetic market. Options traded on futures without price limits are thus also referred to as synthetic options.

The price of an actual futures contract can be expressed as the sum of a long position in a risk-free asset and a bullish spread.

Formally:

$$F_t = (F_{t-1}^c - L)e^{rt} + C_1(F_t^*, \sigma, K_1, t, r) - C_2(F_t^*, \sigma, K_2, t, r), \tag{9.1}$$

where

$$\begin{aligned}
t &= \text{observation date,} \\
t-1 &= \text{previous trading date,} \\
F_t &= \text{actual futures price in the presence of limits,} \\
F_t^* &= \text{true futures price without limits,} \\
F_{t-1}^c &= \text{closing futures price on previous trading date,} \\
L &= \text{size of daily limit,} \\
C_1, C_2 &= \text{call price for options on } F_t^* \text{ with strike } K_1 \text{ and } K_2 \\
&\quad \text{respectively,} \\
K_1 &= F_{t-1}^c - L, \\
K_2 &= F_{t-1}^c + L, \\
r &= \text{risk-free rate of interest,} \\
\sigma &= \text{volatility of } F_t^*.
\end{aligned}$$

	Current Time	Value at Expiry		
Portfolio A	Price	$F_t^* < K_1$	$K_1 \leq F_t^* \leq K_2$	$F_t^* > K_2$
Long futures contract	$+F_t$	K_1 $= F_{t-1}^c - L$	$+F_t^*$	K_2 $= F_{t-1}^c + L$
Total	$+F_t$	$F_{t-1}^c - L$	$+F_t^*$	$F_{t-1}^c + L$

Table 9.1: Payoff profile of a portfolio consisting of 1 long futures contract in the presence of price limits. The level of the price limit is L. The maximum possible movement of the futures price over a trading day is L.

	Current Time	Value at Expiry		
Portfolio B	Price	$F_t^* < K_1$	$K_1 \leq F_t^* \leq K_2$	$F_t^* > K_2$
Long call at K_1	C_1	0	$F_t^* - K_1$ $= F_t^* - (F_{t-1}^c - L)$	$F_t^* - K_1$ $= F_t^* - (F_{t-1}^c - L)$
Short call at K_2	$-C_2$	0	0	$-[F_t^* - K_2]$ $= -[F_t^* - (F_{t-1}^c + L)]$
Risk-free asset	$(F_{t-1}^c - L)e^{-rt}$	$F_{t-1} - L$	$F_{t-1}^c - L$	$F_{t-1}^c - L$
Total	$C_1 - C_2$ $+(F_{t-1}^c - L)e^{-rt}$	$F_{t-1}^c - L$	$+F_t^*$	$F_{t-1}^c + L$

Table 9.2: Payoff profile of a portfolio consisting of a long call option at strike K_1, a short call option at strike K_2 and a risk-free investment of $F_{t-1} - L$. The options are traded in a market where no price limits exist and the underlying asset is a futures contract without price limits.

The relationship in equation 9.1 can be shown to hold by considering the payoffs of portfolio A and portfolio B.

Let portfolio A consist of a long position in a futures contract in the presence of price limits. The price of the future at the end of the trading day must therefore lie in the range $(F_{t-1}^c - L, F_{t-1}^c + L)$.

Let portfolio B consist of two synthetic call options and a risk-free investment of $F_{t-1}^c - L$. The first option position is a long position in a call with a strike price equal to the lower bound of the futures price, $K_1 = F_{t-1}^c - L$. The second option position is a short call with a strike price equal to the upper limit of the futures price, $K_2 = F_{t-1}^c + L$. Both options have a term to maturity of 1 day. They are effectively entered into at the beginning of the trading day for expiry at the end of the day.

Tables 9.1 and 9.2 demonstrate that the payoff of portfolio A is identical to that of portfolio B under all circumstances. Thus the value of the two portfolios must be the same. Hence the relationship in equation 9.1 must hold.

9.3 Unbundling the True Futures Price

A comparison of the actual futures price, F_t, and the true futures price, F_t^*, is required to measure the effect of the price limit.

The true futures price can be derived by expanding equation 9.1:

$$\begin{aligned} F_t &= (F_{t-1}^c - L)e^{rt} + C_1(F_t^*, \sigma, K_1, t, r) - C_2(F_t^*, \sigma, K_2, t, r) \\ &= (F_{t-1}^c - L)e^{rt} + e^{rt}[F_t^* N(x_1) - K_1 N(x_1 - \sigma\sqrt{t})] \\ &\quad -e^{rt}[F_t^* N(x_2) - K_2 N(x_2 - \sigma\sqrt{t})], \end{aligned} \tag{9.2}$$

where

$$x_1 = \frac{\ln\frac{F_t^*}{K_1} + \frac{\sigma^2}{2}t}{\sigma\sqrt{t}}, \tag{9.3}$$

$$x_2 = \frac{\ln\frac{F_t^*}{K_2} + \frac{\sigma^2}{2}t}{\sigma\sqrt{t}}. \tag{9.4}$$

$N()$ is the usual cumulative distribution function of a standard normal distribution. The synthetic options are assumed to be priced according to Black's formula. In fact, any option pricing formula can replace Black's formula in order to price C_1 and C_2.

The value of expressing F_t as in equation 9.2 is that F_t^*, which is actually unobservable, can be derived. By examining the theoretical futures price around limit moves, the two hypotheses, information and overreaction, can be tested.

The procedure of unbundling the theoretical futures price is similar to the standard methodology of estimating the implied volatilities of options.

9.4 Methodology and Conclusions

Holder *et al.* (2002) used intraday trading data of treasury bonds on the Chicago Board of Trade (CBOT) for the period 1 January 1980 to 31 December 1988. Only trading days where the price limit was hit were considered for the study.

The average actual and theoretical price changes on days of limit moves were analysed at different points throughout the trading day. It was shown

that changes in the theoretical futures price started deviating significantly from the actual futures price changes prior to the activation of the price limit. On average the true price started deviating from the actual price three hours before the price limits were triggered.

Two important results were shown. Firstly, at the time of a limit move, the theoretical price was shown to lie significantly outside the limit range. This suggests that price limits are restricting the movements of actual futures prices. Secondly, soon after trade began following a limit move, the theoretical price was shown to move quickly back within the limit range. This observation suggests that the market overreacts to the arrival of information.

Finally, Holder *et al.* (2002) conclude that there is evidence to suggest that both the information and overreaction hypotheses are valid. However, the overreaction hypothesis seems to be more appropriate at explaining the market volatility causing limit moves. The fact that the true futures price deviates from the actual futures price on average three hours prior to a limit move implies that price limit moves may be predicted.

Chapter 10

Conclusions

This study investigates the stochastic behaviour of white maize, yellow maize and wheat futures. The futures price is modelled, using the Sørensen model, as the sum of two stochastic state variables and a deterministic seasonal component.

Model parameters are estimated using the state space formulation and applying the Kalman filter methodology. Data for white maize, yellow maize wheat futures prices from SAFEX is used. The dataset for white and yellow maize constitutes weekly closing prices for the period 08 January 1997 to 31 May 2006 and the dataset for wheat comprises weekly closing prices for the period 07 January to 31 May 2006.

White and yellow maize futures prices are shown to peak for March and December expiry and dip for July and September expiry. Wheat futures on the other hand are shown to peak for July expiry and dip for December expiry. The specific seasonality of each agricultural commodity is caused by their specific harvesting season.

The estimated model parameters also give insight into the shape of the futures curve for the various commodities. White maize, yellow maize and wheat futures prices are all shown to exhibit contango.

Parameters are also estimated using different samples of the data. One sample excludes prices for the period 22 August 2001 to 19 February 2003, the period corresponding to the sharp decline in the value of the rand and its subsequent recovery. Another sample constituted futures prices converted to their equivalent dollar price. The resulting parameters estimates are similar to the estimates using the full dataset, suggesting a strong persistence of the

dynamics of the model for each commodity.

The seasonal parameters, and hence implied seasonal components, of the model are shown to be consistent with the time series data of futures prices. These parameters are very robust with regards to the choice of the initial parameters. However, the non-seasonal parameters, specifically the drift parameters, do not seem to be consistent with the data. The drift parameters for white and yellow maize futures are inconsistent with the actual evolution of prices over the sample period. Moreover, the risk premium parameters for white and yellow maize suggest an unreasonable shape of the futures curve.

These questionable parameter estimates are possibly a result of the high volatility of the futures prices over the sample period or the small size of the sample. A simulated dataset of futures prices is established in order to test the accurateness of the parameter estimation procedure. Parameters are predefined and futures prices are attained using the dynamics of the Sørensen model. The resulting parameter estimates for the simulated dataset indicate that the seasonal parameter estimates are highly accurate and robust. The non-seasonal parameter estimates are shown to produce sufficiently accurate approximations to the true parameters to suggest that the estimation procedure is correct. This is especially so, considering that futures prices, under the Sørensen model, are modelled as a function of two stochastic state variables. Thus a certain degree of inaccuracy in the parameter estimates is not unexpected. However, the risk premium parameter estimates, and to a lesser extent the drift parameter estimates, are unreasonably inaccurate for both the simulated dataset and for white and yellow maize futures. As a result, the optimisation procedure, including the 'fmincon' Matlab numerical optimisation function, is questionable under circumstances of high volatility and small sample sizes.

The natural extension to this study is the modelling and parameter estimation of agricultural futures for a greater sample of futures prices. The history of agricultural futures traded on the SAFEX only dates back to May 1996. Consequently, including daily prices and all traded contracts, not just closest- and farthest-to-maturity, are the only means by which to attain larger sample sizes. Other possible extensions include the comparison of different models for commodity derivative valuation as well as incorporating price limits into futures price formulae.

Bibliography

Bjerksund, P. (1991). Contingent claims evaluation when the convenience yield is stochastic: Analytical results, working paper.

Black, F. (1975). The pricing of commodity contracts. *Journal of Financial Econometrics*.

Black, F. & Scholes, M. (1973). The pricing of options and corporate liabilities. *Journal of Political Economy*, **81**, 637–654.

Brennan, F. (1986). The costs of convenience and the pricing of commodity contingent claims, working Paper.

Cox, J.C., Ingersoll, J.E. & Ross, S.A. (1981). The relation between forward prices and futures prices. *Journal of Financial Economics*, **9(4)**, 321–346.

Fama, E. & French, K. (1987). Commodity futures prices: Some evidence on forecast power, premiums, and the theory of storage. *Journal of Business*, **60(1)**, 55–73.

Fama, E. & French, K. (1988). Business cycles and the behavior of metals prices. *Journal of Finance*, **43**, 1075–1094.

Gibson, R. & Schwartz, E.S. (1990). Stochastic convenience yield and the pricing of oil contingent claims. *Journal of Finance*, **45**, 959–976.

Harvey, A.C. (1989). *Forecasting, Structural Time Series Models and the Kalman Filter*. Cambridge University Press.

Holder, M.E., Ma, C.K. & Mallet, J.E. (2002). Futures price limit moves as options. *The Journal of Futures Markets*, **22(9)**, 901–913.

Jamshidian, F. & Fein, M. (1990). Closed-form solutions for oil futures and european options in the gibson-schwartz model, working Paper.

Korn, O. (2005). Drift matters: An analysis of commodity derivatives. *Journal of Futures Markets*, **25(3)**, 211–241.

Laughton, D.G. & Jacoby, H.D. (1993). Reversion, timing options, and long-term decision making. *Financial Management*, **33**, 225–240.

Laughton, D.G. & Jacoby, H.D. (1995). *The effects of reversion on commodity projects of different length*, vol. Real Options in Capital Investment: Models, Strategies and Applications. Prager, Westport, CT.

Schwartz, E.S. (1997). The stochastic behavior of commodity prices: Implications for valuation and hedging. *Journal of Finance*, **52**, 923–973.

Schwartz, E.S. & Smith, J.E. (2000). Short-term variations and long-term dynamics in commodity prices. *Management Science*, **46(7)**, 893–911.

Sørensen, C. (2002). Modeling seasonality in agricultural commodity futures. *Journal of Futures Markets*, **22**, 393–426.

Appendix A

Properties and Derivations of Prices for the Sørensen Model

A.1 Real World Dynamics

The real world dynamics of the state variables x_t andz_t are as follows:

$$\begin{aligned} dx_t &= (\mu - \frac{1}{2}\sigma^2)dt + \sigma dW_{1t}, \\ dz_t &= -\kappa z_t dt + \nu dW_{2t}. \end{aligned}$$

These dynamics imply that

$$\begin{aligned} x_t - x_s &= \int_s^t (\mu - \frac{1}{2}\sigma^2)du + \int_s^t \sigma dW_{1u}, \\ z_t - z_s &= -\int_s^t \kappa z_u du + \int_s^t \nu dW_{2u}. \end{aligned}$$

Converting to the discrete form:

$$\begin{aligned} x_t - x_{t-\Delta t} &= (\mu - \frac{1}{2}\sigma^2)\Delta t + \sigma(W_{1t} - W_{1(t-\Delta t)}) \\ &= (\mu - \frac{1}{2}\sigma^2)\Delta t + \sigma W_{1\Delta t}, \\ z_t - z_{t-\Delta t} &= -\kappa z_{t-\Delta t}\Delta t + \nu W_{2\Delta t}. \end{aligned}$$

Let $\Delta t = \frac{t}{n}$:

$$\begin{aligned}
\Rightarrow x_n - x_{n-1} &= (\mu - \frac{1}{2}\sigma^2)\Delta t + \sigma(W_{1t} - W_{1(t-\Delta t)}) \\
x_n &= x_{n-1} + (\mu - \frac{1}{2}\sigma^2)\Delta t + \sigma W_{1\Delta t}, \\
z_n &= z_{n-1} - \kappa z_{n-1}\Delta t + \nu W_{2\Delta t} \\
&= z_{n-1}(1 - \kappa\Delta t) + \nu W_{2\Delta t}.
\end{aligned}$$

In vector form:

$$Y_n = \begin{bmatrix} x_n \\ z_n \end{bmatrix} + \begin{bmatrix} 1 & 0 \\ 0 & 1 - \kappa\Delta t \end{bmatrix} \begin{bmatrix} x_{n-1} \\ z_{n-1} \end{bmatrix} + \begin{bmatrix} \sigma W_{1\Delta t} \\ \nu W_{2\Delta t} \end{bmatrix}.$$

i.e..

$$\mathbf{Y}_n = \mathbf{C} + \mathbf{Q}\mathbf{Y}_{n-1} + \eta,$$

where

$$\begin{aligned}
\mathbf{C} &= \begin{bmatrix} (\mu - \frac{1}{2}\sigma^2)\Delta t \\ 0 \end{bmatrix}, \\
\mathbf{Q} &= \begin{bmatrix} 1 & 0 \\ 0 & 1 - \kappa\Delta t \end{bmatrix} \\
&= \begin{bmatrix} 1 & 0 \\ 0 & \phi \end{bmatrix}, \\
\phi &= 1 - \kappa\Delta t, \\
\eta &= \begin{bmatrix} \sigma W_{1\Delta t} \\ \nu W_{2\Delta t} \end{bmatrix}, \\
\mathrm{E}[\eta] &= 0, \\
\mathrm{Cov}[\eta] &= \begin{bmatrix} \sigma^2\Delta t & \rho\sigma\nu\Delta t \\ \rho\sigma\nu\Delta t & \nu^2\Delta t \end{bmatrix} = \mathbf{W}.
\end{aligned}$$

This is clearly a recursive representation. Assume $\mathbf{Y}_0 = (x_0, z_0)'$ is known and $Var(\mathbf{Y}_0) = 0$.

$$\begin{aligned}
\mathbf{Y}_{n-1} &= \mathbf{C} + \mathbf{Q}\mathbf{Y}_{n-2} + \eta \\
\mathbf{Y}_n &= \mathbf{C} + \mathbf{Q}(\mathbf{C} + \mathbf{Q}\mathbf{Y}_{n-2} + \eta) + \eta \\
&= \mathbf{C} + \mathbf{Q}\mathbf{C} + \mathbf{Q}^2\mathbf{Y}_{n-2} + \mathbf{Q}\eta + \eta \\
&\vdots \\
&= \mathbf{C} + \mathbf{Q}\mathbf{C} + \ldots + \mathbf{Q}^{n-1}\mathbf{C} + \mathbf{Q}^n\mathbf{Y}_0 + \eta + \mathbf{Q}\eta + \ldots + \mathbf{Q}^{n-1}\eta.
\end{aligned}$$

Now

$$\begin{aligned}
\mathbf{C} &= \begin{bmatrix} (\mu - \frac{1}{2}\sigma^2)\Delta t \\ 0 \end{bmatrix}, \\
\mathbf{QC} &= \begin{bmatrix} (\mu - \frac{1}{2}\sigma^2)\Delta t \\ 0 \end{bmatrix} \begin{bmatrix} 1 & 0 \\ 0 & \phi \end{bmatrix} = \mathbf{C}, \\
\mathbf{Q}^n &= \begin{bmatrix} 1 & 0 \\ 0 & \phi \end{bmatrix}^n \\
&= \begin{bmatrix} 1 & 0 \\ 0 & \phi^n \end{bmatrix}, \\
\mathbf{Q}^n\mathbf{C} &= \mathbf{C}, \\
\Rightarrow \mathbf{Y}_n &= \mathbf{C} + \ldots + \mathbf{C} + \begin{bmatrix} 1 & 0 \\ 0 & \phi^n \end{bmatrix} \begin{bmatrix} x_0 \\ z_0 \end{bmatrix} + (1 + \mathbf{Q} + \ldots + \mathbf{Q}^{n-1})\eta.
\end{aligned}$$

Therefore:

$$\begin{aligned}
\mathrm{E}[\mathbf{Y}_n|\mathbf{Y}_0] &= \begin{bmatrix} n(\mu - \frac{1}{2}\sigma^2)\Delta t \\ 0 \end{bmatrix} + \begin{bmatrix} x_0 \\ \phi^n z_0 \end{bmatrix} \\
&= \begin{bmatrix} n(\mu - \frac{1}{2}\sigma^2)\Delta t + x_0 \\ \phi^n z_0 \end{bmatrix},
\end{aligned}$$

and

$$\begin{aligned}
\mathrm{Var}[\mathbf{Y}_n|\mathbf{Y}_0] &= \mathrm{Var}[\eta + \mathbf{Q}\eta + \mathbf{Q}^2\eta + \ldots + \mathbf{Q}^{n-1}\eta] \\
&= \mathrm{Var}[\eta] + \mathrm{Var}[\mathbf{Q}\eta] + \ldots + \mathrm{Var}[\mathbf{Q}^{n-1}\eta] \\
&= \mathrm{Var}[\eta] + \mathbf{Q}\mathrm{Var}[\eta]\mathbf{Q}' + \ldots + \mathbf{Q}^{n-1}\mathrm{Var}[\eta][\mathbf{Q}^{n-1}]' \\
&= \mathbf{W} + \mathbf{QWQ}' + \ldots + \mathbf{Q}^{n-1}\mathbf{W}[\mathbf{Q}^{n-1}]'.
\end{aligned}$$

Note:

$$\begin{aligned}
\mathbf{Q} &= \begin{bmatrix} 1 & 0 \\ 0 & \phi \end{bmatrix}, \\
\mathbf{Q}^n &= \begin{bmatrix} 1 & 0 \\ 0 & \phi^n \end{bmatrix} \\
&= [\mathbf{Q}^n]'.
\end{aligned}$$

Now,

$$\mathbf{QWQ}' = \begin{bmatrix} 1 & 0 \\ 0 & \phi \end{bmatrix} \begin{bmatrix} \sigma^2\Delta t & \rho\sigma\nu\Delta t \\ \rho\sigma\nu\Delta t & \nu^2\Delta t \end{bmatrix} \begin{bmatrix} 1 & 0 \\ 0 & \phi \end{bmatrix}$$

$$\begin{aligned} &= \begin{bmatrix} 1 & 0 \\ 0 & \phi \end{bmatrix} \begin{bmatrix} \sigma^2\Delta t & \phi\rho\sigma\nu\Delta t \\ \rho\sigma\nu\Delta t & \phi\nu^2\Delta t \end{bmatrix} \\ &= \begin{bmatrix} \sigma^2\Delta t & \phi\rho\sigma\nu\Delta t \\ \phi\rho\sigma\nu\Delta t & \phi^2\nu^2\Delta t \end{bmatrix}, \\ \Rightarrow \mathbf{Q}^n\mathbf{W}[\mathbf{Q}^n]' &= \begin{bmatrix} \sigma^2\Delta t & \phi^n\rho\sigma\nu\Delta t \\ \phi^n\rho\sigma\nu\Delta t & \phi^{2n}\nu^2\Delta t \end{bmatrix}. \end{aligned}$$

Therefore:

$$\mathrm{Var}[\mathbf{Y}_n|\mathbf{Y}_0] = \begin{bmatrix} \sigma^2\Delta t & \sum_{i=0}^{n-1}\phi^i\rho\sigma\nu\Delta t \\ \sum_{i=0}^{n-1}\phi^i\rho\sigma\nu\Delta t & \sum_{i=0}^{n-1}\phi^{2i}\nu^2\Delta t \end{bmatrix},$$

but

$$\begin{aligned} \sum_{i=0}^{n-1}\phi^i &= \frac{1-\phi^{n-1}}{1-\phi}, \\ \text{and} \qquad \sum_{i=0}^{n-1}\phi^{2i} &= \frac{1-\phi^{2n-1}}{1-\phi^2}. \end{aligned}$$

Hence:

$$\mathrm{Var}[\mathbf{Y}_n|\mathbf{Y}_0] = \begin{bmatrix} \sigma^2\Delta t & (\frac{1-\phi^{n-1}}{1-\phi})\rho\sigma\nu\Delta t \\ (\frac{1-\phi^{n-1}}{1-\phi})\rho\sigma\nu\Delta t & (\frac{1-\phi^{2n-1}}{1-\phi^2})\nu^2\Delta t \end{bmatrix}.$$

Now let $n \to \infty$, $\Delta t = \frac{t}{n} \to 0$,

$$\begin{aligned} \phi^n &= (1-\kappa\Delta t)^n \\ &= (1-\kappa\frac{t}{n})^n \\ &\to e^{-\kappa t}, \\ \text{and} \qquad \phi^{2n} &\to e^{-2\kappa t}. \end{aligned}$$

Then,

$$\begin{aligned} (\frac{1-\phi^{n-1}}{1-\phi})\Delta t &\to \frac{1-e^{-\kappa t}}{\kappa}, \\ \text{and} \qquad (\frac{1-\phi^{2n-1}}{1-\phi^2})\Delta t &\to \frac{1-e^{-2\kappa t}}{2\kappa}. \end{aligned}$$

Thus

$$\mathrm{Var}[\mathbf{Y}_t|\mathbf{Y}_0] = \mathrm{Var}\left[\begin{array}{c|c} x_t & x_0 \\ z_t & z_0 \end{array}\right] = \begin{bmatrix} \sigma^2 t & (\frac{1-e^{-\kappa t}}{\kappa})\rho\sigma\nu \\ (\frac{1-e^{-\kappa t}}{\kappa})\rho\sigma\nu & (\frac{1-e^{-2\kappa t}}{2\kappa})\nu^2 \end{bmatrix}.$$

Also,

$$\begin{aligned} \mathrm{E}[\mathbf{Y}_n|\mathbf{Y}_0] &= \mathrm{E}\left[\begin{array}{c|c} x_n & x_0 \\ z_n & z_0 \end{array}\right] = \left[\begin{array}{c} x_0 + n(\mu - \frac{1}{2}\sigma^2)\Delta t \\ \phi^n z_0 \end{array}\right], \\ \Rightarrow \mathrm{E}[\mathbf{Y}_t|\mathbf{Y}_0] &= \mathrm{E}\left[\begin{array}{c|c} x_t & x_0 \\ z_t & z_0 \end{array}\right] = \left[\begin{array}{c} x_0 + t(\mu - \frac{1}{2}\sigma^2) \\ e^{-\kappa t} z_0 \end{array}\right]. \end{aligned}$$

$\mathrm{E}[\mathbf{Y}_t|\mathcal{F}_0]$ and $\mathrm{Var}[\mathbf{Y}_t|\mathcal{F}_0]$ can be rewritten as $\mathrm{E}[\mathbf{Y}_t|\Im_0]$ and $\mathrm{Var}[\mathbf{Y}_t|\Im_0]$ respectively. $\mathcal{F}_0$ is the filtration at time 0 and contains all information known at that time. In this case $\mathcal{F}_0$ contains information about the state variables x_0 and z_0, i.e. $\mathbf{Y}_0 = (x_0, z_0)'$.

At this point we can generalise the expectation and variance of $\mathbf{Y}_t$ for valuation at any time period s where $0 \leq s \leq t$. i.e.. $\mathrm{E}[\mathbf{Y}_t|\mathcal{F}_s]$ and $\mathrm{Var}[\mathbf{Y}_n|\mathcal{F}_s]$ where $\mathcal{F}_s$, the filtration at time period s, contains all known information at time period s, specifically $\mathbf{Y}_s = (x_s, z_s)'$.

$$\mathrm{E}[\mathbf{Y}_t|\mathbf{Y}_s] = \mathrm{E}\left[\begin{array}{c|c} x_t & x_s \\ z_t & z_s \end{array}\right] = \left[\begin{array}{c} x_s + (t-s)(\mu - \frac{1}{2}\sigma^2) \\ e^{-\kappa(t-s)} z_s \end{array}\right],$$

$$\mathrm{Var}[\mathbf{Y}_t|\mathbf{Y}_s] = \mathrm{Var}\left[\begin{array}{c|c} x_t & x_s \\ z_t & z_s \end{array}\right] = \left[\begin{array}{cc} \sigma^2(t-s) & (\frac{1-e^{-\kappa(t-s)}}{\kappa})\rho\sigma\nu \\ (\frac{1-e^{-\kappa(t-s)}}{\kappa})\rho\sigma\nu & (\frac{1-e^{-2\kappa(t-s)}}{2\kappa})\nu^2 \end{array}\right].$$

From here on all results are presented in the more general form, i.e.. conditional on information know at time period s where $0 \leq s \leq t$.

Now that the expectation and variance of the state variables have been derived, the properties of the log spot price p_t can be derived as well. p_t is normally distributed with mean and variance:

$$\begin{aligned} \mathrm{E}[p_t|\mathcal{F}_s] &= \mathrm{E}[lnP_t|\mathcal{F}_s] \\ &= \mathrm{E}[s(t) + x_t + z_t|\mathcal{F}_s] \\ &= \mathrm{E}[x_t|\mathcal{F}_s] + \mathrm{E}[z_t|\mathcal{F}_s] + \mathrm{E}[s(t)|\mathcal{F}_s] \\ &= x_s + (t-s)(\mu - \frac{1}{2}\sigma^2) + e^{-\kappa(t-s)} z_s + s(t), \end{aligned}$$

$$\begin{aligned} \mathrm{Var}[p_t|\mathcal{F}_s] &= \mathrm{Var}[lnP_t|\mathcal{F}_s] \\ &= \mathrm{Var}[s(t) + x_t + z_t|\mathcal{F}_s] \\ &= \mathrm{Var}[x_t + z_t|\mathcal{F}_s] \\ &= \mathrm{Var}[x_t|\mathcal{F}_s] + \mathrm{Var}[z_t|\mathcal{F}_s] + 2\mathrm{Cov}[x_t z_t|\mathcal{F}_s] \\ &= \sigma^2(t-s) + (\frac{1-e^{-2\kappa(t-s)}}{2\kappa})\nu^2 + 2(\frac{1-e^{-\kappa(t-s)}}{\kappa})\rho\sigma\nu. \end{aligned}$$

The spot price P_t conditioned at time s is thus lognormally distributed with mean $\mathrm{E}[P_t|\mathcal{F}_s]$ and variance $\mathrm{Var}[P_t|\mathcal{F}_s]$.

Only concerned with $\mathrm{E}[P_t|\mathcal{F}_s]$:

$$\begin{aligned}
\mathrm{E}[P_t|\mathcal{F}_s] &= exp\{\mathrm{E}[p_t|\mathcal{F}_s] + \frac{1}{2}\mathrm{Var}[p_t|\mathcal{F}_s]\} \\
&= exp\{(t-s)(\mu - \frac{1}{2}\sigma^2) + x_s + s(t) + e^{-\kappa(t-s)}z_s \\
&\quad + \frac{1}{2}[\sigma^2(t-s) + (\frac{1-e^{-2\kappa(t-s)}}{2\kappa})\nu^2 + 2(\frac{1-e^{-\kappa(t-s)}}{\kappa})\rho\sigma\nu]\} \\
&= exp\{\mu(t-s) + x_s + s(t) + e^{-\kappa(t-s)}z_s \\
&\quad + \frac{1}{2}[(\frac{1-e^{-2\kappa(t-s)}}{2\kappa})\nu^2 + 2(\frac{1-e^{-\kappa(t-s)}}{\kappa})\rho\sigma\nu]\} \\
&= e^{\mu(t-s)}exp\{x_s + s(t) + e^{-\kappa(t-s)}z_s \\
&\quad + \frac{1}{2}[(\frac{1-e^{-2\kappa(t-s)}}{2\kappa})\nu^2 + 2(\frac{1-e^{-\kappa(t-s)}}{\kappa})\rho\sigma\nu]\}.
\end{aligned}$$

A.2 Risk-Neutral Dynamics

The risk-neutral dynamics of the state variables x_t andz_t are as follows:

$$\begin{aligned}
dx_t &= (\mu - \lambda_x - \frac{1}{2}\sigma^2)dt + \sigma dW_{1t}^Q, \\
dz_t &= -(\lambda_z + \kappa z_t)dt + \nu dW_{2t}^Q.
\end{aligned}$$

Following a similar derivation as that for the real world dynamics, it can be shown that the state variables have the following properties.

$(x_t, z_t)'$ is normally distributed with mean and variance:

$$\begin{aligned}
\mathrm{E}^*[\mathbf{Y}_t|\mathcal{F}_s] &= \mathrm{E}^*\begin{bmatrix} x_t \\ z_t \end{bmatrix} = \begin{bmatrix} x_s + (t-s)(\mu - \frac{1}{2}\sigma^2 - \lambda_x) \\ e^{-\kappa(t-s)}z_s - (1-e^{-\kappa(t-s)})\frac{\lambda_z}{\kappa} \end{bmatrix}, \\
\mathrm{Var}^*[\mathbf{Y}_t|\mathcal{F}_s] &= \mathrm{Var}[\mathbf{Y}_t|\mathcal{F}_s] \\
&= \mathrm{Var}\begin{bmatrix} x_t \\ z_t \end{bmatrix} \\
&= \begin{bmatrix} \sigma^2(t-s) & (\frac{1-e^{-\kappa(t-s)}}{\kappa})\rho\sigma\nu \\ (\frac{1-e^{-\kappa(t-s)}}{\kappa})\rho\sigma\nu & (\frac{1-e^{-2\kappa(t-s)}}{2\kappa})\nu^2 \end{bmatrix}.
\end{aligned}$$

From this we can derive the properties of the log spot price p_t. p_t is normally distributed with mean and variance:

$$\begin{aligned}
\mathrm{E}^*[p_t|\mathcal{F}_s] &= \mathrm{E}^*[lnP_t|\mathcal{F}_s] \\
&= \mathrm{E}^*[s(t)+x_t+z_t|\mathcal{F}_s] \\
&= \mathrm{E}^*[s(t)|\mathcal{F}_s]+\mathrm{E}^*[x_t|\mathcal{F}_s]+\mathrm{E}^*[z_t|\mathcal{F}_s] \\
&= s(t)+x_s+(t-s)(\mu-\frac{1}{2}\sigma^2-\lambda_x)+e^{-\kappa(t-s)}z_s \\
&\quad -(1-e^{-\kappa(t-s)})\frac{\lambda_z}{\kappa},
\end{aligned}$$

$$\begin{aligned}
\mathrm{Var}^*[p_t|\mathcal{F}_s] &= \mathrm{Var}[p_t|\mathcal{F}_s] \\
&= \sigma^2(t-s)+(\frac{1-e^{-2\kappa(t-s)}}{2\kappa})\nu^2+2(\frac{1-e^{-\kappa(t-s)}}{\kappa})\rho\sigma\nu.
\end{aligned}$$

Again, the spot price P_t conditional on information at time s is lognormally distributed with mean $\mathrm{E}^*[P_t|\mathcal{F}_s]$ and variance $\mathrm{Var}^*[P_t|\mathcal{F}_s]$.

Again, only concerned with $\mathrm{E}^*[P_t|\mathcal{F}_s]$:

$$\begin{aligned}
\mathrm{E}^*[P_t|\mathcal{F}_s] &= exp\{\mathrm{E}^*[p_t|\mathcal{F}_s]+\frac{1}{2}\mathrm{Var}^*[p_t|\mathcal{F}_s]\} \\
&= exp\{\mathrm{E}^*[p_t|\mathcal{F}_s]+\frac{1}{2}\mathrm{Var}[p_t|\mathcal{F}_s]\} \\
&= exp\{(t-s)(\mu-\frac{1}{2}\sigma^2-\lambda_x)+x_s+s(t) \\
&\quad +e^{-\kappa(t-s)}z_s-(1-e^{-\kappa(t-s)})\frac{\lambda_z}{\kappa} \\
&\quad +\frac{1}{2}[\sigma^2(t-s)+(\frac{1-e^{-2\kappa(t-s)}}{2\kappa})\nu^2+2(\frac{1-e^{-\kappa(t-s)}}{\kappa})\rho\sigma\nu]\} \\
&= exp\{(\mu-\lambda_x)(t-s)+x_s+s(t) \\
&\quad +e^{-\kappa(t-s)}z_s-(1-e^{-\kappa(t-s)})\frac{\lambda_z}{\kappa} \\
&\quad +\frac{1}{2}[(\frac{1-e^{-2\kappa(t-s)}}{2\kappa})\nu^2+2(\frac{1-e^{-\kappa(t-s)}}{\kappa})\rho\sigma\nu]\} \\
&= exp[(\mu-\lambda_x)(t-s)+x_s+s(t)+e^{-\kappa(t-s)}z_s \\
&\quad -(1-e^{-\kappa(t-s)})(\frac{\lambda_z-\rho\sigma\nu}{\kappa})+\frac{\nu^2}{4}(\frac{1-e^{-2\kappa(t-s)}}{\kappa})].
\end{aligned} \tag{A.1}$$

Now the formula of the future price $F_t(T)$ can be obtained:

$$\begin{aligned} F_t(T) &= \mathrm{E}^*[P_t(T)] \\ &= exp[(\mu-\lambda_x)(T-t)+x_t+s(T)+e^{-\kappa(T-t)}z_t \\ &\quad -(1-e^{-\kappa(T-t)})(\frac{\lambda_z-\rho\sigma\nu}{\kappa})+\frac{\nu^2}{4}(\frac{1-e^{-2\kappa(T-t)}}{\kappa})] \\ &= exp[s(T)+A(T-t)+x_t+z_te^{-\kappa(T-t)}], \end{aligned}$$

where

$$A(T-t)=(\mu-\lambda_x)(T-t)-\frac{\lambda_z-\rho\sigma\nu}{\kappa}(1-e^{-\kappa(T-t)})+\frac{\nu^2}{4\kappa}(1-e^{-2\kappa(T-t)}).$$

Also, the futures price $f_t(T)$ is normally distributed with mean and variance:

$$\begin{aligned} \mathrm{E}^*[f_t(T)|\mathcal{F}_s] &= \mathrm{E}^*[lnF_t(T)|\mathcal{F}_s] \\ &= \mathrm{E}^*[s(T)+A(T-t)+x_t+z_te^{-\kappa(T-t)}|\mathcal{F}_s] \\ &= s(T)+A(T-t)+\mathrm{E}^*[x_t|\mathcal{F}_s]+e^{-\kappa(T-t)}\mathrm{E}^*[z_t|\mathcal{F}_s] \\ &= s(T)+A(T-t)+x_s+(t-s)(\mu-\frac{1}{2}\sigma^2-\lambda_x) \\ &\quad +e^{-\kappa(T-t)}[e^{-\kappa(t-s)}z_s-(1-e^{-\kappa(t-s)})\frac{\lambda_z}{\kappa}] \\ &= s(T)+A(T-t)+x_s+(t-s)(\mu-\frac{1}{2}\sigma^2-\lambda_x) \\ &\quad +e^{-\kappa(T-s)}z_s-e^{-\kappa(T-t)}[1-e^{-\kappa(t-s)}]\frac{\lambda_z}{\kappa} \\ &= s(T)+A(T-t)+x_s+(t-s)(\mu-\frac{1}{2}\sigma^2-\lambda_x) \\ &\quad +e^{-\kappa(T-s)}z_s+[e^{-\kappa(T-s)}-e^{-\kappa(T-t)}]\frac{\lambda_z}{\kappa}, \end{aligned}$$

$$\begin{aligned} \mathrm{Var}^*[f_t(T)|\mathcal{F}_s] &= \mathrm{Var}^*[lnF_t(T)|\mathcal{F}_s] \\ &= \mathrm{Var}^*[s(T)+A(T-t)+x_t+z_te^{-\kappa(T-t)}|\mathcal{F}_s] \\ &= \mathrm{Var}^*[x_t+z_te^{-\kappa(T-t)}|\mathcal{F}_s] \\ &= \mathrm{Var}[x_t+z_te^{-\kappa(T-t)}|\mathcal{F}_s] \\ &= \mathrm{Var}[f_t(T)|\mathcal{F}_s] \\ &= \sigma^2(t-s)+\frac{e^{-2\kappa T}}{2\kappa}\nu^2(e^{2\kappa t}-e^{2\kappa s})+\frac{2e^{-\kappa T}}{\kappa}\rho\sigma\nu(e^{\kappa t}-e^{\kappa s}). \end{aligned}$$

Appendix B

Derivation of Option Prices

Option prices are derived here where the underlying is a futures contract. 2 different differential equations (DE's) yield different formulae for option prices. Firstly, The Standard Black DE produces formulae for European options. The second method uses the SAFEX Black DE.

B.1 Standard Black

The general form of the value of a European option on a future is as follows:

$$C_{\mathrm{E}} = e^{-r\tau}[FN(d_1) - KN(d_2)], \tag{B.1}$$
$$P_{\mathrm{E}} = e^{-r\tau}[KN(-d_2) - FN(-d_1)], \tag{B.2}$$

where

$$d_1 = \frac{\ln(F/K) + (\sigma^2/2)\tau}{\sigma\sqrt{\tau}},$$
$$d_2 = \frac{\ln(F/K) - (\sigma^2/2)\tau}{\sigma\sqrt{\tau}}.$$

C_{E} and P_{E} denote the value of a European call and a European put respectively. F is the current price of the underlying futures and K is the strike price. $\tau = T - t$ denotes the time to expiry of the option. σ^2 is the volatility of the underlying asset, in this case F. Hence, the term $\sigma^2\tau$ is the volatility of the underlying asset over the duration of the option. r is the prevailing risk-free rate and $N(x)$ denotes the cumulative normal standard normal integral, i.e..

$$N(x) = \frac{1}{\sqrt{2\pi}} \int_{-\infty}^{x} e^{-\frac{t^2}{2}} dt.$$

Note, B.1 and B.2 give values for the price of options at valuation time 0. The option expires at time τ, but the expiry of the underlying is not explicitly specified. The expiry of the underlying is factored into its price. In fact, $F = F_0(T_2)$ where τ_2 denotes the expiry of the futures contract.

Let t be the valuation date, T_1 be the expiry of the option contract, and T_2 be the expiry of the underlying futures contract. Note, $T_1 \leq T_2$.

Consider firstly a valuation date of $t = 0$. It is assumed that information about the state variables x_0 and z_0 is known.

Before proceeding, two important results are needed:

Firstly,

$$F_0(T_2) = \mathrm{E}^*[F_{T_1}(T_2)|\mathcal{F}_0]. \tag{B.3}$$

The proof of B.3 follows by considering the left-hand side (LHS) and right-hand side (RHS) separately.

$$\begin{aligned} LHS &= F_0(T_2) \\ &= \mathrm{E}^*[P(T_2)|\mathcal{F}_0]. \end{aligned}$$

$$\begin{aligned} RHS &= \mathrm{E}^*[F_{T_1}(T_2)|\mathcal{F}_0] \\ &= \mathrm{E}^*\{\mathrm{E}^*[P(T_2)|\mathcal{F}_{T_1}]|\mathcal{F}_0\} \\ &= \mathrm{E}^*[P(T_2)|\mathcal{F}_{T_1}|\mathcal{F}_0] \\ &= \mathrm{E}^*[P(T_2)|\mathcal{F}_0]. \end{aligned}$$

Clearly LHS = RHS. This implies that under risk-neutral valuation the current futures price $f_0(T_2)$ is equal to the expected futures price $\mathrm{E}^*[F_{T_1}(T_2)|\mathcal{F}_0]$ at time T_1. In, fact it can be shown that $f_0(T_2)$ is equal to to the expected futures price $\mathrm{E}^*[F_s(T_2)|\mathcal{F}_0]$ where s is any time between 0 and T_2, i.e.. $0 \leq s \leq T_2$.

This result is very important and is used in the derivation the price of an option on a future.

Secondly, the distribution of $f_{T_1}(T_2)$ conditioned at time 0 is needed. Recall equations **??** and **??**. $\phi = f_{T_1}(T_2)$ is normally distributed with mean and variance:

$$\begin{aligned}\mu_\phi(0,T_1,T_2) &= \mathrm{E}^*[f_{T_1}(T_2)|\mathcal{F}_0] \\ &= s(T_2) + A(T_2-T_1) + x_0 + T_1(\mu - \frac{1}{2}\sigma^2 - \lambda_x) + e^{-\kappa T_2}z_0 \\ &\quad + [e^{-\kappa T_2} - e^{-\kappa(T_2-T_1)}]\frac{\lambda_z}{\kappa},\end{aligned}$$

$$\begin{aligned}\sigma^2_\phi(0,T_1,T_2) &= \mathrm{Var}^*[f_{T_1}(T_2)|\mathcal{F}_0] \\ &= \sigma^2 T_1 + \frac{e^{-2\kappa T_2}}{2\kappa}\nu^2(e^{2\kappa T_1}-1) + \frac{2e^{-\kappa T_2}}{\kappa}\rho\sigma\nu(e^{\kappa T_1}-1).\end{aligned}$$

Let $C_{\mathrm{E},0}$ and $P_{\mathrm{E},0}$ denote the value of a European call and a European put at valuation date $t = 0$ respectively.

$$\begin{aligned}C_{\mathrm{E},0} &= e^{-rT_1}\mathrm{E}^*[max(F_{T_1}(T_2) - K, 0)] \\ &\vdots \\ &= e^{-rT_1}[F_0(T_2)N(d_1) - KN(d_2)],\end{aligned} \tag{B.4}$$

and

$$\begin{aligned}P_{\mathrm{E},0} &= e^{-rT_1}\mathrm{E}^*[max(K - F_{T_1}(T_2), 0)] \\ &\vdots \\ &= e^{-rT_1}[KN(-d_2) - F_0(T_2)N(-d_1)],\end{aligned} \tag{B.5}$$

where

$$\begin{aligned}d_1 &= \frac{\ln(F_0(T_2)/K) + \sigma^2_\phi(0,T_1,T_2)/2}{\sigma_\phi(0,T_1,T_2)}, \\ d_2 &= \frac{\ln(F_0(T_2)/K) - \sigma^2_\phi(0,T_1,T_2)/2}{\sigma_\phi(0,T_1,T_2)}.\end{aligned}$$

Note, the term $\sigma_\phi(0,T_1,T_2)$ is equivalent to the term $\sigma\sqrt{\tau}$ used in general form.

The futures price $F_0(T_2)$ is that defined by equation 4.18.

Equations B.6 and B.6 present closed form solutions for option prices at valuation date 0.

The derivation of the above equations can be extended to allow for a valuation date t where $0 \leq t \leq T_1$. Again it is assumed that at the valuation date the state variables x_t and z_t are known.

The two results needed to derive the option prices are altered slightly:

Firstly,

$$F_t(T_2) = \mathrm{E}^*[F_{T_1}(T_2)|\mathcal{F}_t],$$

and secondly, the distribution of $\phi = f_{T_1}(T_2)$ conditioned at time t is normally distributed with mean and variance:

$$\begin{aligned}
\mu_\phi(t, T_1, T_2) &= \mathrm{E}^*[f_{T_1}(T_2)|\mathcal{F}_t] \\
&= s(T_2) + A(T_2 - T_1) + x_t + (T_1 - t)(\mu - \frac{1}{2}\sigma^2 - \lambda_x) + \\
&\quad e^{-\kappa(T_2-t)} z_t + [e^{-\kappa(T_2-t)} - e^{-\kappa(T_2-T_1)}]\frac{\lambda_z}{\kappa},
\end{aligned}$$

$$\begin{aligned}
\sigma^2_\phi(t, T_1, T_2) &= \mathrm{Var}^*[f_{T_1}(T_2)|\mathcal{F}_t] \\
&= \sigma^2(T_1 - t) + \frac{e^{-2\kappa T_2}}{2\kappa}\nu^2(e^{2\kappa T_1} - e^{2\kappa t}) + \frac{2e^{-\kappa T_2}}{\kappa}\rho\sigma\nu(e^{\kappa T_1} - e^{\kappa t}).
\end{aligned}$$

Now the values for the option prices at time t can be determined:

$$\begin{aligned}
C_{\mathrm{E},t} &= e^{-r(T_1-t)}[F_t(T_2)N(d_1) - KN(d_2)], \\
P_{\mathrm{E},t} &= e^{-r(T_1-t)}[KN(-d_2) - F_t(T_2)N(-d_1)],
\end{aligned}$$

where

$$\begin{aligned}
d_1 &= \frac{\ln(F_t(T_2)/K) + \sigma^2_\phi(t, T_1, T_2)/2}{\sigma_\phi(t, T_1, T_2)} \\
d_2 &= \frac{\ln(F_t(T_2)/K) - \sigma^2_\phi(t, T_1, T_2)/2}{\sigma_\phi(t, T_1, T_2)}
\end{aligned}$$

Again, $F_t(T_2)$ is defined by equation 4.18.

B.2 SAFEX Black

The general form of the solution to option prices using the SAFEX Black DE is presented:

$$\begin{aligned} C_{\mathrm{A}} &= [FN(d_1) - KN(d_2)], \\ P_{\mathrm{A}} &= [KN(-d_2) - FN(-d_1),] \end{aligned}$$

where

$$d_1 = \frac{\ln(F/K) + (\sigma^2/2)\tau}{\sigma\sqrt{\tau}},$$
$$d_2 = \frac{\ln(F/K) - (\sigma^2/2)\tau}{\sigma\sqrt{\tau}}.$$

The option price formulae for $C_{\mathrm{A},t}$ and $P_{\mathrm{A},t}$ follow similarly to the derivation of prices $C_{\mathrm{E},t}$ and $P_{\mathrm{E},t}$:

$$\begin{aligned} C_{\mathrm{A},t} &= [F_t(T_2)N(d_1) - KN(d_2)], \\ P_{\mathrm{A},t} &= [KN(-d_2) - F_t(T_2)N(-d_1)], \end{aligned}$$

where

$$d_1 = \frac{\ln(F_t(T_2)/K) + \sigma_\phi^2(t, T_1, T_2)/2}{\sigma_\phi(t, T_1, T_2)},$$
$$d_2 = \frac{\ln(F_t(T_2)/K) - \sigma_\phi^2(t, T_1, T_2)/2}{\sigma_\phi(t, T_1, T_2)}.$$

The terms $F_t(T_2)$ and $\sigma_\phi^2(t, T_1, T_2)$ have the same meaning as in the Standard Black model.

Appendix C

Parameter Estimates For White Maize Futures

	$K=1$	$K=2$	$K=3$
μ	0.0920	0.0815	0.0700
κ	0.7282	0.6283	0.6268
σ	0.4591	0.4986	0.4974
ν	0.5242	0.5740	0.5720
ρ	-0.7341	-0.7817	-0.7803
λ_x	-0.0150	-0.0344	-0.0463
λ_z	-0.5151	-0.4580	-0.4288
x_1	5.5578	5.5449	5.5405
σ_e	0.0000	0.0001	0.0000
γ_1	0.0177	0.0198	-0.0109
γ_1^*	0.0160	0.0144	0.0065
γ_2		-0.0048	-0.0310
γ_2^*		0.0040	-0.0176
γ_3			0.0449
γ_3^*			-0.0448
l	1865.1	1870.2	1872.6
AIC	-3.7762	-3.7825	-3.7833
SC	-3.7214	-3.7178	-3.7725

Table C.1: Full set of parameter estimates together with the resulting values for the log likelihood function, l, and the information criterion AIC and SC. Estimates are obtained by means of maximum likelihood and Kalman filtering. Sample: Weekly closing prices for nearest- and farthest- to maturity white maize futures contracts. Sample Period: 08 Jan 1997 to 31 May 2006.

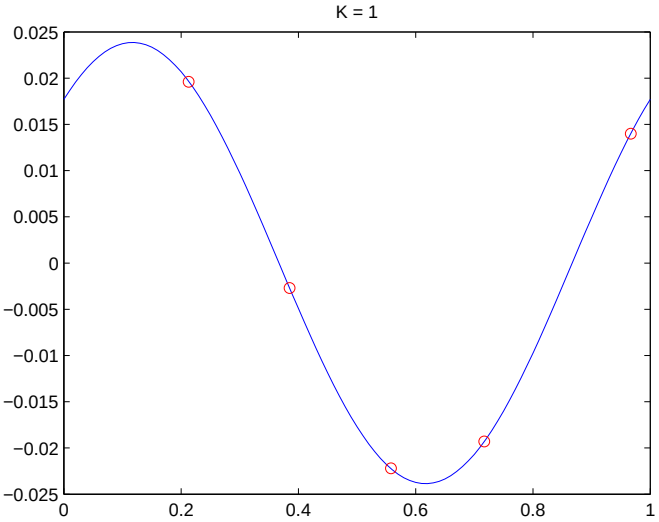

Figure C.1: Plot of $s(T)$ vs T for $K = 1$. $s(T)$ denotes the seasonal component of a futures contract expiring at T. Sample: Weekly closing prices for nearest- and farthest-to maturity white maize futures contracts. Sample period: 08 Jan 1997 to 31 May 2006.

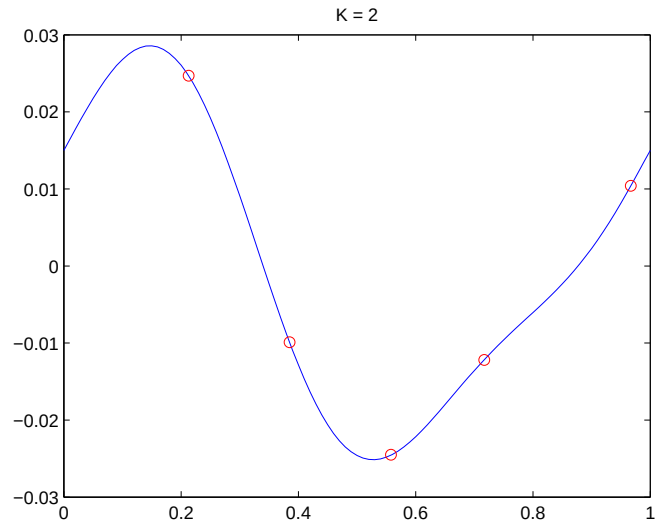

Figure C.2: Plot of $s(T)$ vs T for $K = 2$. $s(T)$ denotes the seasonal component of a futures contract expiring at T. Sample: Weekly closing prices for nearest- and farthest-to maturity white maize futures contracts. Sample period: 08 Jan 1997 to 31 May 2006.

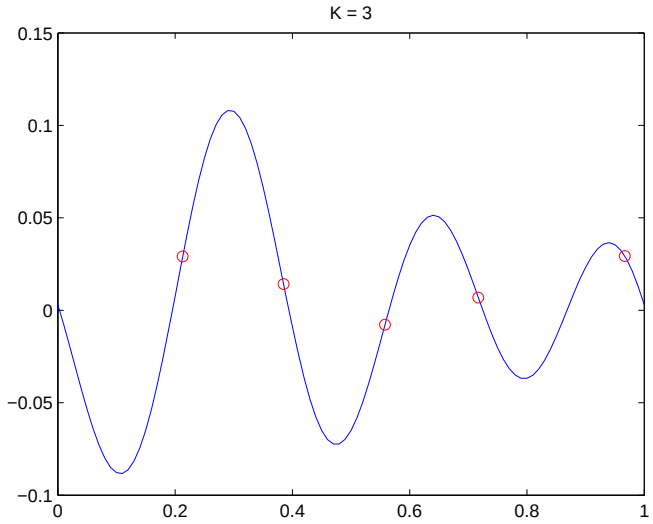

Figure C.3: Plot of $s(T)$ vs T for $K = 3$. $s(T)$ denotes the seasonal component of a futures contract expiring at T. Sample: Weekly closing prices for nearest- and farthest-to maturity white maize futures contracts. Sample period: 08 Jan 1997 to 31 May 2006.

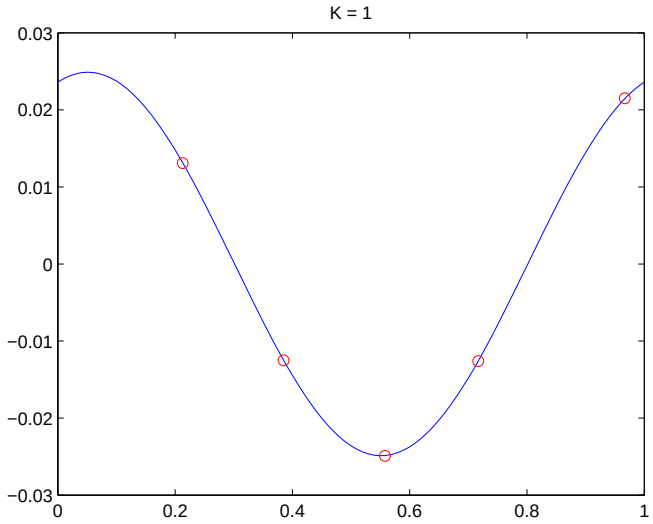

Figure C.4: Plot of $s(T)$ vs T for $K = 1$. $s(T)$ denotes the seasonal component of a futures contract expiring at T. Sample: Weekly closing nearest- and farthest- to maturity white maize futures prices. Sample Period: 08 Jan 1997 to 31 May 2006 excluding observations between the period 22 Aug 2001 to 19 Feb 2003.

	$K = 1$	$K = 2$
μ	0.2666	0.2365
κ	0.5199	0.5324
σ	0.5805	0.5572
ν	0.6623	0.6379
ρ	-0.8473	-0.8346
λ_x	0.1398	0.1213
λ_z	-0.3582	-0.3657
x_1	5.5834	5.6184
σ_e	0.0020	0.0032
γ_1	0.0236	0.0229
γ_1^*	0.0079	0.0058
γ_2		-0.0058
γ_2^*		-0.0045
l	1562.4	1565.5
AIC	-3.7655	-3.7682
SC	-3.7026	-3.6938

Table C.2: Full set of parameter estimates together with the resulting values for the log likelihood function, l, and the information criterion AIC and SC. Estimates are obtained by means of maximum likelihood and Kalman filtering. Sample: Weekly closing prices for nearest- and farthest- to maturity white maize futures contracts. Sample Period: 08 Jan 1997 to 31 May 2006 excluding observations between the period 22 Aug 2001 to 19 Feb 2003.

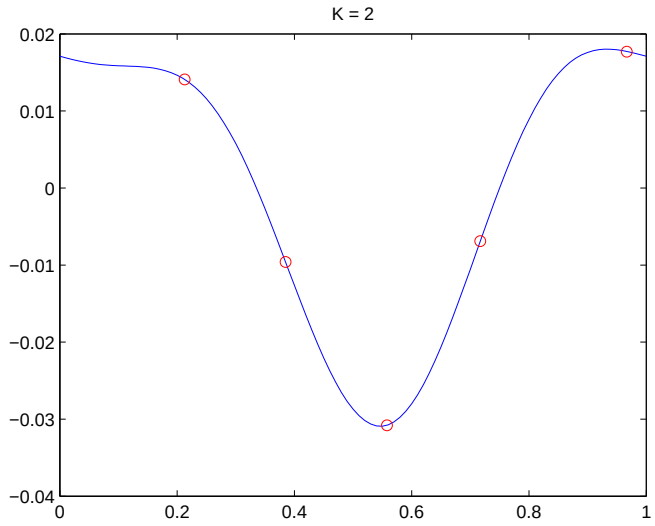

Figure C.5: Plot of $s(T)$ vs T for $K = 2$. $s(T)$ denotes the seasonal component of a futures contract expiring at T. Sample: Weekly closing prices for nearest- and farthest-to maturity white maize futures contracts. Sample Period: 08 Jan 1997 to 31 May 2006 excluding observations between the period 22 Aug 2001 to 19 Feb 2003.

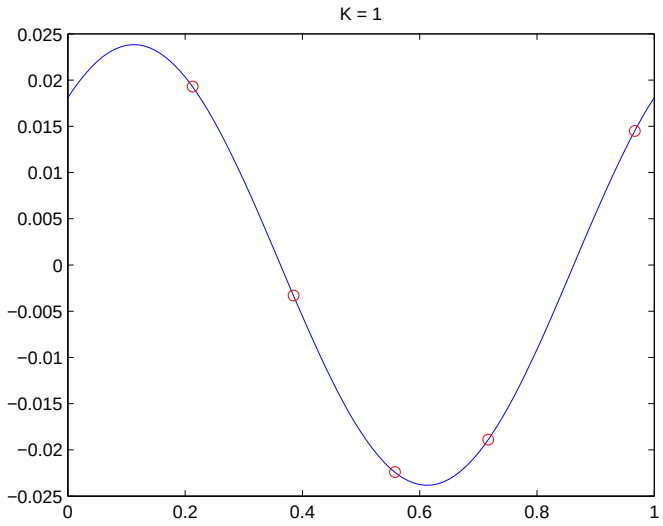

Figure C.6: Plot of $s(T)$ vs T for $K = 1$. $s(T)$ denotes the seasonal component of a futures contract expiring at T. Sample: Weekly closing prices for nearest- and farthest-to maturity white maize futures contracts converted to a dollar price. Sample Period: 08 Jan 1997 to 31 May 2006.

	$K = 1$	$K = 2$
μ	0.1037	-0.0859
κ	0.7019	0.6033
σ	0.5191	0.5559
ν	0.5368	0.5856
ρ	-0.7125	-0.7565
λ_x	-0.0238	-0.2245
λ_z	-0.4771	-0.4171
x_1	4.0168	4.0086
σ_e	0.0000	0.0018
γ_1	0.0181	0.0200
γ_1^*	0.0155	0.0141
γ_2		-0.0046
γ_2^*		0.0036
l	1788.9	1799.3
AIC	-3.6210	-3.6381
SC	-3.5662	-3.5734

Table C.3: Full set of parameter estimates together with the resulting values for the log likelihood function, l, and the information criterion AIC and SC. Estimates are obtained by means of maximum likelihood and Kalman filtering. Sample: Weekly closing prices for nearest- and farthest- to maturity white maize futures contracts converted to a dollar price. Sample Period: 08 Jan 1997 to 31 May 2006.

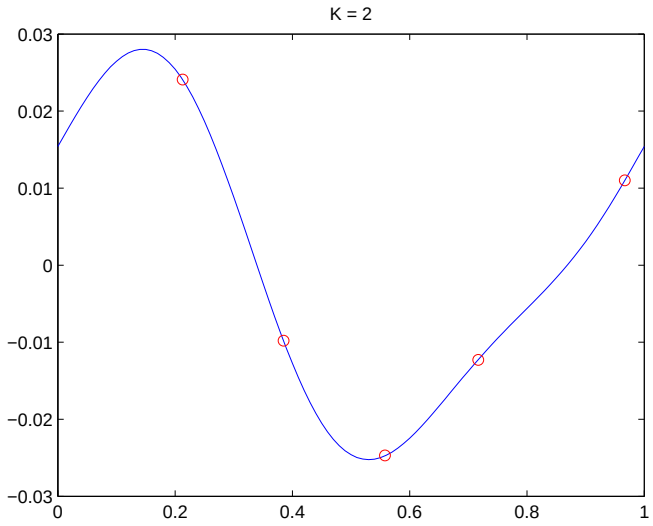

Figure C.7: Plot of $s(T)$ vs T for $K = 2$. $s(T)$ denotes the seasonal component of a futures contract expiring at T. Sample: Weekly closing prices for nearest- and farthest-to maturity white maize futures contracts converted to a dollar price. Sample Period: 08 Jan 1997 to 31 May 2006.

Appendix D

Parameter Estimates For Yellow Maize Futures

	$K=1$	$K=2$
μ	0.1556	0.2369
κ	0.4160	0.3178
σ	0.5461	0.6774
ν	0.6840	0.8116
ρ	-0.9030	-0.9381
λ_x	-0.2468	-0.3186
λ_z	0.2406	0.3375
x_1	5.9343	5.7670
σ_e	0.0084	0.0089
γ_1	0.0177	0.0211
γ_1^*	0.0091	0.0097
γ_2		-0.0029
γ_2^*		0.0112
l	1979.4	1988.1
AIC	-4.0090	-4.0226
SC	-3.9542	-3.9579

Table D.1: Full set of parameter estimates together with the resulting values for the log likelihood function, l, and the information criterion AIC and SC. Estimates are obtained by means of maximum likelihood and Kalman filtering. Sample: Weekly closing prices for nearest- and farthest- to maturity yellow maize futures contracts. Sample Period: 08 Jan 1997 to 31 May 2006.

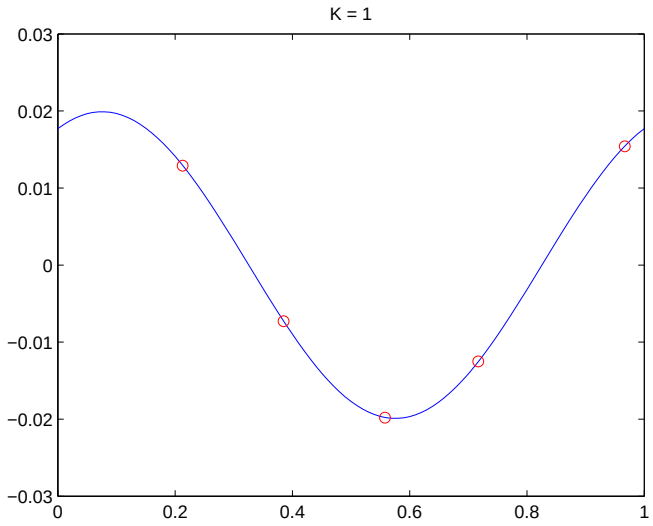

Figure D.1: Plot of $s(T)$ vs T for $K = 1$. $s(T)$ denotes the seasonal component of a futures contract expiring at T. Sample: Weekly closing prices for nearest- and farthest-to maturity yellow maize futures contracts. Sample period: 08 Jan 1997 to 31 May 2006.

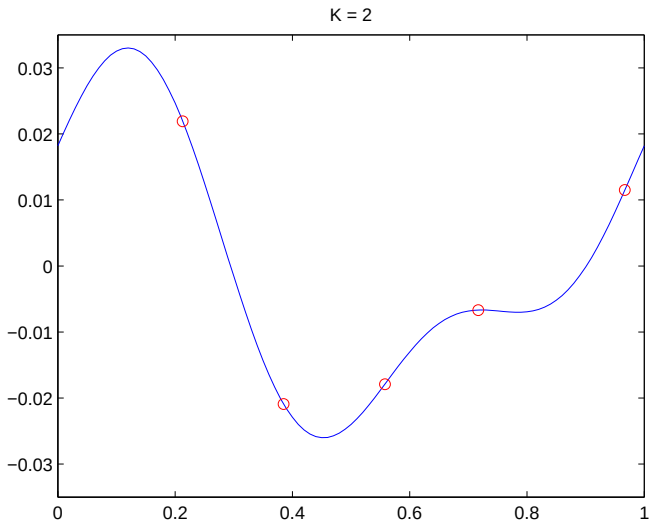

Figure D.2: Plot of $s(T)$ vs T for $K = 2$. $s(T)$ denotes the seasonal component of a futures contract espying at T. Sample: Weekly closing prices for nearest- and farthest- to maturity yellow maize futures contracts. Sample period: 08 Jan 1997 to 31 May 2006.

	$K=1$	$K=2$
μ	0.1574	0.1710
κ	0.4549	0.4252
σ	0.5285	0.5521
ν	0.6463	0.6623
ρ	-0.8943	-0.9035
λ_x	-0.2254	-0.2338
λ_z	-0.2342	0.2157
x_1	6.0194	5.8782
σ_e	0.0093	0.0095
γ_1	0.0224	0.0244
γ_1^*	0.0078	0.0079
γ_2		-0.0032
γ_2^*		0.0073
l	1641.4	1654.4
AIC	-3.9573	-3.9840
SC	-3.8943	-3.9096

Table D.2: Full set of parameter estimates together with the resulting values for the log likelihood function, l, and the information criterion AIC and SC. Estimates are obtained by means of maximum likelihood and Kalman filtering. Sample: Weekly closing prices for nearest- and farthest- to maturity yellow maize futures contracts. Sample Period: 08 Jan 1997 to 31 May 2006 excluding observations between the period 22 Aug 2001 to 19 Feb 2003.

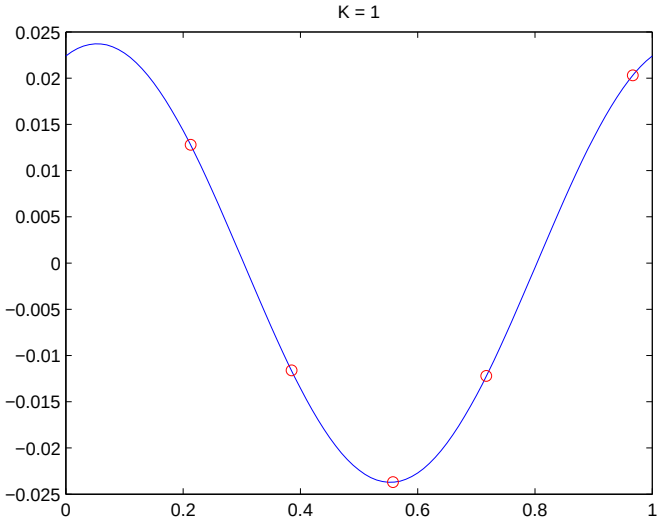

Figure D.3: Plot of $s(T)$ vs T for $K = 1$. $s(T)$ denotes the seasonal component of a futures contract espying at T. Sample: Weekly closing prices for nearest- and farthest-to maturity yellow maize futures contracts. Sample Period: 08 Jan 1997 to 31 May 2006 excluding observations between the period 22 Aug 2001 to 19 Feb 2003.

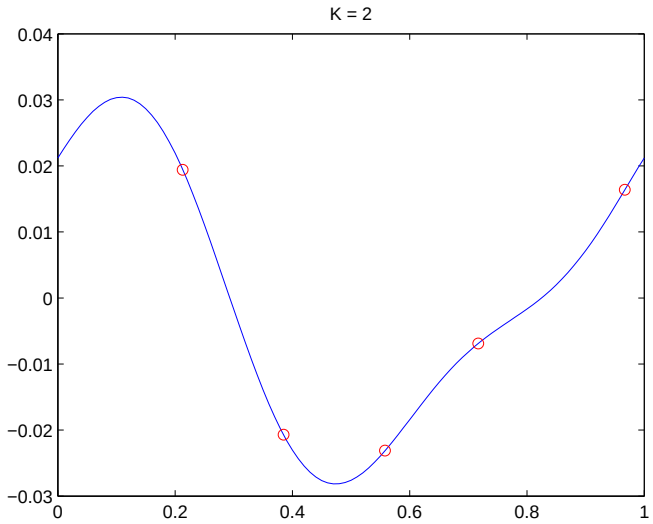

Figure D.4: Plot of $s(T)$ vs T for $K = 2$. $s(T)$ denotes the seasonal component of a futures contract espying at T. Sample: Weekly closing prices for nearest- and farthest-to maturity yellow maize futures contracts. Sample Period: 08 Jan 1997 to 31 May 2006 excluding observations between the period 22 Aug 2001 to 19 Feb 2003.

	$K = 1$	$K = 2$
μ	0.2856	0.5537
κ	0.2886	0.1935
σ	0.7524	1.0496
ν	0.8725	1.1797
ρ	-0.9183	-0.9590
λ_x	-0.3421	-0.5092
λ_z	0.4109	0.6332
x_1	4.1725	4.1308
σ_e	0.0099	0.0102
γ_1	0.0189	0.0221
γ_1^*	0.0091	0.0094
γ_2		-0.0039
γ_2^*		0.0103
l	1860.6	1869.4
AIC	-3.7670	-3.7809
SC	-3.7122	-3.7161

Table D.3: Full set of parameter estimates together with the resulting values for the log likelihood function, l, and the information criterion AIC and SC. Estimates obtained by means of maximum likelihood and Kalman filtering. Sample: Weekly closing prices for nearest- and farthest- to maturity yellow maize futures contracts converted to a dollar price. Sample Period: 08 Jan 1997 to 31 May 2006.

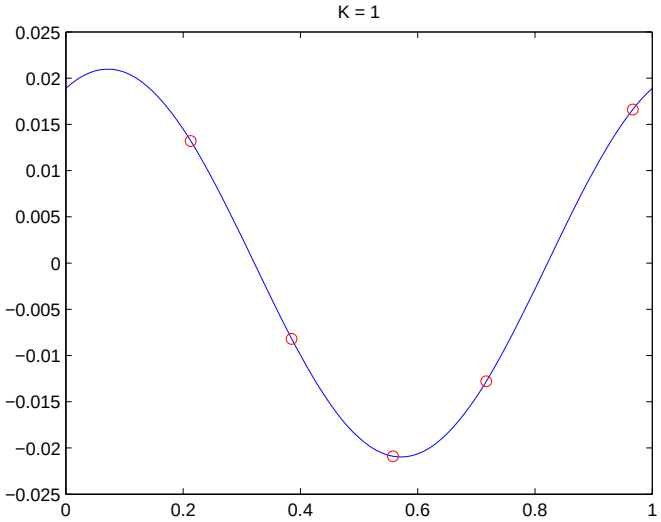

Figure D.5: Plot of $s(T)$ vs T for $K = 1$. $s(T)$ denotes the seasonal component of a futures contract espying at T. Sample: Weekly closing prices for nearest- and farthest- to maturity yellow maize futures contracts converted to a dollar price. Sample Period: 08 Jan 1997 to 31 May 2006.

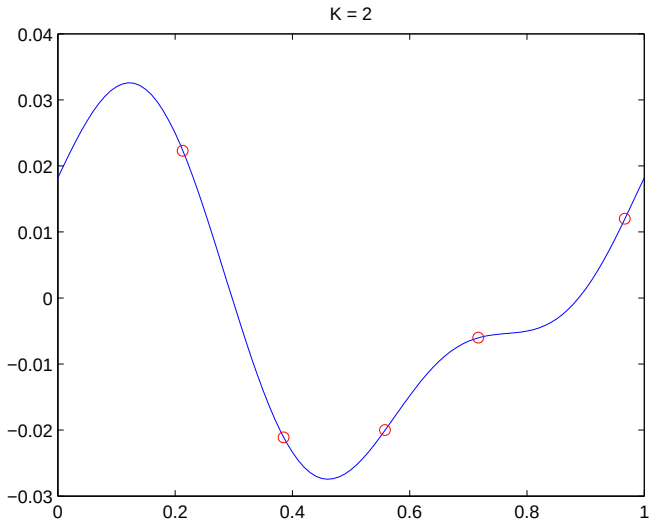

Figure D.6: Plot of $s(T)$ vs T for $K = 2$. $s(T)$ denotes the seasonal component of a futures contract espying at T. Sample: Weekly closing prices for nearest- and farthest- to maturity yellow maize futures contracts converted to a dollar price. Sample Period: 08 Jan 1997 to 31 May 2006.

Appendix E

Parameter Estimates For Wheat Futures

	$K=1$	$K=2$
μ	0.0504	0.0832
κ	0.9144	0.6399
σ	0.2901	0.3885
ν	0.3783	0.4848
ρ	-0.8710	-0.9313
λ_x	-0.0424	-0.0318
λ_z	-0.1045	-0.3111
x_1	7.7789	7.1896
σ_e	0.0064	0.0062
γ_1	-0.0240	-0.0227
γ_1^*	-0.0041	-0.0110
γ_2		-0.0078
γ_2^*		-0.0041
l	2114.9	2125.8
AIC	-4.8477	-4.8682
SC	-4.7873	-4.7968

Table E.1: Full set of parameter estimates together with the resulting values for the log likelihood function, l, and the information criterion AIC and SC. Estimates are obtained by means of maximum likelihood and Kalman filtering. Sample: Weekly closing prices for nearest- and farthest- to maturity wheat futures contracts. Sample Period: 07 Jan 1998 to 31 May 2006.

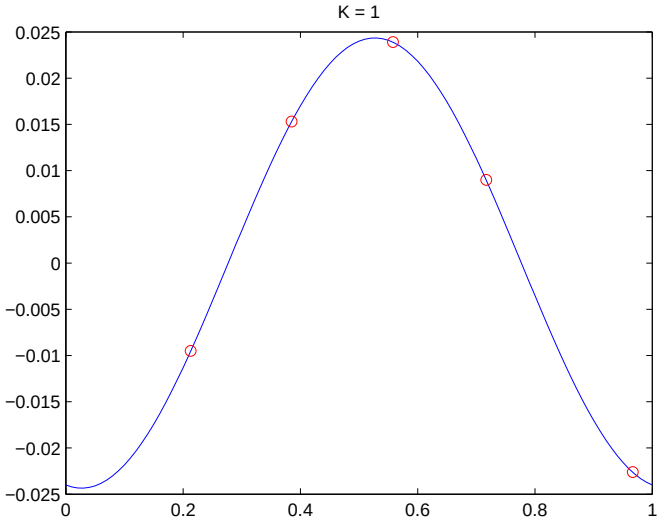

Figure E.1: Plot of $s(T)$ vs T for $K = 1$. $s(T)$ denotes the seasonal component of a futures contract expiring at T. Sample: Weekly closing prices for nearest- and farthest-to maturity wheat futures contracts. Sample Period: 07 Jan 1998 to 31 May 2006.

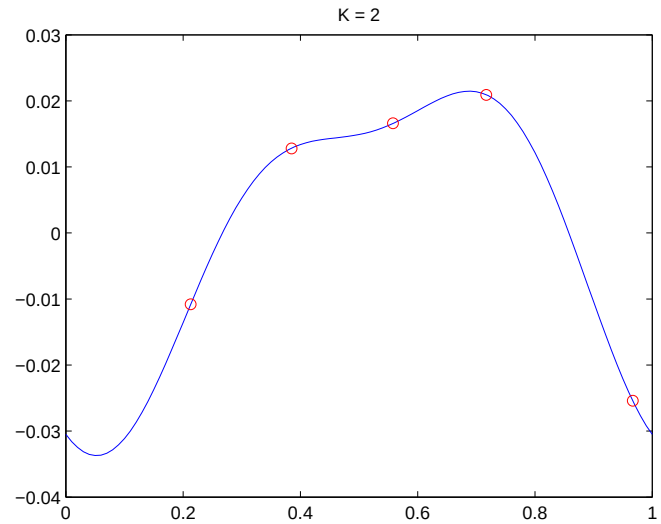

Figure E.2: Plot of $s(T)$ vs T for $K = 2$. $s(T)$ denotes the seasonal component of a futures contract expiring at T. Sample: Weekly closing prices for nearest- and farthest-to maturity wheat futures contracts. Sample Period: 07 Jan 1998 to 31 May 2006.

	$K=1$	$K=2$
μ	0.0495	0.0535
κ	1.0566	0.9524
σ	0.2656	0.2846
ν	0.3393	0.3608
ρ	-0.8735	-0.8923
λ_x	-0.1086	-0.1028
λ_z	0.0619	0.0132
x_1	7.8886	7.8700
σ_e	0.0064	0.0061
γ_1	-0.0248	-0.0236
γ_1^*	-0.0070	-0.0151
γ_2		-0.0088
γ_2^*		-0.0057
l	1769.1	1780.5
AIC	-4.9524	-4.9789
SC	-4.8817	-4.8953

Table E.2: Full set of parameter estimates together with the resulting values for the log likelihood function, l, and the information criterion AIC and SC. Estimates are obtained by means of maximum likelihood and Kalman filtering. Sample: Weekly closing prices for nearest- and farthest- to maturity wheat futures contracts. Sample Period: 07 Jan 1998 to 31 May 2006 excluding observations between the period 22 Aug 2001 to 19 Feb 2003.

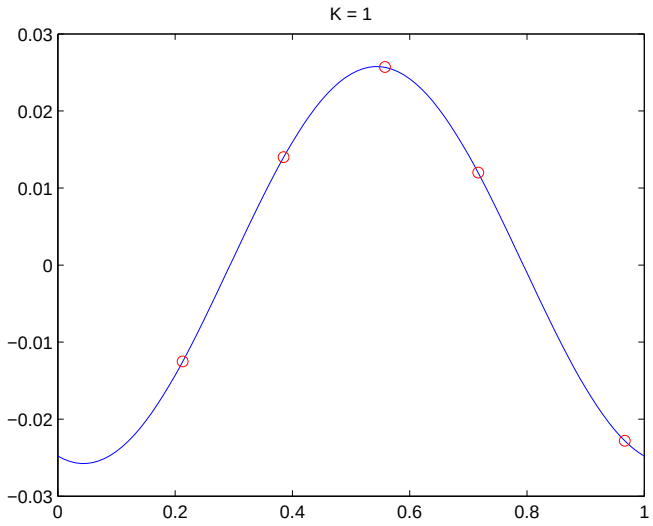

Figure E.3: Plot of $s(T)$ vs T for $K = 1$. $s(T)$ denotes the seasonal component of a futures contract expiring at T. Sample: Weekly closing prices for nearest- and farthest- to maturity wheat futures contracts. Sample Period: 07 Jan 1998 to 31 May 2006 excluding observations between the period 22 Aug 2001 to 19 Feb 2003.

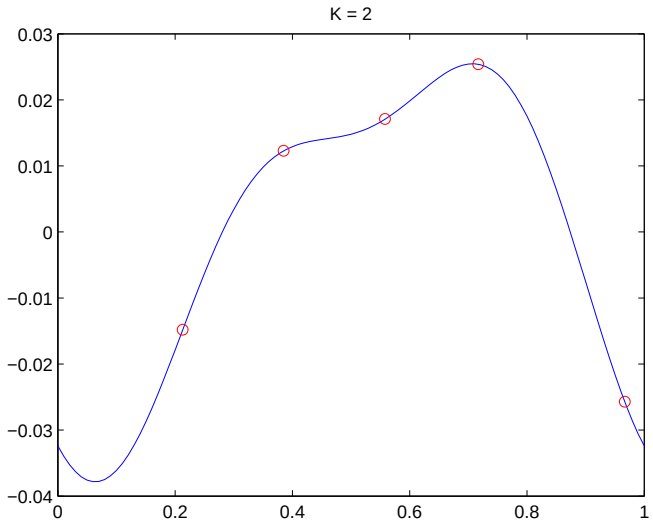

Figure E.4: Plot of $s(T)$ vs T for $K = 2$. $s(T)$ denotes the seasonal component of a futures contract expiring at T. Sample: Weekly closing prices for nearest- and farthest- to maturity wheat futures contracts. Sample Period: 07 Jan 1998 to 31 May 2006 excluding observations between the period 22 Aug 2001 to 19 Feb 2003.

	$K = 1$	$K = 2$
μ	0.0437	0.0499
κ	0.9387	0.7562
σ	0.3777	0.4175
ν	0.3619	0.4154
ρ	-0.6825	-0.7495
λ_x	-0.0805	-0.0896
λ_z	-0.1321	-0.2355
x_1	6.0289	5.7518
σ_e	0.0070	0.0068
γ_1	-0.0241	-0.0228
γ_1^*	-0.0047	-0.0109
γ_2		-0.0070
γ_2^*		-0.0036
l	1788.9	1799.3
AIC	-4.0965	-4.1159
SC	-4.0361	-4.0445

Table E.3: Full set of parameter estimates together with the resulting values for the log likelihood function, l, and the information criterion AIC and SC. Estimates are obtained by means of maximum likelihood and Kalman filtering. Sample: Weekly closing prices for nearest- and farthest- to maturity wheat futures contracts converted to a dollar price. Sample Period: 07 Jan 1998 to 31 May 2006.

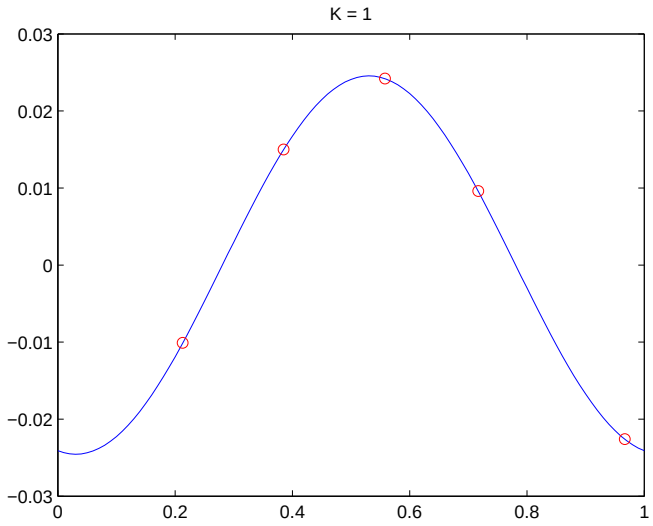

Figure E.5: Plot of $s(T)$ vs T for $K = 1$. $s(T)$ denotes the seasonal component of a futures contract expiring at T. Sample: Weekly closing prices for nearest- and farthest-to maturity wheat futures contracts converted to a dollar price. Sample Period: 07 Jan 1998 to 31 May 2006.

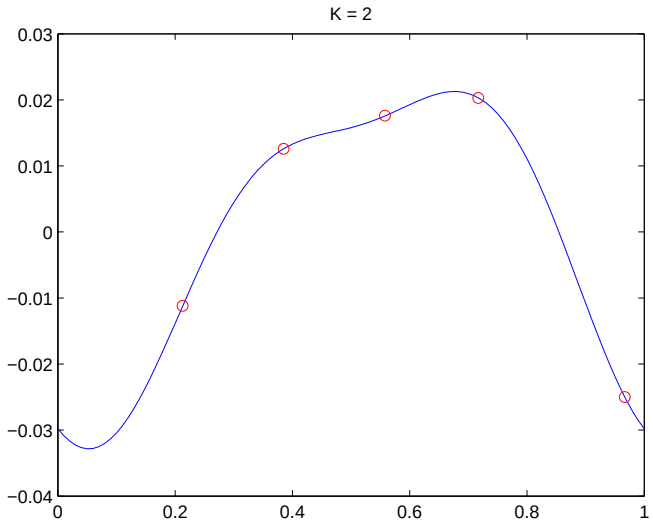

Figure E.6: Plot of $s(T)$ vs T for $K = 2$. $s(T)$ denotes the seasonal component of a futures contract expiring at T. Sample: Weekly closing prices for nearest- and farthest-to maturity wheat futures contracts converted to a dollar price. Sample Period: 07 Jan 1998 to 31 May 2006.